Università Degli Studi Di Napoli
Federico II

Scuola Politecnica e delle Scienze di Base

Dipartimento di Matematica e Applicazioni
"Renato Caccioppoli"

Tesi per il dottorato di ricerca in
Matematica e Applicazioni
XXXVI Ciclo

Infectious Disease Outbreak Simulation: Accurate and Dynamically Consistent Numerical Methods for Integro-Differential Epidemic Models

MARIO PEZZELLA

infectious disease outbreak simulation: accurate and dynamically consistent numerical methods for integro-differential epidemic models.

mario pezzella
ph.d. in "mathematics and applications", xxxvi cycle.
university of naples federico ii.

PREFACE

Mathematical epidemiology is the cross-disciplinary branch of mathematics that investigates infectious disease outbreaks and associated mortality patterns within human populations. It employs mathematical models as analytical tools to comprehend and assess the spread of epidemics, forecast their impact on humanity and devise a priori strategies for infection prevention and control. Daniel Bernoulli is credited with the earliest mathematical contributions to epidemiology, dating back to 1760 [10] and 1766 [11]. In his works, he addressed the effectiveness of the *variolation*[1] technique in reducing the mortality rate of smallpox (see [41] for a contemporary reformulation of Bernoulli's approach in terms of differential equations). In the early twentieth century, William Hamer [53] and Ronald Ross [87] proposed the mass-action principle of transmission, a pivotal concept in mathematical epidemiology. This principle was based on the idea that the net rate of spread is jointly proportional to the number of infectious individuals and the number of susceptible people, i.e. those who may get the infection.

The pioneering work of Kermack and McKendrick [58] in 1927 established the basic foundations of mathematical epidemiology with the age-of-infection model

$$S'(t) = \beta S(t) \int_0^\infty S'(t-s)A(s)\, ds, \tag{1}$$

for which we refer to [20, 39] and references therein. Here, $S(t)$ is the number of susceptibles at time t, $\beta > 0$ represents the constant rate of effective contacts and $A(s) \in L^1(\mathbb{R}_0^+)$ is the non-negative mean infectivity of an individual who became infected s units of time ago. It has been proved that, provided the initial value is positive, the solution $S(t)$ to (1) is positive, mono-

1 The variolation procedure involved the intentional introduction of pulverized dried smallpox scabs or pustule fluid into an individual's skin. This method yielded a milder manifestation of the disease with a reduced mortality rate compared to natural smallpox infection. However, it did not prevent transmission and could even facilitate the spread of other diseases, such as syphilis and hepatitis.

tonically non-increasing and convergent to the final size $S(\infty) \in (0, +\infty)$ as $t \to +\infty$. The value $S(\infty)$ represents the number of individuals who have not been infected during the epidemic and provides a quantification of its impact on the population. It is related to the basic reproduction number R_0 (i.e. the average number of new infections generated by a single infected individual) through a transcendental equation known as the final size relation [16, 20].

The age-of-infection model (1) inherently accounts for the dependence of the infectivity on the time elapsed since the infection. Furthermore, it is general enough to encompass compartmental differential models with an arbitrary number of compartments [14, 18, 46] and multiple infective and treatment stages [15–17]. Several extensions of the original Kermack and McKendrick model have appeared in the scientific literature over time, enriching the class of age-of-infection models based on non-linear Integral and Integro-Differential Equations (IEs and IDEs, respectively). In [14, 16, 24, 36] the model (1) was expanded to incorporate demographic turnover and disease deaths. A more general age-of-infection epidemic model with two pathways, covering symptomatic and asymptomatic infections, was presented in [7]. An extensive examination on the effect of restrictive interventions such as quarantine and vaccination policies was conducted in [14–16, 46]. More recently, some variants of the original model exploring heterogeneously mixed populations [17, 20, 23, 33, 36, 50, 62] have emerged, with the aim to investigate the impact of multifaceted human interactions on the transmission of the disease.

Modeling epidemics using IEs and IDEs leads to a more realistic depiction of the infection's spread, as it allows for the consideration of arbitrarily distributed disease stages [36, 46], improving traditional approaches based on differential equations. Moreover, the integral operators naturally incorporate incubation and latent periods of diseases, as well as the delay between the introduction of restrictive measures and the observation of their effect on the course of the epidemics. These peculiarities make age-of-infection models suitable to describe the dynamics of infectious diseases like smallpox [2], AIDS [3, 91, 92], SARS [14, 15], cholera [22], COVID-19 [42, 47, 56, 57] and influenza [48].

Numerical simulations assume a crucial role in the field of mathematical epidemiology by providing timely responses to epidemics and offering

early or real-time insights. Classical numerical approaches, such as collocation methods [26] or Runge-Kutta and block-by-block schemes [63], represent accurate integrators for problem (1). However, achieving the continuous dynamics may require small time steps, resulting in significant computational costs. Moreover, attaining an asymptotic behaviour for the numerical solution that mirrors the one of the continuous model can be challenging. In this perspective, the interest arises to devise dynamically consistent numerical methods able to replicate, at the discrete-time level and with no limitations on the stepsize, the dynamical and asymptotic properties of the solution to (1). Our primary goal is then to develop positivity-preserving schemes that consistently yield positive numerical solutions, regardless of the discretization stepsize. Furthermore, given the significant role of the final size of the epidemic

$$S(\infty) = \lim_{t \to +\infty} S(t),$$

we are interested in providing approximations of the solution to (1) which retain its asymptotic behaviour. We emphasize that classic error analysis is typically performed over bounded intervals and that the convergence of a numerical scheme is not sufficient to meet the requirement above. Therefore, accounting for these aspects and motivated by the dearth of established numerical methods with the described attributes in the scientific literature, we present in this dissertation a set of ad hoc strategies specifically designed to address the original Kermack and McKendrick integro-differential model (1) and some of its variants.

Non-Standard Finite Difference (NSFD) discretizations are extensively employed for epidemic models governed by non-linear Ordinary Differential Equations (ODEs) to design unconditionally positive numerical methods [6, 59, 93, 96]. The NSFD approach, initially introduced by Mickens in the latter half of the last century [78–80], has only recently found application to integral problems [64]. In [71], we introduce a novel non-standard numerical method to integrate the problem (1). In [75] we extend the same technique to a multidimensional Volterra integro-differential system, which generalizes (1) and includes a variety of age-of-infection epidemic models. In both cases, the proposed linearly implicit schemes preserve the positivity, monotonicity and boundedness of the continuous-time solution without any constraint on

the stepsize. Furthermore, the asymptotic limit of the numerical solution, as the number of time steps tends to infinity, behaves coherently with respect to the reference problem. Nevertheless, such methods exhibit only linear convergence and may become too demanding from a computational perspective for long-term integration tasks, requiring a delicate balance between accuracy and computational costs.

Direct Quadrature (DQ) [28] numerical methods for Volterra IEs and IDEs are highly effective and widely employed computational techniques that directly discretize the integral operators, providing accurate and stable numerical solutions [30, 68, 77]. However, ensuring the properties of the continuous-time solution to (1) for this kind of methods, may lead to severe restrictions on the stepsize, posing practical limitations in the context of long-time simulations. To overcome this drawback, while retaining the benefits of a DQ approach, we exploit in [72] an equivalent exponential form of the evolution operator in (1) and integrate it by DQ method of any order. The resulting scheme possesses the dual advantage of automatically providing positive numerical solutions and of attaining high accuracy. Under the assumption of the existence of a discrete final size, intended as the limit of the numerical solution as the number of time steps goes to infinity, we prove that the proposed method replicates the asymptotic behaviour of the model.

The open problem of the existence of the numerical final state and of its convergence to the continuous limit drives our investigation towards the wider domain of discrete Volterra equations, of which the method in [72] is a specific instance. A comprehensive analysis of non-linear implicit Volterra discrete equations of convolution type is then carried out in [74]. There, sufficient conditions for their solutions to converge to a finite limit are provided, with applications to the stability analysis of linear methods for implicit Volterra Integral Equations (VIEs).

Finally, in [73] the DQ discretization based on the exponential reformulation is applied to the system of IDEs representing the multi-group age-of-infection model with heterogeneous mixing. The proposed method yields accurate, unconditionally positive and long-time behaviour preserving approximations of the continuous solution. Given these properties and the generality of the scenarios to which the multi-dimensional model refers, the numerical method presented in [73] completely fulfills the requirement for approximation schemes that provide precise simulations over extended time

intervals. Consequently, it represents an efficient and reliable tool for comprehending infectious disease outbreaks.

The present dissertation comprises four parts and six chapters, organized as follows. Chapter 1 serves as an introduction to the rest of the thesis and aims to familiarize the reader with some well-established theoretical findings concerning the class of age-of-infection models. Starting from (1), heterogeneity is gradually introduced in the population by initially differentiating symptomatic patients from asymptomatic ones, and later by extending this distinction to an arbitrary number of groups. The corresponding continuous models are considered with a particular emphasis on the qualitative and asymptotic properties of the solution. A comprehensive integro-differential framework that unifies the specific age-of-infection models examined in Chapter 1 is then formulated.

Chapter 2 and Chapter 3 constitute the Part II of the thesis, where the dynamically consistent approximation of the continuous-time solution to the scalar model (1) is addressed. A linearly implicit, first order numerical method based on a non-standard finite difference discretization of the integral term is presented in Chapter 2. The proposed method preserves the essential properties of the continuous model, unconditionally with respect to the integration step-length h, and replicates the continuous dynamics as $h \to 0$.

Aiming to attain higher accuracy in the simulation, we reformulate the Kermack and McKendrick model as an implicit Volterra integral equation in Chapter 3. Then, the discretization of this equation by direct quadrature schemes with Gregory convolution weights results in an accurate numerical method able to replicate the asymptotic behaviour of the epidemic. Specifically, we prove that the numerical solution remains positive and bounded for any step size h and that it inherits the arbitrarily high order of convergence from the underlying quadrature rule. We introduce the discrete equivalents of the basic reproduction number and of the final size relation and demonstrate that they play a role in the discrete dynamics that exactly mirrors their counterparts in the continuous model.

A thorough investigation of the solutions to non-linear implicit Volterra discrete equations is carried out with the Part III and Chapter 4. There, we obtain results about the existence, uniqueness and boundedness of such solutions under mild assumptions on the non-linearity. Emphasis is placed on the

asymptotic analysis of implicit discrete VIEs, along with the identification of conditions governing the convergence of the state variable to a finite limit or the onset of oscillations. Since the analysis is conducted across a general discrete time framework, it proves well-suited for capturing the dynamics of intrinsic discrete time models and of numerical methods, as well. Specifically, our theoretical findings are relevant in the context of approximating renewal equations for age-of-infection epidemic models and estimating their final size. As a matter of fact, the open question raised in Chapter 3 concerning the existence of the asymptotic limit of the DQ numerical solution to (1), is there addressed. Furthermore, the convergence of this limit, as the stepsize vanishes, towards the continuous final size is proved.

Considered the benefits of the NSFD and DQ techniques in approximating the solution to the original model (1), it naturally follows to apply these approaches to multidimensional age-of-infection models as well. These extensions are elaborated in Part IV (Ch. 5 and Ch. 6) of the thesis. More specifically, in Chapter 5 we present a direct quadrature method for the integro-differential system describing an outbreak in a mixed host population. For the proposed scheme, two crucial properties are established: the unconditional positivity and the inheritance of the high order convergence from the underlying Gregory quadrature rule. Additionally, for some choices of the convolution weights and realistic infectivity functions, the monotonicity of the continuous solution is retained too. The theoretical findings of Chapter 4 regarding implicit Volterra discrete systems are then employed to show the existence, uniqueness and positivity of the asymptotic limit of the numerical solution. Remarkably it is proved that the discrete final size converges, as h approaches zero, towards the continuous one. This theoretical achievement represents the central outcome of Chapter 5, as it establishes the asymptotic numerical solution as an accurate approximation of the continuous-time solution's limit.

Chapter 6 delves into the non-local approximation of the general renewal type system outlined in Chapter 1, which includes several age-of-infection models. The aim is to provide a comprehensive NSFD numerical framework to analyze a wider class of problems whose continuous dynamic is well known in the literature and to deepen the investigation in cases where the theory lacks. In general, the study carried out in Chapter 6 can be regarded as a stability numerical investigation on a class of epidemic problems that act as

test equations. The role of the test equations is twofold. Primarily, as the proposed method unconditionally preserves the qualitative characteristics of the continuous solution, it exhibits reliability in facilitating quantitative assessments, including crucial aspects such as the detection of epidemic peaks and of the final size. Additionally, the method's inherent properties suggest its potential effectiveness in addressing more complex problems, such as models incorporating disease-induced mortality or time-varying coefficients.

Each chapter includes numerical experiments and simulations designed to validate the theoretical results, accompanied by pseudo-code sketches of the algorithms. Some remarks and insights on future works conclude the dissertation.

"If I have been able to see further,
it was only because I stood
on the shoulders of giants"

— Sir Isaac Newton.

"Macte nova virtute, puer,
sic itur ad astra"

— Publius Vergilius Maro,
Aeneid, Book IX, 641.

ACKNOWLEDGEMENTS

First and foremost, I express my deepest gratitude to my supervisor Professor Eleonora Messina, whose contribution has been essential to this thesis. Her enduring guidance, invaluable insights and firm encouragements have been a constant presence throughout my academic journey, from my undergraduate studies through my master's degree and into my doctoral research. I am truly grateful to the Research Director Antonia Vecchio as well, for her diligent oversight of my work over these three years and for having provided me with profound suggestions, stimulating discussions and constant support. I wish also to thank Professor Giuseppe Izzo for having embraced my recent proposals and guided the shift of my research towards topics different from those of the thesis, readily offering his experience and expertise to me.

A further acknowledgment to my tutor Professor Paola Festa, who consistently demonstrated a keen awareness and genuine concern for my academic needs. I would also like to thank Professor Gioconda Moscariello, the coordinator of the Ph.D. programme in -Mathematics and Applications, XXXVI cycle- and Professor Cristina Trombetti, the head of the *Department of Mathematics and Applications Renato Caccioppoli*, for having solicitously organized the related courses and activities.

During my Ph.D. I spent a research visiting period in Germany as a guest of the *Institut für Mathematik, Martin-Luther-Universität Halle-Wittenberg*. There, I had the chance to deepen my investigations on Modified Patankar Linear Multistep methods. In this regard, I am thankful to Doctor Helmut Podhaisky, who enthusiastically supported my ideas and provided me with valuable advice and discussions. I wish also to thank Professor Martin Arnold

and Professor Raphael Kruse for their hearty hospitality, as they treated me as a member of their department, not just as a guest.

The sincerest acknowledgment goes to my family, the place where I started from and will always go back to.

To my long-time friends Antonio, Cira, Claudia, Domenico, Federica, Francesca, Francesco, Marco, Pasquale and Roberta, whose support has been invaluable throughout these years. To Amir, Antoni, Aslı, Aslıhan, Denise, Erik, Felix, Karl, Kévin, Nermana, Şebnem and Skerdi, thanks to whom Germany felt more like home. To Alba, Andrea, Peppe, Vincenzo and the other friends and colleagues. This work would not have been the same without all of them.

"D'altronde ho capito di essere solo un uomo
e nessuno può essere grande da solo"

— M.P., *L'umiltà di contare i passi*.

CONTENTS

ACRONYMS 1
LIST OF FIGURES 2
LIST OF TABLES 4

I THE CLASS OF AGE-OF-INFECTION EPIDEMIC MODELS 5
1 INTRODUCTION 6
1.1 The Age-of-Infection Model 6
1.1.1 Asymptotic Behaviour and Final Size Relation 9
1.1.2 Reformulation in Terms of the Force of Infection 10
1.1.3 Derivation of Compartmental Models 11
The SIR model 11
The SEIR model 12
The General Compartmental Model 12
1.2 The Symptomatic and Asymptomatic Age-of-Infection Model 13
1.2.1 Asymptotic Behaviour and Final Size Relation 15
1.3 The Age-of-Infection Model with Heterogeneous Mixing 16
1.3.1 Asymptotic Behaviour and Final Size Relation 18
1.4 A Comprehensive Renewal Equation Framework 19
1.4.1 Derivation of Age-of-infection Models 22

II DYNAMICALLY CONSISTENT NUMERICAL METHODS FOR THE AGE-OF-INFECTION MODEL 24
2 A NON-STANDARD FINITE DIFFERENCE SCHEME 25
2.1 The Non-Standard Numerical Method 25
2.1.1 Qualitative Properties of the Numerical Solution 26
2.1.2 Error Analysis and Convergence 28
2.2 Discrete Asymptotic Dynamics 31
2.3 Numerical Experiments 37
3 UNCONDITIONALLY POSITIVE AND HIGH ORDER DQ SCHEME 41
3.1 Gregory Quadrature Rules 42
3.2 The Direct-Quadrature Method 44
3.2.1 Qualitative Properties of the Numerical Solution 45

Trapezoidal Discretization in Some Realistic Cases 46
3.2.2 Error Analysis and Convergence 48
3.3 Asymptotic Behaviour of the Numerical Solution 50
3.4 Numerical Experiments 52

III ASYMPTOTIC SOLUTIONS OF NON-LINEAR IMPLICIT VOLTERRA DISCRETE EQUATIONS 59

4 VOLTERRA DISCRETE EQUATIONS: THEORETICAL AND NUMERICAL INSIGHTS 60
4.1 Implicit Volterra Discrete Equations 60
4.1.1 Existence and Uniqueness of a Solution 64
4.2 Implicit Volterra Discrete Systems 66
4.3 From Discrete Equations to Numerical Analysis 68
4.3.1 Continuous Volterra Integral Equations 68
4.3.2 Numerical Approximations of Implicit VIEs 70
Error Analysis and Convergence 72
4.3.3 Existence of the Limit and Asymptotic Convergence 73
4.3.4 Numerical Experiments 77
4.4 The Age-of-infection Case Study 79

IV UNCONDITIONALLY POSITIVE LONG-TIME BEHAVIOUR PRESERVING NUMERICAL METHODS FOR MULTI-DIMENSIONAL AGE-OF-INFECTION MODELS 83

5 DQ DISCRETIZATION OF THE HETEROGENEOUSLY MIXED AGE-OF-INFECTION MODEL 84
5.1 The Direct Quadrature Method 86
5.1.1 Existence and Uniqueness of a Positive Numerical Solution 87
5.1.2 Error Analysis and Convergence 91
5.2 Asymptotic Properties of the Numerical Solution 93
5.2.1 Convergence of the Numerical Final Size 95
5.2.2 The Proportionate Mixing Case 98
5.3 Numerical Experiments 98
5.3.1 Age Structured Simulation of Influenza in Italy 101

6 NON-LOCAL DISCRETIZATION OF A CLASS OF RENEWAL TYPE EPIDEMIC MODELS 106
6.1 The Non-local Finite Difference Scheme 106

6.1.1 Non Negativity, Monotonicity and Boundedness Preservation 107
6.1.2 Error Analysis and Convergence 109
6.2 Asymptotic Behaviour of the Numerical Solution 112
6.2.1 Numerical Final State and Asymptotic Convergence 113
6.3 Numerical Experiments 120
The Age-of-infection Model 121
The Symptomatic and Asymptomatic Age-of-Infection Model 122
The Age-of-Infection Model with Heterogeneous Mixing 124
The Virus Shedding Model 126

CONCLUSIONS AND FUTURE INSIGHTS 129

BIBLIOGRAPHY 132

ACRONYMS

AIDS Acquired Immune Deficiency Sindrome

COVID-19 COrona VIrus Disease 2019

DQ Direct Quadrature

FoI Force of Infection

HIT Herd Immunity Threshold

HIV Human Immunodeficiency Virus

IE Integral Equation

IDE Integro-Differential Equation

NG Next Generation

NLFD Non-Local Finite Difference

NSFD Non-Standard Finite Difference

ODE Ordinary Diferenttial Equation

SARS Severe Acute Respiratory Syndrome

SEIR Susceptible-Exposed-Infective-Recovered

SIR Susceptible-Infective-Recovered

VIE Volterra Integral Equation

LIST OF FIGURES

Figure 1	Flowcharts of SIR and SEIR Compartmental Models	12
Figure 2	Flowchart of the Symptomatic and Asymptomatic Age-of-infection Model	15
Figure 3	Experimental Convergence of the NSFD Method	38
Figure 4	Long Time Behaviour of the Numerical Solution by the NSFD Method	40
Figure 5	Comparison of the NSFD Method and the Composite Trapezoidal Discretization	40
Figure 6	Experimental Convergence of the DQ Method	54
Figure 7	Work Precision Diagram for the DQ Method	54
Figure 8	Long Time Behaviour of the Numerical Solution by the DQ Method	55
Figure 9	Comparison of the DQ Method and the Composite Trapezoidal Discretization	57
Figure 10	Final State Convergence for the DQ Numerical Solution to Non-linear Implicit VIEs	80
Figure 11	Onset of oscillations for the DQ Numerical Solution to Non-linear Implicit VIEs	81
Figure 12	Commutative Diagram of the Theoretical Outcomes for the DQ approximation of the Age-of-Infection Model with Static Heterogeneity	97
Figure 13	Experimental Convergence of the DQ Method for the Heterogeneously Mixed Age-of-infection Model	100
Figure 14	Long Time Behaviour of the DQ Numerical Solution to the Heterogeneously Mixed Age-of-infection Model	102
Figure 15	Age Structured Simulation of Influenza in Italy	104
Figure 16	Long Time Behaviour of the NLFD Numerical Solution to the Kermack and McKendrick Model	122
Figure 17	Long Time Behaviour of the NLFD Numerical Solution to the Symptomatic and Asymptomatic Age-of-Infection Model	124

Figure 18 Long Time Behaviour of the NLFD Numerical Solution to the Heterogeneously Mixed Age-of-Infection Model 125
Figure 19 Long Time Behaviour of the NLFD Numerical Solution to the Virus Shedding Model 128

LIST OF TABLES

Table 1	Experimental Convergence of the NSFD Method	39
Table 2	Long Time Behaviour of the Numerical Solution by the NSFD Method	39
Table 3	Experimental Convergence of the DQ Method	53
Table 4	Long Time Behaviour of the Numerical Solution by the DQ Method	56
Table 5	Experimental Convergence of the DQ Method for Nonlinear Implicit VIEs	78
Table 6	Final State Convergence for the DQ Solution to Nonlinear Implicit VIEs	79
Table 7	Experimental Convergence of the DQ Method for the Heterogeneously Mixed Age-of-infection Model	99
Table 8	Convergence of the Numerical Final Size by the DQ Method for the Heterogeneously Mixed Age-of-infection Model	103
Table 9	Age structure Partition and Contact Patterns of Italian Population.	104
Table 10	Convergence of the Numerical Final Size by the NLFD Method for the Heterogeneously Mixed Age-of-infection Model	126
Table 11	Convergence of the Numerical Final Size by the NLFD Method for the Virus Shedding Model	127

Part I

THE CLASS OF AGE-OF-INFECTION EPIDEMIC MODELS

In this introductory chapter, we discuss equivalent formulations of the age-of-infection model (1) and underline its relation to compartmental differential models. A comprehensive overview of the main theoretical results is provided, with a specific emphasis on the asymptotic behavior of the solution. Furthermore, the extensions of the model to more general situations are addressed. More specifically, we consider the model accounting for the difference between symptomatic and asymptomatic infections and its generalization to a heterogeneous multi-group population. Finally, we formulate a unified framework based on renewal integral equations which encompasses all the aforementioned models and scenarios.

1 INTRODUCTION

1.1 THE AGE-OF-INFECTION MODEL

The original Kermack and McKendrick model (1) delineates the dynamics of an epidemic within a closed population, for which demographic and mortality effects are neglected. The age-of-infection model's key feature is the time-varying total infectivity

$$\varphi(t) = -\int_0^{+\infty} A(s)S'(t-s)ds,$$

which depends on the time elapsed since the infection (the age of infection). The function $\varphi(t)$ accounts for the contribution of the entire history of the epidemic to the total infectivity. As a matter of fact, it traces the number of new infections, $-S'(\tau)$ at time $\tau = t - s$, for all $\tau \leq t$. Here, $S(t)$ denotes the number of susceptible individuals, i.e. those who may contract the infection. Our investigation builds upon the assumption that the time $t = 0$ corresponds to the disease outbreak, so that $S(t) = N$ for all $t < 0$ (we refer to [14, 16, 20, 22] and references therein for a detailed description). Equation (1) can be rewritten as follows

$$\begin{aligned} S'(t) &= -\beta S(t)\varphi(t) \\ \varphi(t) &= \varphi_0(t) + \beta \int_0^t A(t-s)S(s)\varphi(s)\, ds, \end{aligned} \tag{1.1}$$

where the given function $\varphi_0(t) = -\int_t^{\infty} A(s)S'(t-s)\, ds \geq 0$ is the total infectivity, at time t, of members of the population who were infected at $t = 0$ (see [14] for further details). In general the inequality

$$\varphi_0(t) \leq A(t)(N - S_0), \tag{1.2}$$

holds true for $t \in \mathbb{R}_0^+$, where $N > 0$ is the constant population size and $S_0 = S(0) \in (0, N]$ is the initial number of susceptible individuals. Thus,

(1.2) turns to an equality when the supplementary assumption is made that all initial infectives have infection-age zero at the disease outbreak (see, for instance, [16]). The first equation of (1.1) incorporates the standard bilinear mass-action principle ([53, 87]) for the incidence[1] at time t. There, $\beta > 0$ is the constant rate of effective contacts and $A(s) \in L^1(\mathbb{R}_0^+)$ is the non-negative mean infectivity of members of the population with infection age s, including those who are no longer infectious. More specifically, $A(s) = \pi(s)B(s)$, where $0 \leq B(s) \in L^1(\mathbb{R}_0^+)$ is the fraction of infected members remaining infected at infection age s, and $0 \leq \pi(s) \leq 1$ is the mean infectivity of infected individuals at infection age s ([14, 19]). The number $I(t)$ of infected (and infective) members of the population at time t is then given by

$$I(t) = -\beta \int_0^{+\infty} B(s)S'(t-s)\, ds = I_0(t) + \beta \int_0^t B(t-s)S(s)\varphi(s)\, ds, \quad (1.3)$$

with $0 \leq I_0(t) \leq B(t)(N - S_0)$, for $t \geq 0$.

Henceforward, we will equivalently refer to (1) or (1.1) as needed. There is ample literature which deals with the description and analysis of the age-of-infection epidemic model of the form (1.1). Here we outline the main facts, that will represent our guidelines for constructing dynamically consistent numerical schemes.

- The functions $S(t)$ and $\varphi(t)$ are non-negative. Additionally, the positivity assumption on the initial value $S_0 = S(0)$ implies that $S(t) > 0$ for $t \geq 0$.
- From the first of (1.1), $S(t)$ is a non-increasing function which decreases to the finite value $S(\infty)$, as $t \to \infty$. Further details on the asymptotic behaviour of the solution are provided in Subsection 1.1.1.
- When $\varphi_0(t) = 0$ for all $t \geq 0$, the solution to (1.1) is constant. Therefore, owing to (1.2), the condition $S_0 = N$ leads to the disease-free equilibrium $(S(t), \varphi(t)) = (N, 0)$, $t \in \mathbb{R}_0^+$, representing a population in which the disease does not spread.

1 The *incidence* is the number of instances of illness commencing, or of persons falling ill, during a given period in a specified population [84].

- The basic reproduction number [16],

$$R_0 = \beta N \int_0^\infty A(s)\, ds, \tag{1.4}$$

is the number of secondary disease cases produced by one typical primary case and represents an important indicator of the risk of epidemic. Its role can be clarified through the following *invasion criterion*. Based on the consideration that at the disease outbreak the entire population is susceptible ($S(t) \approx N$), the linearization around the disease free equilibrium of (1) yields

$$S'(t) = \beta N \int_0^\infty [S'(t-s)]A(s)\, ds,$$

which has a solution $S(t) = Ne^{rt}$, with an exponential growth rate r, if

$$1 = \beta N \int_0^\infty A(s)e^{-rs}\, ds.$$

Therefore R_0 can be expressed in terms of the initial growth rate

$$R_0 = \frac{\int_0^\infty A(s)\, ds}{\int_0^\infty A(s)e^{-rs}\, ds}, \tag{1.5}$$

and it points out that an epidemic situation, for which initially the solution grows exponentially (see [18]), is characterized by

$$r > 0 \qquad \Leftrightarrow \qquad R_0 > 1.$$

Moreover, the relation (1.5) provides a mean to estimate the basic reproduction number from measurements of the initial exponential growth rate provided the infectivity distribution is known.

1.1.1 *Asymptotic Behaviour and Final Size Relation*

In this section, we present well-established results pertaining to the asymptotic behavior of the solution to the age-of-infection model (1.1). The final size of the epidemic $S(\infty) = \lim_{t\to+\infty} S(t)$ provides insights on the impact of the outbreak on the population. As a matter of fact, $S(\infty)$ quantifies the portion of the population unaffected by the infection, while $N - S(\infty)$ corresponds to the total number of individuals infected over the course of the epidemic.

Here we report the *final size relation*, a transcendental equation relating the final size to the basic reproduction number defined in (1.4) and show that $S(\infty) > 0$. Furthermore we underline that, under regularity assumptions on the known functions of problem (1.1), $\varphi(t) \overset{t\to+\infty}{\longrightarrow} 0$. Dividing both members of (1.1) by $S(t)$, integrating with respect to t from zero up to infinity and taking advantage of Dirichlet's formula (see, for instance, [28, p. 11]), yields

$$\begin{aligned}
\log\left(\frac{S_0}{S(\infty)}\right) &= \beta\int_0^{+\infty}\varphi_0(t)\,dt - \beta\int_0^{+\infty}\left(\int_0^t A(s)S'(t-s)\,ds\right)\,dt \\
&= \beta\int_0^{+\infty}\varphi_0(t)\,dt - \beta\int_0^{+\infty}A(s)\left(\int_s^{+\infty}S'(t-s)\,dt\right)\,ds \\
&= \beta\int_0^{+\infty}(\varphi_0(t) - (N-S_0)A(t))\,dt + \beta\,(N-S(\infty))\int_0^{+\infty}A(s)\,ds,
\end{aligned} \tag{1.6}$$

which shows the positivity of the final size. Therefore, $S(\infty)$ satisfies the non-linear equation

$$\log\left(\frac{S_0}{S(\infty)}\right) = \left(1 - \frac{S(\infty)}{N}\right)R_0 + \beta\int_0^{+\infty}(\varphi_0(t) - (N-S_0)A(t))\,dt, \tag{1.7}$$

commonly referred to as the *final size relation*[2]. A slight generalization of the results in [16], corresponding to the scenario where (1.2) holds as an equality, leads to a proof of uniqueness for the solution to the final size relation (1.7) lying within the interval $(0, S_0]$.

2 The quantity $1 - S(\infty)/N$ represents the *attack ratio* [16], indicating the proportion of infected individuals in the population.

The asymptotic behaviour of the function $\varphi(t)$ can be examined by the same arguments. As a matter of fact, by integrating the second equation in (1.1) with respect to t over the interval $[0, +\infty)$, we obtain:

$$\int_0^{+\infty} \varphi(t)\, dt \leq (N - S(\infty)) \int_0^{+\infty} A(s)\, ds.$$

Assume that the known functions $A(t)$ and $\varphi_0(t)$ are smooth enough to ensure the differentiability of the solution to (1.1). Therefore $\varphi(t) \geq 0$ belongs to $C^1(\mathbb{R}_0^+) \cap L^1(\mathbb{R}_0^+)$ and the total infectivity vanishes as t approaches infinity. A similar result for the function $I(t)$ can be derived from (1.3).

1.1.2 *Reformulation in Terms of the Force of Infection*

The original model (1) is equivalently restated in terms of the Force of Infection[3] (FoI) function

$$F(t) = -\int_0^{+\infty} S'(t-s)A(s)\, ds,$$

in [36, 39]. The incidence at time t is expressed as the product $F(t)S(t)$ and it is evident that the current value of the FoI depends on the past incidence. In this context, the non-negative kernel $A(s) \in L^1(\mathbb{R}_0^+)$ represents the expected contribution to the force of infection from an individual with an age of infection s. The age-of-infection model then reads

$$\begin{aligned} S'(t) &= -S(t)F(t) \\ F(t) &= \int_{-\infty}^{t} F(s)S(s)A(t-s)\, ds. \end{aligned} \tag{1.8}$$

Although the distinct epidemiological interpretations of the involved functions, a direct comparison of the incidence equations reveals that the system (1.8) coincides with (1.1) when $F(t) = \beta\varphi(t)$. Thus, the two formulations are equivalent from a mathematical perspective and share the same qualitative

3 The *force of infection* is by definition the probability per unit of time for a susceptible to become infected [36].

properties. In the following subsection, as we explore the connection with differential epidemic models, we exploit both formulations interchangeably.

1.1.3 *Derivation of Compartmental Models*

Compartmental epidemic models partition the population into distinct compartments based on the individuals' disease status. By tracking the transitions between these clusters, they provide valuable insights into the progression of an epidemic and aid in assessing various control measures. Here, we illustrate how to derive well-established compartmental models from the age-of-infection model.

THE SIR MODEL The Susceptible-Infective-Recovered model (see, for instance [54] and [67, ch. 2]) is obtained from (1.1) by assuming that the infectious period follows an exponential distribution with parameter α, or equivalently that infectives have a constant probability per unit of time α to become removed [14]. Assume that all initial infective have infection-age zero at $t = 0$. In this case (1.2) holds as an equality,

$$A(t) = e^{-\alpha t}, \qquad A'(t) = -\alpha A(t), \qquad B(t) = A(t), \qquad \pi(t) = 1$$

and the differentiation with respect to t of the second equation in (1.1) yields

$$\begin{aligned}\varphi'(t) &= \varphi_0'(t) + \beta A(0) S(t)\varphi(t) + \beta \int_0^t A'(t-s) S(s)\varphi(s)\, ds \\ &= \beta S(t)\varphi(t) - \alpha\varphi(t).\end{aligned}$$

Finally, from (1.3), $I(t) = \varphi(t)$ and the age-of-infection model reduces to

$$\begin{aligned}S'(t) &= -\beta S(t) I(t), \\ I'(t) &= \beta S(t) I(t) - \alpha I(t), \\ R'(t) &= \alpha I(t),\end{aligned}$$

where the last equation is derived from the relation $N = S(t) + I(t) + R(t)$ for all $t \geq 0$, corresponding to the assumption of a closed population. The flowchart of the SIR model is reported in Figure 1a.

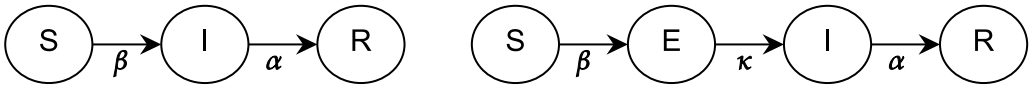

(a) Flowchart of SIR model. (b) Flowchart of SEIR model.

Figure 1: Diagrammatic frameworks of compartmental models. The solid arrows represent the transitions between different compartments.

THE SEIR MODEL There is ample evidence that exponential distributions of stay in compartments are much less realistic than gamma distributions [16, 46], which can be expressed as the sum of exponential ones. These considerations allow to view the Susceptible-Exposed-Infective-Recovered model as an age-of-infection model of the form (1.1). Assume that κ is the probability per unit of time for an exposed member to become infective at infection age s, while α denotes the probability for an infective individual to transition into the removed state [14]. In this case,

$$A(t) = \frac{\kappa(e^{-\alpha t} - e^{-\alpha t})}{\kappa - \alpha}, \qquad B(t) = \frac{\kappa e^{-\alpha t} - \alpha e^{-\kappa t}}{\kappa - \alpha}, \qquad \pi(t) = 1.$$

Therefore, taking $E(t) = \beta \int_0^{+\infty} B(s)S(t-s)\varphi(t-s)\, ds - \varphi(t)$, $I(t) = \varphi(t)$ and $R(t) = N - (S(t) + E(t) + I(t))$ in (1.1) leads to the differential model

$$\begin{aligned} S'(t) &= -\beta S(t)I(t), \\ E'(t) &= \beta S(t)I(t) - \kappa E(t), \\ I'(t) &= \kappa E(t) - \alpha I(t), \\ R'(t) &= \alpha I(t), \end{aligned}$$

whose flowchart is reported in Figure 1b.

THE GENERAL COMPARTMENTAL MODEL As detailed in [35, Sec. 9.3] and [38, Sec. 4 and Sec. 6], a general compartmental model with n compartments assumes the following *standard form*

$$\begin{aligned} S'(t) &= -F(t)S(t), \\ Y'(t) &= \Sigma Y(t) + (F(t)S(t))V, \\ F(t) &= UY(t), \end{aligned} \tag{1.9}$$

where $U \in \mathbb{R}^{1\times n}$, $V \in \mathbb{R}^{n\times 1}$ and $\Sigma \in \mathbb{R}^{n\times n}$. In this context, the components of the vector $Y(t) \in \mathbb{R}^{n\times 1}$ represent the states of the model at time t, whose contribution to the force of infection $F(t)$ is expressed through the components of U. The vector V contains crucial information about the incidence, while the matrix Σ governs the autonomous Markov chain dynamics of the states. Notably, the model (1.9) aligns with the age-of-infection model (1.8) with

$$A(t) = Ue^{t\Sigma}V \qquad \text{and} \qquad Y(t) = \int_0^{+\infty} e^{s\Sigma}VF(t-s)S(t-s)\,ds.$$

1.2 THE SYMPTOMATIC AND ASYMPTOMATIC AGE-OF-INFECTION MODEL

Substantial evidence highlights the significant impact of asymptomatic cases on infectious disease progression, including COVID-19 (see [65, 69, 88, 90] and references therein). Therefore the distinction between symptomatic and asymptomatic infections in an epidemic model is a key element for comprehending transmission dynamics and anticipating long-term consequences.

An age-of-infection model accounting for both infection pathways is described in [7], by the following system

$$\begin{aligned} S'(t) &= -\frac{a}{N}S(t)(\varphi^s(t)+\varphi^a(t)),\\ \varphi^s(t) &= \varphi_0^s(t) + \frac{a}{N}\int_0^t f(t-s)A^s(t-s)S(s)(\varphi^s(s)+\varphi^a(s))\,ds,\\ \varphi^a(t) &= \varphi_0^a(t) + \frac{a}{N}\int_0^t (1-f(t-s))A^a(t-s)S(s)(\varphi^s(s)+\varphi^a(s))\,ds. \end{aligned} \tag{1.10}$$

Model (1.10) tracks the evolution of the epidemic by differentiating between the infectivity functions of symptomatic and asymptomatic individuals, denoted as $\varphi^s(t)$ and $\varphi^a(t)$, respectively. The total infectivity, given by

$$\varphi(t) = \varphi^s(t) + \varphi^a(t),$$

plays a crucial role in the incidence equation. An analogous distinction is made for the non-negative functions

$$\varphi_0^s(t) \leq (N - S_0)A^s(t) \qquad \text{and} \qquad \varphi_0^a(t) \leq (N - S_0)A^a(t),$$

which describe the contribution to the total infectivity of people who got infected before the initial time (the positive value $S_0 = S(0)$ is given).

Regarding the known parameters of the model, $N > 0$ is the total size of the closed population and $a > 0$ is the average number of contacts made by a member per unit of time. The function $f(t) \in (0,1)$ denotes the probability at time t for an individual to develop symptoms after infection and can be formulated as a Heaviside function or its smooth approximations (e.g. generalized logistic functions). Consequently, $1 - f(t)$ represents the probability at time t for an infected individual to become asymptomatic. Furthermore, $A^s(s) = B^s(s)\pi^s(s) \in L^1(\mathbb{R}_0^+)$ and $A^a(s) = B^a(s)\pi^a(s) \in L^1(\mathbb{R}_0^+)$ represent the mean infectivity of symptomatic and asymptomatic individuals (infectious or not) with infection age s, respectively. More specifically, the integrable non-negative functions $B^s(s)$ and $B^a(s)$ denote the fractions of infected symptomatic and asymptomatic members remaining infected at infection age s, while $0 \leq \pi^s(s) \leq 1$ and $0 \leq \pi^a(s) \leq 1$ are the mean infectivity of infected individuals.

The equations

$$\begin{aligned} I^s(t) &= I_0^s(t) + \frac{a}{N}\int_0^t f(t-s)B^s(t-s)S(s)(\varphi^s(s) + \varphi^a(s))\,ds, \\ I^a(t) &= I_0^s(t) + \frac{a}{N}\int_0^t (1 - f(t-s))B^a(t-s)S(s)(\varphi^s(s) + \varphi^a(s))\,ds, \end{aligned} \tag{1.11}$$

govern the number of symptomatic and asymptomatic patients at time t, $I^s(t)$ and $I^a(t)$, respectively. Here, the non-negative functions $I_0^s(t) \leq (N - S_0)B^s(t)$ and $I_0^a(t) \leq (N - S_0)B^a(t)$ account for individuals who were infected before the initial outbreak. Furthermore, the absence of demographic turnover leads to the equation

$$R(t) = N - (S(t) + I^a(t) + I^s(t)),$$

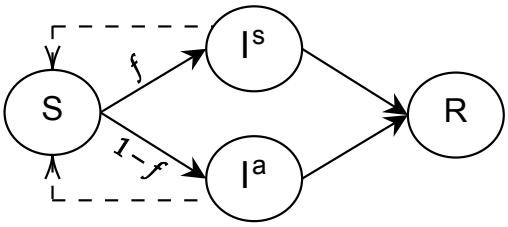

Figure 2: Flowchart of the symptomatic and asymptomatic age-of-infection model. The solid and dashed arrows represent the transitions between different compartments and the occurrences of new infections, respectively.

for the number of recovered people at time t. The modeling flowchart of (1.10) is depicted in Figure 2. In this scenario, the basic reproduction number, given by

$$R_0 = af(0)\int_0^{+\infty} A^s(s)\,ds + a(1-f(0))\int_0^{+\infty} A^a(s)\,ds, \tag{1.12}$$

depends on the initial ratio $f(0)$, as well as on the mean period in each infective stage, but not on the specific distribution of the stages.

1.2.1 *Asymptotic Behaviour and Final Size Relation*

To investigate the asymptotic behaviour of the continuous–time solution to (1.10), we assume that $f(t) = f$ and $1 - f(t) = \tilde{f}$ for all $t \geq 0$. The function $S(t)$ is positive, monotonically non-increasing and converges to the positive final size $S(\infty)$. Given the definition of R_0 in (1.12), by the same arguments of Subsection 1.1.1, we outline that

$$\begin{aligned}
\log\left(\frac{S_0}{S(\infty)}\right) &= \frac{a}{N}\left(\int_0^{+\infty}\left(\varphi_0^s(t) + \varphi_0^a(t) - \int_0^t (fA^s(s) + \tilde{f}A^a(s))S'(t-s)\,ds\right)dt\right) \\
&= \frac{a}{N}\left(\int_0^{+\infty}\left(\varphi_0^s(s) + \varphi_0^a(s) - \int_s^{+\infty} (fA^s(s) + \tilde{f}A^a(s))S'(t-s)\,dt\right)ds\right) \\
&= \frac{a}{N}\int_0^{+\infty}(\varphi_0^s(s) + \varphi_0^a(s))\,ds + R_0\,\frac{S_0 - S(\infty)}{N},
\end{aligned} \tag{1.13}$$

which corresponds to the *final size relation* for the model (1.10). Intuitively, the final size provides insights on the total number of symptomatic and asymptomatic patients, $(S_0 - S(\infty))f$ and $(S_0 - S(\infty))\tilde{f}$, respectively. A more detailed derivation of this relationship, based on additional integro-differential equations for the removed class, is available in [7, pp. 81-82].

The integration over $\mathbb{R}_0^+$ of the second equation in (1.10) and the first in (1.11) yields

$$\int_0^{+\infty} \varphi^s(t)\, dt \leq N_{S(\infty)} \|A^s\|_{L^1(\mathbb{R}_0^+)}, \qquad \int_0^{+\infty} I^s(t)\, dt \leq N_{S(\infty)} \|B^s\|_{L^1(\mathbb{R}_0^+)},$$

with $N_{S(\infty)} = N - S(\infty)$. Assuming the known functions are sufficiently smooth, the inequalities above suggest that both the number of infected symptomatic people and their mean infectivity tend to zero as t approaches infinity. Thus, analogous results may be carried out for the asymptomatic infectious pathway and the functions $\varphi^a(t)$ and $I^a(t)$.

1.3 THE AGE-OF-INFECTION MODEL WITH HETEROGENEOUS MIXING

The original age-of-infection model (1) lacks population heterogeneity and the ability to incorporate multifaceted human interactions and individualized responses to contagion. To overcome this issue, several extensions of the original model addressing heterogeneously mixed population have recently been presented in the literature (see, for instance, [17, 33, 38, 50, 62] and references therein). In [13], for instance, a time since infection model involving static heterogeneity is devised to assess the efficiency of face masks as non-pharmaceutical interventions to reduce the spread of the disease (see also [12] for further details on the model and its relation the Herd Immunity Threshold (HIT)).

Here, we examine the multi-group age–of–infection model with mixing

$$\frac{\partial S}{\partial t}(t,\zeta) = a(\zeta)S(t,\zeta) \int_\Sigma \frac{p(\zeta,z)}{N(z)} \left(\int_0^{+\infty} \frac{\partial S}{\partial t}(t-s,z)A(s,z)\, ds \right) dz, \qquad (1.14)$$

as proposed in [23], where $S(t,\zeta)$ is the number of susceptible members of group ζ (i.e. with trait ζ) at time t and $A(s,z)$ is the mean infectivity of individuals of group z with infection-age s. In (1.14) the variable $\zeta \in \Sigma$, identifies the subpopulation of size $N(\zeta,t)$ at time t. Here, the traits are considered static and do not change during the life of the host individual, who always belongs to one and only one group. Furthermore, we assume that the state space Σ consists of discrete states, so the integral in (1.14) turns to a finite sum. Under this assumption, $\Sigma = \{1,2,\dots,d\}$ and the population is partitioned into d disjoint sub-groups $\mathcal{P}_i$ of constant sizes N_i, $i = 1,\dots,d$. Let $a_i \geq 0$ be the contact rate for members of group $\mathcal{P}_i$, and p_{ij} be the fraction of contacts made by a member of $\mathcal{P}_i$ with a member of $\mathcal{P}_j$. Therefore $\sum_{j=1}^{d} p_{ij} = 1$ and, if $i \neq j$, a balance [23] or consistency [13] relation

$$a_i p_{ij} N_i = a_j p_{ji} N_j, \tag{1.15}$$

governs the total number of contacts made in unit time by members of group i with members of group j. In this multi-group heterogeneous setting, the epidemic model (1.14) reads

$$\begin{aligned} S_i'(t) &= -a_i S_i(t) \sum_{j=1}^{d} \frac{p_{ij}}{N_j} \varphi_j(t), \\ \varphi_i(t) &= \varphi_{0i}(t) - \int_0^t A_i(s) S_i'(t-s)\, ds, \qquad\qquad i = 1,\dots,d. \end{aligned} \tag{1.16}$$

Here $t = 0$ corresponds to the disease outbreak and the initial value $S_i^0 = S_i(0)$, $i = 1,\dots,d$ is given. Furthermore, $0 \leq S_i(t) \leq S_i^0$ and $0 \leq A_i(s) \in L^1(\mathbb{R}^+)$ are the number of susceptibles belonging to $\mathcal{P}_i$ at time t and the mean infectivity of members of this group with infection age s, respectively. The non-negative function

$$\varphi_{0i}(t) = -\int_t^{+\infty} A_i(s) S_i'(t-s)\, ds, \qquad i = 1,\dots,d,$$

belonging to $L^1(\mathbb{R}^+)$, represents the infectivity, at time t, of members of $\mathcal{P}_i$ who were infected before the initial time $t = 0$. It is $\varphi_{0i}(t) \leq (N_i - S_i^0) A_i(t)$,

where the equality holds if all the initial infectives of group $\mathcal{P}_i$ are supposed to have infection-age zero at $t = 0$ (see, for instance, [16]).

We emphasize that the framework (1.16) is devised to address diverse patterns of contact and a wide range of scenarios, including social interactions among different age groups, workplace-specific mixing patterns and the influence of educational and socioeconomic factors. A known type of mixing between groups is the *proportionate*[4] one, introduced by Barbour in 1978 [8]. Based on the assumption that the number of contacts between groups is proportional to the relative activity levels, it yields

$$p_{ij} = p_j, \qquad \text{for all} \qquad 1 \leq i, j \leq d. \tag{1.17}$$

Further details on the model can be found in [20, Sec.5.4] and [23], where it is proved that the solution $S_i(t)$, $i = 1, \dots, d$, to (1.16) remains positive, bounded from above by the initial value and non-increasing. Furthermore, $\varphi(t) \geq 0$, for $t \geq 0$ and $i = 1, \dots, d$.

1.3.1 *Asymptotic Behaviour and Final Size Relation*

Let $S_i(\infty) = \lim_{t \to +\infty} S_i(t)$, be the final size of the epidemic. Then, manipulating (1.16) and integrating with respect to $t \in [0, +\infty)$ leads to the *final size relation*

$$\begin{aligned}
\log\left(\frac{S_i^0}{S_i(\infty)}\right) &= a_i \sum_{j=1}^{d} \frac{p_{ij}}{N_j} \left(\int_0^{+\infty} \varphi_{0j}(t)\, dt - \int_0^{+\infty} \left(\int_0^t A_j(s) S_j'(t-s)\, ds \right) dt \right) \\
&= a_i \sum_{j=1}^{d} \frac{p_{ij}}{N_j} \left(\int_0^{+\infty} \varphi_{0j}(t)\, dt - \int_0^{+\infty} A_j(s) \left(\int_s^{+\infty} S_j'(t-s)\, dt \right) ds \right) \\
&= a_i \sum_{j=1}^{d} \frac{p_{ij}}{N_j} \left(\int_0^{+\infty} \varphi_{0j}(t)\, dt + (S_j^0 - S_j(\infty)) \int_0^{+\infty} A_j(s)\, ds \right),
\end{aligned} \tag{1.18}$$

4 From a biological perspective, (1.17) corresponds to a scenario where the distribution of people who get infected is independent of the distribution of those who transmitted the infection [37]. For this reason, it is also referred to as a specific instance of *separate mixing*.

for $i = 1, \dots, d$. Therefore, if $\varphi_{0j}(t) = (N_j - S_j^0)A_j(t)$ for each $1 \leq j \leq d$, the final size relation reads

$$\log\left(\frac{S_i^0}{S_i(\infty)}\right) = a_i \sum_{j=1}^{d} p_{ij}\left(1 - \frac{S_j(\infty)}{N_j}\right)\int_0^{+\infty} A_j(s)\, ds \qquad i = 1, \dots, d,$$

where $1 - S_j(\infty)/N_j$ represents the attack ratio for the group $\mathcal{P}_j$.

Since the computation of the dominant eigenvalue of the Next Generation (NG) operator is, in general, not an easy task, the calculation of the basic reproduction number R_0 for the model (1.16) is involved [23, 37]. However, when proportionate mixing is assumed, the condition (1.17) results in a separable NG operator and $R_0 = \sum_{j=1}^{d} p_j a_j \int_0^{+\infty} A_j(s)\, ds$. Furthermore, in this case, (1.18) simplifies and if $a_i > 0$, $i = 1, \dots, d$, the final size can be computed as

$$S_i(\infty) = S_i^0 \sigma^{a_i}, \qquad i = 1, \dots, d,$$

where σ solves the scalar non-linear equation

$$\log(\sigma) + \sum_{j=1}^{d} \frac{p_j}{N_j}\left(\int_0^{+\infty} \varphi_{0j}(s)\, ds + S_j^0(1 - \sigma^{a_j})\int_0^{+\infty} A_j(s)\, ds\right) = 0. \quad (1.19)$$

A straightforward extension of the results of the previous sections yields the boundedness of $\int_0^{+\infty} \varphi_i(s)\, ds$ for $i = 1, \dots, d$. Therefore, under smoothness assumptions for the given functions, we can conclude $\lim_{t \to +\infty} \varphi_i(t) = 0$, $i = 1, \dots, d$.

1.4 A COMPREHENSIVE RENEWAL EQUATION FRAMEWORK

While the previous sections focus on the analysis of specific epidemic models, here we take a broader approach and formulate a comprehensive framework that encompasses several scenarios, including the previously investigated

age-of-infection models. Consider the following $2M+1$ dimensional system of Volterra integro-differential equations

$$\begin{aligned} S_i'(t) &= -\beta_i S_i(t) V_i(t), \\ \varphi_i(t) &= \varphi_{i0}(t) + \beta_i \int_0^t A_i(t-s) S_i(s) V_i(s)\, ds, \\ P(t) &= P_0(t) + \int_0^t B(t-s) \sum_{r=1}^{M} c_r \varphi_r(s)\, ds, \end{aligned} \tag{1.20}$$

where $t \in \mathbb{R}_0^+$ and, for $i = 1, \ldots, M$,

$$V_i(t) = \textstyle\sum_{r=1}^{M} \beta_{ir} \varphi_r(t) + \alpha_i P(t).$$

Here $\varphi_{i0}(t)$, $A_i(t)$, $i = 1, \ldots, M$, $P_0(t)$ and $B(t)$ are given functions and $S_i^0 = S_i(0) > 0$ and $\alpha_i, \beta_i, c_i, \beta_{ir} \geq 0$, $i, r = 1, \ldots, M$, are given constants.

We introduce the following assumptions to facilitate a theoretical examination of the properties of the solution to (1.20) and of its numerical approximation, as well. Specifically, we assume that the known functions in (1.20) belong to $C[0, +\infty) \cap L^1[0, +\infty)$ and that:

ASSUMPTIONS A for $i = 1, \ldots, M$:

- $\alpha_i \geq 0,\ \beta_{ir} \geq 0,\ r = 1, \ldots, M,$
- $S_i^0 = S_i(0) > 0,\ \varphi_{i0}(t) \geq 0,\ A_i(t) \geq 0,\ t \geq 0,$

and

- $P_0(t) \geq 0,\ \ B(t) \geq 0,\ \ t \geq 0.$

ASSUMPTIONS B there exist positive constants $\varphi_{0,max}$, $P_{0,max}$, A_{max}, and $\bar{B}$ such that:

- $\varphi_0(t) \leq \varphi_{0,max},\ P_0(t) \leq P_{0,max},\ t \geq 0,$
- $A_i(t) \leq A_{max},\ i = 1, \ldots, M,\ t \geq 0,$
- $h \sum_{n=0}^{\infty} B(nh) \leq \bar{B},\ h > 0.$

ASSUMPTIONS C there exist positive constants $\bar{A}$, $\bar{\varphi}_0$, $\bar{P}_0$ such that for $h > 0$:

- $h \sum_{n=0}^{+\infty} A_i(nh) \leq \bar{A},\ i = 1, \ldots, M,$
- $h \sum_{n=0}^{+\infty} \varphi_{0i}(nh) \leq \bar{\varphi}_0,\ i = 1, \ldots, M,$

- $h\sum_{n=0}^{+\infty} P_0(nh) \leq \bar{P}_0$.

The third of Assumptions B and the Assumptions C imply that the functions $\varphi_{i0}(t)$, $A_i(t)$, $i = 1, \ldots, M$, $P_0(t)$ and $B(t)$ tend to 0 as $t \to +\infty$. Furthermore, these assumptions are particular instances of the condition

$$h\sum_{n=0}^{+\infty} Q(nh) \leq \bar{Q}, \qquad \text{with} \qquad Q \in L^1(\mathbb{R}_0^+), \qquad \bar{Q} > 0, \qquad h > 0,$$

which is certainly accomplished, for example, when the function $Q'(t) \in L^1(\mathbb{R}_0^+)$ (see [71]) or when $Q(t)$ is strictly non-increasing, which is often the case in realistic situations.

A thorough analysis of the qualitative properties of the continuous-time solution to (1.20) may be performed by a generalization of the theoretical findings in [19, 20, 33]. It can be proved that, under the Assumptions A,

$$S_i(t) > 0, \quad \varphi_i(t) \geq 0, \quad P(t) \geq 0, \quad \text{for all} \quad t \in \mathbb{R}_0^+, \quad i = 1, \ldots, M.$$

If in addition Assumptions B hold, then $S_i(t)$, $\varphi_i(t)$, $i = 1, \ldots, M$ and $P(t)$ are bounded from above. To investigate the asymptotic behaviour of the solution $S_i(\infty) = \lim_{t\to+\infty} S_i(t)$, we reformulate the first equation of (1.20) as follows

$$\begin{aligned}\log\left(\frac{S_i(\infty)}{S_i^0}\right) = &-\beta_i \sum_{r=1}^{M}\left(\alpha_i c_r \int_0^{+\infty}\left(\int_0^t B(t-s)\varphi_r(s)\,ds\right)dt + \beta_{ir}\int_0^{+\infty}\varphi_r(t)\,dt\right)\\ &-\beta_i\alpha_i\int_0^{+\infty} P_0(t)\,dt, \qquad i = 1, \ldots, M.\end{aligned} \tag{1.21}$$

From Dirichlet's formula (see, for instance, [28, p. 11]),

$$\int_0^{+\infty}\varphi_r(t)\,dt = \int_0^{+\infty}\varphi_{0r}(t)\,dt + \beta_i(S_r^0 - S_r(\infty))\int_0^{+\infty} A_r(t)\,dt,$$
$$\int_0^{+\infty}\left(\int_0^t B(t-s)\varphi_r(s)\,ds\right)dt = \left(\int_0^{+\infty} B(t)\,dt\right)\left(\int_0^{+\infty}\varphi_r(t)\,dt\right), \quad r = 1, \ldots, M$$

and therefore $S_i(\infty)$ satisfies the limiting algebraic system $R_i(x) = 0$, $i = 1, \dots, M$, where $R_i : \mathbb{R}^M \to \mathbb{R}$ is given by

$$R_i(x) = \log\left(\frac{S_i^0}{x_i}\right) - \beta_i \alpha_i \int_0^{+\infty} P_0(t)\, dt - \beta_i \sum_{r=1}^{M} \left(\beta_{ir} + \alpha_i c_r \int_0^{+\infty} B(t)\, dt\right) \cdot \left(S_r^0 \left(1 - \frac{x_r}{S_r^0}\right) \int_0^{+\infty} A_r(t)\, dt + \int_0^{+\infty} \varphi_{0r}(t)\, dt\right), \tag{1.22}$$

with $x = [x_1, \dots, x_M]^T$, if a solution to the system exists. Moreover, from the Assumptions B,

$$\|\varphi_i\|_{L^1(\mathbb{R}_0^+)} \leq \|\varphi_{0i}\|_{L^1(\mathbb{R}_0^+)} + \beta_i S_i^0 \|A_i\|_{L^1(\mathbb{R}_0^+)},$$

which leads to $\lim_{t\to+\infty} \varphi_i(t) = 0$, $i = 1, \dots, M$, under differentiability hypotheses for the known functions.

1.4.1 *Derivation of Age-of-infection Models*

As already pointed out, the motivation for considering system (1.20) is that it represents a general problem that includes a variety of epidemic mathematical models that, taking into account the age of infection, involve memory terms. We report some examples and demonstrate how to recover the models examined in the previous sections.

I. The unified framework (1.20) reduces to the original age-of-infection model (1.1) when

$$M = 1, \quad \alpha_1 = 0, \quad \beta_{11} = 1, \quad \beta_1 = \beta, \quad c_1 = 0, \quad B(t) = P_0(t) = 0,$$

for $t \geq 0$. The final size relation (1.6) coincides with the equation $R_1(S(\infty)) = 0$, with $R_1(x)$ defined in (1.22).

II. The age-of-infection model accounting for both symptomatic and asymptomatic infections (1.10) corresponds to the general system (1.20) with

$$M = 2, \qquad \alpha_i = 0, \qquad \beta_{ij} = 1 \qquad \beta_i = a/N, \qquad c_i = 0,$$

for $i, j \in \{1, 2\}$ and

$$\begin{aligned} &S_1(t) = S(t), \quad A_1(t) = f(t)A^s(t), \quad \varphi_1(t) = \varphi^s(t), \quad B(t) = 0, \\ &S_2(t) = S(t), \quad A_2(t) = (1 - f(t))A^a(t), \quad \varphi_2(t) = \varphi^a(t), \quad P(t) = 0, \end{aligned}$$

for $t \geq 0$. Due to these identifications, the system $R_i(S(\infty)) = 0$, $i = 1, 2$, matches the final size relation (1.13).

III. The age-of-infection model in a multi-group heterogeneous population (1.16) may be derived from (1.20) by taking

$$M = d, \quad \alpha_i = 0, \quad \beta_{ij} = \frac{p_{ij}}{N_j}, \quad \beta_i = a_i, \quad c_i = 0, \quad B(t) = P_0(t) = 0,$$

for $i, j = 1, \ldots, M$ and $t \geq 0$. Thus, (1.18) directly adheres to the algebraic system $R_i(x) = 0$, $i = 1, \ldots, M$, where $R_i(x)$ is given in (1.22).

IV. In [33] the virus shedding epidemic model is studied

$$\begin{aligned} S_i'(t) &= -\beta_i S_i(t) P(t), \\ \varphi_i(t) &= \varphi_{i0}(t) + \beta_i \int_0^t A_i(t-s) S_i(s) P(s)\, ds, \\ P(t) &= P_0(t) + \int_0^t \Gamma(t-s)(r_1\varphi_1(s) + r_2\varphi_2(s))\, ds, \end{aligned} \tag{1.23}$$

$i = 1, 2$, where $P(t)$ is the pathogen shed by infected individuals of each group at a rate r_1 and r_2, respectively. Here, β_i, $i = 1, 2$, are the contact rates, $A_1(s)$ and $A_2(s)$ are the mean infectivity of individuals in group 1 and 2 at age of infection s and $\Gamma(s)$ is the fraction of pathogen remaining s time units after having been shed by an infectious individual (see also [19, p. 168] in case of homogeneous mixing). The comprehensive framework (1.20) coincides with (1.23) when $M = 2$, $\alpha_i = 1$, $\beta_{ij} = 0$, $c_i = r_i$, $i, j = 1, 2$ and $B(t) = \Gamma(t)$, for $t \geq 0$.

Part II

DYNAMICALLY CONSISTENT NUMERICAL METHODS FOR THE AGE-OF-INFECTION MODEL

In this part of the thesis we propose two unconditionally positive numerical methods for approximating the solution to the integro-differential Kermack and McKendrick model (1). Chapter 2 presents a linearly implicit scheme based on a non-local discretization of the memory term. This method preserves positivity, monotonicity and boundedness of continuous-time solutions, as well as the final size relation for the epidemic and plays the role of a discrete epidemic model. Nevertheless, the major drawback of the non-standard approach lies in its linear convergence rate. In fact, despite its straightforward implementation due to its linearly implicit formulation, it may pose high computational costs when aiming for accurate long-term simulations. The issue of low accuracy is then addressed, for the same scalar integro-differential equation, in Chapter 3. There, the direct quadrature discretization of the model, reformulated as an exponential Volterra integral equation, results in a high order and positive numerical scheme. Remarkably, this numerical method retains the asymptotic properties of the solution and, for a fixed accuracy, it outperforms the NSFD method in terms of computational cost.

2 A NON-STANDARD FINITE DIFFERENCE SCHEME

In this chapter we propose a dynamically consistent numerical method for the scalar age-of-infection model (1). We refer to Subsection 1.1 for the notations, the assumptions and the theoretical results that are utilized throughout this chapter.

2.1 THE NON-STANDARD NUMERICAL METHOD

Consider an uniform mesh $t_n = nh$, where $n \geq 0$ and $h > 0$ is the stepsize. We define the following discretization scheme for (1.1)

$$\begin{aligned} S_{n+1} &= S_n - h\beta S_{n+1}\varphi_n \\ \varphi_{n+1} &= \varphi_0(t_{n+1}) + h\beta \sum_{j=0}^{n} A(t_{n+1-j}) S_{j+1}\varphi_j, \end{aligned} \tag{2.1}$$

where $S_0 = S(0)$, $\varphi_0 = \varphi_0(0)$ and $S_n \approx S(t_n)$, $\varphi_n \approx \varphi(t_n)$, for $n \geq 0$. Here, we have discretized the integral in (1.1) by a modified rectangular rule, which is a left approximation in $A(t)\varphi(t)$ and a right approximation in $S(t)$. For this reason, the numerical scheme (2.1) falls into the class of Non-Standard Finite Difference (NSFD) methods, originally introduced for differential equations (see [78] and references therein) and only recently extended to integral problems [64]. In the same fashion, the NSFD discretization of equation (1.3) reads

$$I_{n+1} = I_0(t_{n+1}) + \beta h \sum_{j=0}^{n} B(t_{n+1-j}) S_{j+1}\varphi_j, \qquad n = 0, 1, \ldots, \tag{2.2}$$

where $I_n \approx I(t_n)$ is the approximation of the number of infected individuals at time t_n. A pseudo-code implementation of the linearly implicit method (2.1) is presented with the Algorithm 1.

Algorithm 1 : Non-Standard Finite Difference Scheme for (1.1)

Inputs : $h, T, \beta, S_0, \varphi_0(t), I_0(t), A(t), B(t)$

Outputs : $[t_0, \ldots, t_{\bar{n}}], [S_0, \ldots, S_{\bar{n}}], [\varphi_0, \ldots, \varphi_{\bar{n}}], [I_0, \ldots, I_{\bar{n}}]$

$\bar{n} \leftarrow \lceil T/h \rceil$, $t_0 \leftarrow 0$

for $0 \leq n \leq \bar{n} - 1$ **do**

  $t_{n+1} \leftarrow (n+1)\, h$

  for $0 \leq j \leq n$ **do**

    $a_j \leftarrow A(t_{n+1} - t_j)$

    $b_j \leftarrow B(t_{n+1} - t_j)$

  $S_{n+1} \leftarrow S_n(1 + h\beta\varphi_n)^{-1}$

  $v^{n+1} \leftarrow [S_1, \ldots, S_{n+1}] \circ [\varphi_0, \ldots, \varphi_n]$ // Component-wise product

  $\varphi_{n+1} \leftarrow \varphi_0(t_{n+1}) + h\beta v^{n+1} \cdot a$

  $I_{n+1} \leftarrow I_0(t_{n+1}) + h\beta v^{n+1} \cdot b$

2.1.1 *Qualitative Properties of the Numerical Solution*

In this subsection, we investigate the numerical solution obtained using the NSFD method (2.1) and demonstrate that it exhibits qualitative properties mirroring those of the continuous solution to (1.1), regardless of the integration step-length. From now on, we make the following additional assumptions on the known functions describing problem (1.1)

$$\varphi_0(t) = A(t)(N - S_0), \qquad \text{for} \qquad t \geq 0, \tag{2.3}$$

$$A'(t) \in L^1(\mathbb{R}_0^+). \tag{2.4}$$

The following preliminary lemma is a generalization to the convergence result stated in [34, Cor. p. 208].

Lemma 2.1. *Let $A(t) \in L^1(\mathbb{R}_0^+)$ be a differentiable function satisfying (2.4). Then, for each $h \geq 0$,*

$$h \sum_{n=0}^{+\infty} A(t_{n+1}) \leq \int_0^{+\infty} A(t)dt + h\|A'\|_{L^1(\mathbb{R}_0^+)} \tag{2.5}$$

and

$$\lim_{h\to 0} h \sum_{n=0}^{+\infty} A(t_{n+1}) = \int_0^{+\infty} A(t)dt. \tag{2.6}$$

Proof. Immediately comes from [77, Lem.1]. □

The following result concerns the unconditional preservation at the discrete-time level of the properties of the continuous solution to the age-of-infection model highlighted in Subsection 1.1.

Theorem 2.2. *Let $\{S_n\}_{n\in\mathbb{N}_0}$ and $\{\varphi_n\}_{n\in\mathbb{N}_0}$ be the solutions to the discrete equations in (2.1), with $h > 0$ and non-negative initial values S_0, $\varphi_0 = \varphi_0(0)$. Then:*

- *S_n and φ_n are non-negative, for all $n \in \mathbb{N}$;*
- *the sequence $\{S_n\}_{n\in\mathbb{N}_0}$ is non-increasing;*
- *$\{S_n\}_{n\in\mathbb{N}_0}$ and $\{\varphi_n\}_{n\in\mathbb{N}_0}$ are bounded sequences,*

$$\lim_{n\to\infty} S_n = S_\infty(h) \geq 0 \qquad \text{and} \qquad \lim_{n\to\infty} \varphi_n = 0.$$

Proof. For the first two items we proceed by induction to prove that the statement $S_{n+1} \geq 0$, $\varphi_{n+1} \geq 0$ and $S_{n+1} \leq S_n$, holds for all $n \in \mathbb{N}_0$ and $h > 0$. The case $n = 0$ is true because the initial values are non-negative. Assume $n > 0$ and that the properties hold true for each $j = 1, \ldots, n-1$. Therefore, $1 + h\beta\varphi_n \geq 1$ and from (2.1) and (2.2)

$$0 \leq S_{n+1} = \frac{S_n}{1 + h\beta\varphi_n} \leq S_n,$$
$$\varphi_{n+1} = \varphi_0(t_{n+1}) + h\beta \sum_{j=0}^{n} A(t_{n+1-j}) S_{j+1} \varphi_j \geq 0$$

In order to prove the third item we observe that, for each $h > 0$, since $\{S_n\}_{n\in\mathbb{N}_0}$ is a non-negative, non-increasing sequence, then it is bounded from above by S_0 and convergent to a finite non-negative value $S_\infty(h)$. Furthermore, the second of (2.1) and assumption (2.3) on $\varphi_0(t)$, imply that $\varphi_n \leq N \cdot \sup_{t\in\mathbb{R}_0^+} A(t)$, for all $n \geq 0$, so also $\{\varphi_n\}_{n\in\mathbb{N}_0}$ is bounded by the

same constant that does depend neither on n nor on h. Again from the second of (2.1) and assumption (2.3) we have

$$h\sum_{n=0}^{+\infty}\varphi_{n+1} = (N - S_0)h\sum_{n=0}^{+\infty}A(t_{n+1}) + h\beta\sum_{j=0}^{+\infty}S_{j+1}\varphi_j h\sum_{n=0}^{+\infty}A(t_{n+1}). \tag{2.7}$$

In equation (2.7), the first of (2.1) and condition (2.5) lead to

$$h\sum_{n=0}^{+\infty}\varphi_{n+1} \leq (N - S_\infty(h))\left(\int_0^{+\infty}A(t)dt + h\|A'\|_{L^1(\mathbb{R}_0^+)}\right).$$

It is clear that for h smaller than an arbitrary $\bar{h} > 0$, it is

$$h\sum_{n=0}^{+\infty}\varphi_{n+1} \leq N\left(\int_0^{+\infty}A(t)dt + \bar{h}\|A'\|_{L^1(\mathbb{R}_0^+)}\right) < +\infty. \tag{2.8}$$

Then φ_n converges to zero, as $n \to +\infty$, for any $h > 0$, which completes the proof. □

Remark. *Analogous arguments to those presented in Theorem 2.2 establish a non-negativity result for the solution $\{I_n\}_{n\in\mathbb{N}_0}$ of the discrete equation (2.2). Furthermore, it can be demonstrated that, regardless of $h > 0$, $\lim_{n\to\infty} I_n = 0$.*

2.1.2 *Error Analysis and Convergence*

The non-local integration rule in (2.1), based on a combination of explicit and implicit integrand approximations, is designed to unconditionally preserve the qualitative properties of the continuous solution. However, owing to this non-standard approach, the analysis of the approximation error is not straightforward. Here we refer, when needed, to the equivalent compact notations for the continuous problem (1.1) and the numerical method (2.1), respectively,

$$\begin{bmatrix} S(t) \\ \varphi(t) \end{bmatrix} = \begin{bmatrix} S_0 \\ \varphi_0(t) \end{bmatrix} + \beta\int_0^t \begin{bmatrix} -1 & 0 \\ 0 & A(t-s) \end{bmatrix}\begin{bmatrix} S(s)\varphi(s) \\ S(s)\varphi(s) \end{bmatrix} ds,$$

and

$$\begin{bmatrix} S_{n+1} \\ \varphi_{n+1} \end{bmatrix} = \begin{bmatrix} S_0 \\ \varphi_0(t_{n+1}) \end{bmatrix} + h\beta \sum_{j=0}^{n} \begin{bmatrix} -1 & 0 \\ 0 & A(t_{n+1}-t_j) \end{bmatrix} \begin{bmatrix} S_{j+1}\varphi_j \\ S_{j+1}\varphi_j \end{bmatrix}, \tag{2.9}$$

for $n = 0, 1, \ldots$. The local truncation error of the NSFD scheme (2.9) then reads

$$\begin{aligned} \delta(h; t_n) = &\int_0^{t_n} \begin{bmatrix} -1 & 0 \\ 0 & A(t_n - s) \end{bmatrix} \begin{bmatrix} S(s)\varphi(s) \\ S(s)\varphi(s) \end{bmatrix} ds \\ &-h \sum_{j=0}^{n-1} \begin{bmatrix} -1 & 0 \\ 0 & A(t_n - t_j) \end{bmatrix} \begin{bmatrix} S(t_{j+1})\varphi(t_j) \\ S(t_{j+1})\varphi(t_j) \end{bmatrix}, \qquad n = 0, 1, \ldots. \end{aligned} \tag{2.10}$$

Lemma 2.3. *Assume that the given function $A(t)$, describing problem (1.1), is continuously differentiable on an interval $[0, T]$, with $T < +\infty$. Then the method (2.1) is consistent with (1.1), of order 1.*

Proof. The assumption on $A(t)$ implies that also $S(t)$ and $\varphi(t)$ are continuously differentiable on $[0, T]$. Let $h = T/\bar{n}$, with $\bar{n}$ positive integer. Because of the convergence properties of rectangular quadrature rule (see for example [34]), for each $j = 0, \ldots, \bar{n} - 1$ it is

$$\left\| \int_{t_j}^{t_{j+1}} \begin{bmatrix} -S(s+h)\varphi(s) \\ A(t_n - s)S(s+h)\varphi(s) \end{bmatrix} ds - h \begin{bmatrix} -S(t_{j+1})\varphi(t_j) \\ A(t_{n-j})S(t_{j+1})\varphi(t_j) \end{bmatrix} \right\| \leq ch^2, \tag{2.11}$$

where the constant $c > 0$ does not depend on h. For $0 < n < \bar{n}$, by simple manipulations and the mean value theorem (see, for instance [61, Sec. 1.3]), we write the integral in (2.10) as

$$\begin{aligned} &\sum_{j=0}^{n-1} \int_{t_j}^{t_{j+1}} \begin{bmatrix} -S(s)\varphi(s) \\ A(t_n - s)S(s)\varphi(s) \end{bmatrix} ds \\ &= \sum_{j=0}^{n-1} \int_{t_j}^{t_{j+1}} \left(\begin{bmatrix} -S(s+h)\varphi(s) \\ A(t_n - s)S(s+h)\varphi(s) \end{bmatrix} - h \begin{bmatrix} -S'(s+\theta_j h)\varphi(s) \\ A(t_n - s)S'(s+\theta_j h)\varphi(s) \end{bmatrix} \right) ds, \end{aligned}$$

with $\theta_j \in (0,1)$, for $j = 0, \ldots, n-1$. Therefore, given (2.11), the local truncation error (2.10) satisfies

$$\|\delta(h;t_n)\| \leq c\bar{n}h^2 + h\int_0^T \left\| \begin{bmatrix} -S'(s+\theta_j h)\varphi(s) \\ A(t_n-s)S'(s+\theta_j h)\varphi(s) \end{bmatrix} \right\| ds,$$

$n = 0, \ldots, \bar{n}$ and the regularity properties of the functions involved lead to

$$\max_{0\leq n\leq \bar{n}} \|\delta(h;t_n)\| \leq Ch.$$

Thus, the positive constant C depends on the bounds in $[0,T]$ for the functions and derivatives involved, as well as on T, but not on h. □

Denote by $e(h;t_n) = \begin{bmatrix} S(t_n) \\ \varphi(t_n) \end{bmatrix} - \begin{bmatrix} S_n \\ \varphi_n \end{bmatrix}$ the global error of the discretization (2.9). The following theorem provides sufficient conditions for the convergence of the numerical method.

Theorem 2.4. *Assume that the given function $A(t)$, describing problem (1.1), is continuously differentiable on an interval $[0,T]$, and that $h = T/\bar{n}$, with $\bar{n} \in \mathbb{N}$. Let $\{S_n\}_{0\leq n\leq \bar{n}}$, $\{\varphi_n\}_{0\leq n\leq \bar{n}}$ be the approximations to (1.1), defined by (2.1). Then*

$$\lim_{h\to 0} \max_{0\leq n\leq \bar{n}} \|e(h;t_n)\| = 0.$$

Furthermore, the order of convergence is 1.

Proof. The smoothness of the kernel function and the boundedness of both the continuous and numerical solutions lead to

$$\begin{aligned} \|e(h;t_n)\| &\leq \|\delta(h;t_n)\| + h\beta \left\| \sum_{j=0}^{n-1} \begin{bmatrix} -1 & 0 \\ 0 & A(t_{n+1}-t_j) \end{bmatrix} \begin{bmatrix} S(t_{j+1})\varphi(t_j) - S_{j+1}\varphi_j \\ S(t_{j+1})\varphi(t_j) - S_{j+1}\varphi_j \end{bmatrix} \right\| \\ &\leq \|\delta(h;t_n)\| + h\beta\tilde{c} \sum_{j=0}^{n-1} (\|e(h;t_{j+1})\| + \|e(h;t_j)\|), \qquad n = 0, \ldots, \bar{n}, \end{aligned}$$

with $\tilde{c} > 0$ not depending on h. For a sufficiently small h, the Gronwall discrete inequality (see, for example, [63, p. 101]) yields

$$\begin{aligned}\|e(h;t_n)\| &\leq \frac{\|\delta(h;t_n)\|}{1-h\beta\tilde{c}} + h\frac{2\beta\tilde{c}}{1-h\beta\tilde{c}}\sum_{j=0}^{n-1}\|e(h;t_j)\| \\ &\leq \left(\frac{\max_{0\leq n\leq \bar{n}}\|\delta(h;t_n)\|}{1-h\beta\tilde{c}}\right)\exp\left(\frac{2\beta\tilde{c}T}{1-h\beta\tilde{c}}\right), \qquad n=0,\dots,\bar{n},\end{aligned}$$

which, in conjunction with the outcome from Lemma (2.3), concludes the proof. □

Remark. *The numerical solution computed by* (2.1) *contributes to the approximation of the number of infected individuals, as outlined in* (2.2)*. Proceeding as in the proof of Theorem* 2.4 *and under its assumptions, one may prove that*

$$\lim_{h\to 0}\max_{0\leq n\leq \bar{n}}\|I(t_n)-I_n\| = 0.$$

2.2 DISCRETE ASYMPTOTIC DYNAMICS

In this section, our focus will be on the possibility of replicating the asymptotic dynamics of the continuous model (1.1) with the numerical method (2.1). In this perspective, establishing the boundedness of the local error $\delta(h;t_n)$, as defined in (2.10), for all $n \in \mathbb{N}$ and its convergence to zero as $h \to 0$, becomes pivotal. Stated differently, a theoretical result is required to extend the established consistency over a finite interval, as outlined in Lemma 2.3, to an integration over $[0,+\infty)$.

Here, we make the assumption (2.4) on $A(t)$, which consequently assures sufficient regularity for the solution to (1.1). Furthermore, in this context, the results of Lemma 2.1 and (2.5) hold true.

Theorem 2.5. *Assume that the given function $A(t)$, describing problem* (1.1)*, is continuously differentiable on $\mathbb{R}_0^+$. Then the scheme* (2.1)*, is consistent with* (1.1) *on $\mathbb{R}_0^+$.*

Proof. Since $\int_{t_{j-1}}^{t_j} S(t_{j+1})\varphi(t_j)\,ds = h\,S(t_{j+1})\varphi(t_j)$, for each $j \geq 1$, it follows

$$\int_{t_{j-1}}^{t_j} \begin{bmatrix} -S(s+h)\varphi(s) \\ A(t_n-s)S(s+h)\varphi(s) \end{bmatrix} ds - h \begin{bmatrix} -S(t_{j+1})\varphi(t_j) \\ A(t_n-t_j)S(t_{j+1})\varphi(t_j) \end{bmatrix}$$
$$= -\int_{t_{j-1}}^{t_j} \int_s^{t_j} \frac{d}{d\tau} \begin{bmatrix} -S(\tau+h)\varphi(\tau) \\ A(t_n-\tau)S(\tau+h)\varphi(\tau) \end{bmatrix} d\tau\, ds.$$

Thus, for $n \in \mathbb{N}$,

$$\left\| \int_0^{t_n} \begin{bmatrix} -S(s+h)\varphi(s) \\ A(t_n-s)S(s+h)\varphi(s) \end{bmatrix} ds - h \sum_{j=0}^{n-1} \begin{bmatrix} -S(t_{j+1})\varphi(t_j) \\ A(t_n-t_j)S(t_{j+1})\varphi(t_j) \end{bmatrix} \right\|$$
$$\leq h \int_0^{+\infty} \left\| \frac{d}{d\tau} \begin{bmatrix} -S(\tau+h)\varphi(\tau) \\ A(t_n-\tau)S(\tau+h)\varphi(\tau) \end{bmatrix} \right\| d\tau$$
$$+ h \left\| \begin{bmatrix} -S(t_{n+1})\varphi(t_n) + S(h)\varphi(0) \\ A(0)S(t_{n+1})\varphi(t_n) - A(t_n)S(h)\varphi(0) \end{bmatrix} \right\| \leq \bar{c}h,$$

where the constant $\bar{c} > 0$ does not depend on n and h, since, due to the assumption (2.4) on $A'(t)$, it is $S'(t)$, $\varphi'(t) \in L^1[0,+\infty)$, and $\varphi(t)$ bounded. Then, for the local error defined in (2.10), proceeding as in the proof of Lemma 2.3, we have

$$\sup_{n\geq 0} \|\delta(h;t_n)\| \leq h \left(\bar{c} + \sup_{n\geq 0} \int_0^{t_n} \left\| \begin{bmatrix} S'(s+\theta_n h)\varphi(s) \\ A(t_n-s)S'(s+\theta_n h)\varphi(s) \end{bmatrix} \right\| ds \right),$$

with $\theta_n \in (0,1)$, for all $n = 0, 1, \ldots$. Since, $S'(t) \in L^1[0,+\infty)$, $A(t)$ and $\varphi(t)$ are non-negative and bounded, the proof is completed. □

We define the numerical basic reproduction number

$$R_0(h) = h\beta N \sum_{n=0}^{+\infty} A(t_{n+1}), \tag{2.12}$$

corresponding to the discretization of (1.4). Thus, $R_0(h) = R_0 - \beta N \tau(h)$, where the error

$$\tau(h) = \int_0^{+\infty} A(t)dt - h \sum_{n=0}^{+\infty} A(t_{n+1}), \tag{2.13}$$

tends to zero as h vanishes, accordingly to (2.6). In compliance with the definition of R_0, the discrete reproduction number serves as a threshold parameter within the numerical model. As a matter of fact, the direct discretization of equation (1)

$$\frac{S_{n+1} - S_n}{h} = h\beta S_{n+1} \sum_{j=0}^{\infty} A(t_{j+1}) \frac{S_{n-j} - S_{n-j-1}}{h}, \tag{2.14}$$

is equivalent to (2.1), with $\varphi_n = -h \sum_{j=0}^{+\infty} A(t_{j+1}) \frac{S_{n-j} - S_{n-j-1}}{h}$, and

$$\varphi_0(t_{n+1}) = -h \sum_{j=n}^{+\infty} A(t_{j+1}) \frac{S_{n-j} - S_{n-j-1}}{h}. \tag{2.15}$$

The assumption that all initial infectives have infection age zero at the disease outbreak implies that, at time $t > 0$, no member of the population can have infection age $s > t$. It follows that, since for $n < 0$, $S_n = S(t_n) = N$, the right-hand-side of (2.15) gives back expression (2.3) for $\varphi_0(t_{n+1})$.

Here, we establish a discrete analogue of the *invasion criterion* as introduced in Subsection 1.1. We examine the scenario where the solution to (2.1) exhibits initial exponential growth characterized by $(1 + rh)^n$, in cases where $r > 0$. If we assume that, initially, $S_n \approx N$, the linearization of (2.14) is

$$\frac{S_{n+1} - S_n}{h} = h\beta N \sum_{j=0}^{\infty} A(t_{j+1}) \frac{S_{n-j} - S_{n-j-1}}{h}, \tag{2.16}$$

which has an exponential solution $S_n = (1 + rh)^n$, if

$$1 = h\beta N \sum_{n=0}^{+\infty} A(t_{n+1})(1 + rh)^{-(n+1)}, \tag{2.17}$$

holds true. Furthermore, (2.12) and (2.17) give

$$R_0(h) = \frac{h\sum_{n=0}^{+\infty} A(t_{n+1})}{h\sum_{n=0}^{+\infty} A(t_{n+1})(1+rh)^{-(n+1)}},$$

which is the discrete equivalent to (1.5) and for which $r > 0$ if and only if $R_0(h) > 1$. The role of $R_0(h)$ in depicting the discrete dynamic closely aligns with that of R_0 concerning the disease outbreak. Moreover, the fact that $R_0(h) = R_0 - \beta N \tau(h)$, with $\tau(h) \overset{h\to 0}{\longrightarrow} 0$, and

$$\lim_{h\to 0} R_0(h) = R_0,$$

implies that the NSFD discrete scheme (2.1) retrieves the continuous dynamic when h vanishes.

As highlighted in Section 2.1.1, since $\{S_n\}_{n\in\mathbb{N}_0}$ is a non-negative and monotonically non-increasing sequence regardless of $h > 0$, it converges to a non-negative limit denoted as $S_\infty(h) = \lim_{n\to+\infty} S_n$. Thus, the positiveness of $S_\infty(h)$ is guaranteed for any fixed value of the stepsize $h > 0$. This value is henceforth referred to as the *numerical* or *discrete final size*. From the first of (2.1) it is clear that independently of $h > 0$,

$$S_\infty(h) = \frac{S_0}{\prod_{n=0}^{\infty}(1+h\beta\varphi_n)}, \tag{2.18}$$

thus implying the following relation for the discrete final size of the epidemic

$$\log\left(\frac{S_0}{S_\infty(h)}\right) = \sum_{n=0}^{\infty} \log\left(1+h\beta\varphi_n\right). \tag{2.19}$$

The series at the right-hand side of (2.19) converges if and only if $h\beta\sum_{n=0}^{\infty}\varphi_n$ is finite. This is true because of (2.8). The following result shows how to express this series in terms of the numerical basic reproduction number (2.12).

Theorem 2.6. *Let $\{S_n\}_{n\in\mathbb{N}_0}, \{\varphi_n\}_{n\in\mathbb{N}_0}$ be the numerical solution to (1.1), obtained by the discrete scheme (2.1), and $S_\infty(h)$ be defined in (2.18). Then, for each $h > 0$, it holds:*

$$h\beta \sum_{n=0}^{\infty} \varphi_{n+1} = (N - S_\infty(h))h\beta \sum_{n=0}^{+\infty} A(t_{n+1}) = R_0(h)\left(1 - \frac{S_\infty(h)}{N}\right). \tag{2.20}$$

Proof. From (2.7) and the first of (2.1) it is

$$h\beta \sum_{n=0}^{+\infty} \varphi_{n+1} = \beta(N - S_0)h \sum_{n=0}^{+\infty} A(t_{n+1}) - \beta(S_\infty(h) - S_0)h \sum_{n=0}^{+\infty} A(t_{n+1}).$$

Thus

$$h\beta \sum_{n=0}^{+\infty} \varphi_{n+1} = \beta(N - S_\infty(h))h \sum_{n=0}^{+\infty} A(t_{n+1}). \tag{2.21}$$

The result then comes from the definition of $R_0(h)$ in (2.12). □

From (2.19) and (2.20), we have

$$\log\left(\frac{S_0}{S_\infty(h)}\right) = U(h)R_0(h)\left(1 - \frac{S_\infty(h)}{N}\right) + \mathcal{O}(h),$$

which, under the assumption (2.3), is the discrete equivalent to the final size relation (1.7), for any $h > 0$. The equivalence is more evident as $h \to 0$, since the spurious term

$$U(h) = \frac{\sum_{n=0}^{\infty} \log(1 + h\beta\varphi_n)}{h\beta \sum_{n=0}^{\infty} \varphi_n},$$

tends to 1, as shown in the next theorem.

Theorem 2.7. *Consider the solution $\{\varphi_n\}_{n\in\mathbb{N}_0}$ to the discrete equation (2.1), obtained by a fixed stepsize $h > 0$, and define*

$$u_n(h) = \frac{\log(1 + h\beta\varphi_n)}{h\beta\varphi_n}, \qquad n \in \mathbb{N}_0. \tag{2.22}$$

Then

- $\lim_{h\to 0} u_n(h) = 1$, *uniformly with respect to* n;
- $\lim\limits_{h\to 0} \sum_{n=0}^{\infty} (\log(1+h\beta\varphi_n) - h\beta\varphi_n) = 0$.

Proof. From Theorem 2.2, the sequence $\{\varphi_n\}_{n\in\mathbb{N}_0}$ is bounded by a constant $\bar{\varphi}$, that does not depend on h. Consider $h < (\beta\bar{\varphi})^{-1}$, by Taylor expansion in (2.22) it is $u_n(h) = \sum_{j=0}^{\infty} \frac{(-1)^j (h\beta\varphi_n)^j}{j+1}$ and

$$|u_n(h) - 1| \leq \sum_{j=1}^{\infty} (h\beta\varphi_n)^j \leq \sum_{j=1}^{\infty} (h\beta\bar{\varphi})^j = \frac{h\beta\bar{\varphi}}{1-h\beta\bar{\varphi}}, \qquad n \in \mathbb{N}_0.$$

Since the last term in the previous inequality vanishes as h goes to 0, it follows that

$$\forall \varepsilon > 0, \quad \exists h_\varepsilon > 0 \ : \quad \left(h < h_\varepsilon \quad \Longrightarrow \quad \frac{h\beta\bar{\varphi}}{1-h\beta\bar{\varphi}} < \varepsilon \right).$$

Hence, if $\varepsilon > 0$ is fixed, the choice for $h < \min\left\{h_\varepsilon, (\beta\bar{\varphi})^{-1}\right\}$ leads to $|u_n(h) - 1| < \varepsilon$, $\forall n \in \mathbb{N}_0$. This proves the first part of the theorem.
So, for $h < \bar{h}_\varepsilon$ and $n \in \mathbb{N}$, it is $1 - \varepsilon < u_n(h) < 1 + \varepsilon$ and, since

$$\sum_{n=0}^{\infty} \log(1+h\beta\varphi_n) = h\beta \sum_{n=0}^{\infty} \varphi_n u_n(h),$$

with $h\beta \sum_{n=0}^{\infty} \varphi_n < \infty$, as proved in (2.8), we can state that

$$(1-\varepsilon)h\beta \sum_{n=0}^{\infty} \varphi_n < h\beta \sum_{n=0}^{\infty} \varphi_n u_n(h) = \sum_{n=0}^{\infty} \log(1+h\beta\varphi_n) < (1+\varepsilon)h\beta \sum_{n=0}^{\infty} \varphi_n.$$

Therefore

$$\lim_{h\to 0} \left(\frac{\sum_{n=0}^{\infty} \log(1+h\beta\varphi_n)}{h\beta \sum_{n=0}^{\infty} \varphi_n} \right) = 1,$$

which completes the proof since, from (2.8), the denominator is bounded.

□

As $h \to 0$, we expect to recover the continuous dynamic. We prove the following theorem.

Theorem 2.8. *Let $\{S_n\}_{n\in\mathbb{N}_0}, \{\varphi_n\}_{n\in\mathbb{N}_0}$ be the numerical solution to (1.1), obtained by the discrete scheme (2.1), and $S_\infty(h)$ be defined in (2.18). It holds:*

$$\lim_{h\to 0}\left(\log\frac{S_0}{S_\infty(h)} - h\beta(N - S_\infty(h))\sum_{n=0}^{\infty} A(t_{n+1})\right) = 0.$$

Proof. We use (2.19) and simple algebraic manipulations, to obtain

$$\log\left(\frac{S_0}{S_\infty(h)}\right) - h\beta(N - S_\infty(h))\sum_{n=0}^{\infty} A(t_{n+1}) =$$
$$\left(\sum_{n=0}^{\infty}\log(1 + h\beta\varphi_n) - h\beta\sum_{n=0}^{\infty}\varphi_n\right) + \left(h\beta\sum_{n=0}^{\infty}\varphi_n - h\beta(N - S_\infty(h))\sum_{n=0}^{\infty} A(t_{n+1})\right).$$

The statement is proved by taking the limit for $h \to 0$ of both terms and by using the result of Theorem 2.7 and (2.21). □

Remark. *Assume that there exists $\lim_{h\to 0} S_\infty(h) = S_\infty^* > 0$. For $h \to 0$, $S(\infty)$ and S_∞^* satisfy the same final size relation (1.7), which (see [16] or [20]) has a unique solution in $[0, S_0]$. It follows that $S(\infty) = S_\infty^*$, thus implying that the dynamic of the continuous model (1.1) is preserved by the numerical one (2.1), as $h \to 0$.*

The theoretical insights presented in this chapter provide evidence that the NSFD scheme (2.1) can be considered also as a discrete-time epidemic model, regardless of its association with the continuous-time age-of-infection model (1.1). Therefore, from a distinct perspective, it may serve as an ideal framework for conducting data-driven analyses of infectious disease outbreaks (we refer to [21, 40] for further details on discrete-time modeling).

2.3 NUMERICAL EXPERIMENTS

Aiming to experimentally corroborate the theoretical outcomes of the previous sections, we present some numerical examples. For our experiments we choose illustrative test equations of the form (1.1) and we use the non-standard numerical method detailed in (2.1).

Our first simulation addresses the problem (1.1) for $t \in [0,1]$, with

$$A(t) = \frac{1}{(1+t)^2}, \quad B(t) = \frac{5}{(2+2t)^2}, \quad N = 10, \quad S_0 = 9, \quad \beta = 0.3, \qquad (2.23)$$

$I_0(t) = (N - S_0)B(t)$ and $\varphi_0(t)$ given by (2.3). Table 1 and Figure 3 report the absolute errors $E(h)$ and the experimental order of convergence $\hat{p} = \log_{10}(E(h)/E(0.1h))$ related to the approximations of $S(t)$, $\varphi(t)$, and $I(t)$ computed by (2.1) and (2.2), respectively. In compliance with the results of Theorem 2.4, the reduction of numerical errors as function of the stepsize confirms the expected linear convergence. Here, we have used the numerical solution computed with stepsize $h = 10^{-6}$ as reference solution.

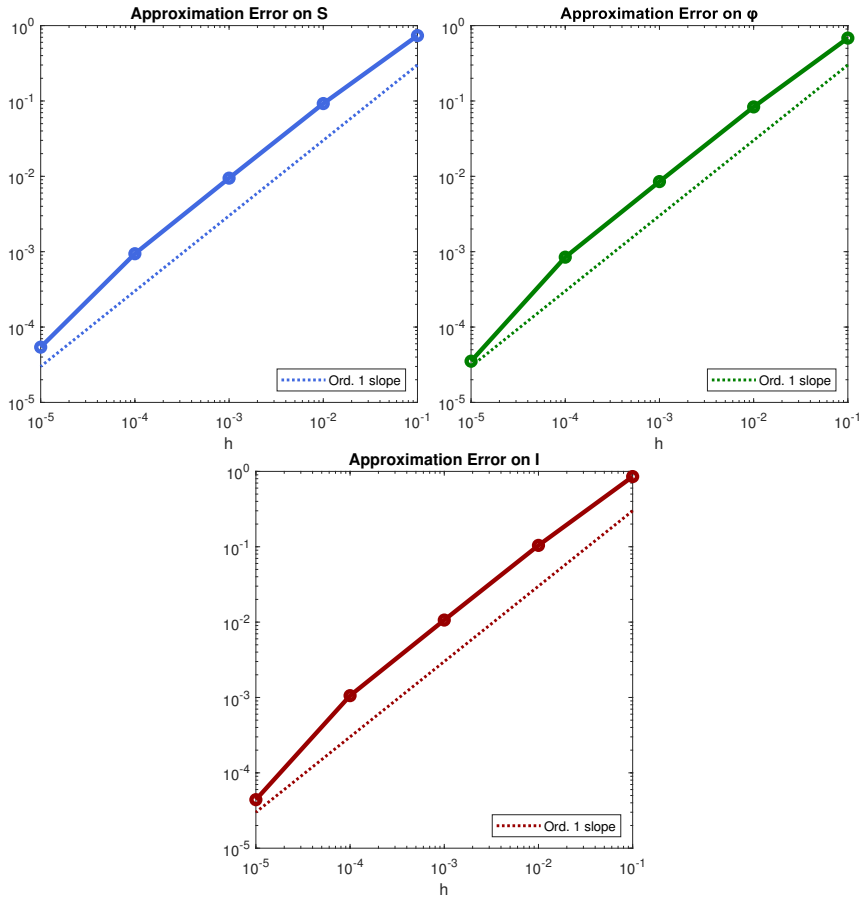

Figure 3: Logarithmic scale plot of the approximation errors and experimental convergence of the NSFD method (2.1).

	APPROXIMATION ERRORS			EXP. ORDER OF CONVERGENCE		
h	Err. on S	Err. on φ	Err. on I	Ord. on S	Ord. on φ	Ord. on I
10^{-1}	$7.37 \cdot 10^{-1}$	$6.83 \cdot 10^{-1}$	$8.53 \cdot 10^{-1}$	\\	\\	\\
10^{-2}	$9.24 \cdot 10^{-2}$	$8.34 \cdot 10^{-2}$	$1.04 \cdot 10^{-1}$	0.90	0.91	0.91
10^{-3}	$9.46 \cdot 10^{-3}$	$8.52 \cdot 10^{-3}$	$1.06 \cdot 10^{-2}$	0.99	0.99	0.99
10^{-4}	$9.40 \cdot 10^{-4}$	$8.46 \cdot 10^{-4}$	$1.06 \cdot 10^{-3}$	1.00	1.00	1.00

Table 1: Approximation errors and experimental rate of convergence for the NSFD method (2.1).

In order to examine the long time behaviour of the numerical solution, we consider problem (1.1), with a Gaussian distribution for the infectivity function. More specifically, we take

$$A(t) = \frac{1}{\sigma\sqrt{2\pi}} e^{-\frac{(t-\mu)^2}{2\sigma^2}}, \quad N = 10^5, \quad S_0 = 99950, \quad \mu = 0.2, \quad \sigma = 2\mu, \tag{2.24}$$

$\beta = 3 \cdot 10^{-5}$ and $\varphi_0(t)$ given by (2.3). In Figure 4 the behaviour of the numerical solution is reported for $h = 10^{-3}$. Notably, an epidemic outbreak is evident accordingly to the value of the numerical basic reproduction number $R_0(h) \approx 1.29$, derived from equation (2.12). By running the code on a sufficiently large interval, we obtain the values reported in Table 2 for $S_\infty(h)$ and $\varphi_\infty(h) = \lim_{n\to+\infty} \varphi_n$. These outcomes align with the value $S_\infty = 1.8389 \cdot 10^4$, achieved through iterative resolution of the non-linear final size relation (1.7).

	LONG TIME BEHAVIOUR	
h	$S_\infty(h)$	$\varphi_\infty(h)$
10^{-1}	$2.3211 \cdot 10^4$	$6.8092 \cdot 10^{-7}$
10^{-2}	$1.8852 \cdot 10^4$	$2.1778 \cdot 10^{-9}$
10^{-3}	$1.8435 \cdot 10^4$	$1.1588 \cdot 10^{-9}$

Table 2: Long time behaviour of the NSFD numerical solution to problem (1.1)-(2.24).

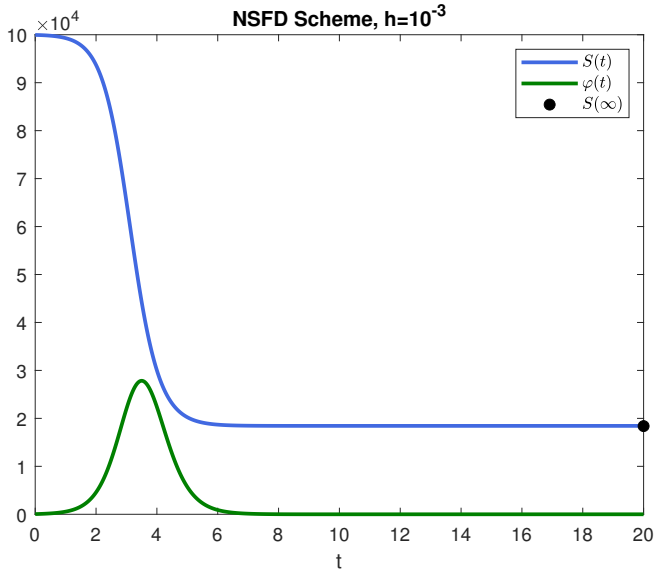

Figure 4: Long time behaviour of the NSFD solution to problem (1.1)-(2.24).

In our last example we assess the effectiveness of the NSFD scheme (2.1) by comparing it to the direct quadrature Trapezoidal method's performance. We integrate problem (1.1)-(2.24) with $\beta = 5.8 \cdot 10^{-5}$, and using a relatively large stepsize $h = 0.25$. It is evident from Figure 5 that, despite the higher order of convergence, the Trapezoidal Direct Quadrature method fails to preserve the positivity and monotonicity of the solution.

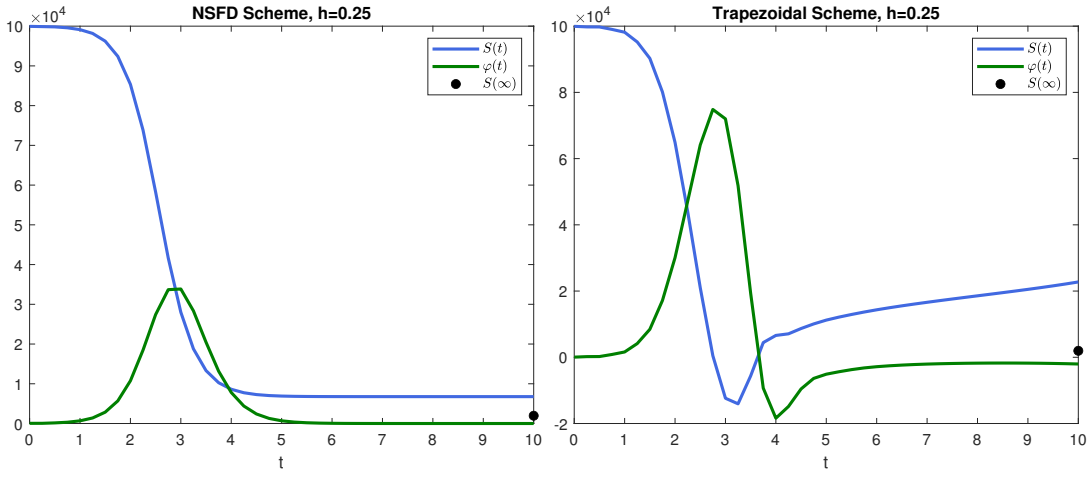

Figure 5: Comparison of the NSFD method and the composite trapezoidal discretization for the problem (1.1)-(2.24) with $\beta = 5.8 \cdot 10^{-5}$.

3 UNCONDITIONALLY POSITIVE AND HIGH ORDER DQ SCHEME

In Chapter 2, we employed a non-standard discretization technique to numerically integrate problem (1). The linearly implicit method there presented is computationally efficient and suitable for a straightforward implementation. Its primary strength lies in the unconditional preservation of the essential features of the continuous model. As a matter of fact, the numerical solution generated by the NSFD scheme exhibits positivity, boundedness and monotonicity properties for any positive value of h. Moreover, the scheme provides a reliable approximation of the asymptotic dynamic and can be interpreted as a discrete-time epidemic model. Nevertheless, the drawback of the non-standard approach arises from its limited accuracy due to its linear convergence, resulting in a computationally demanding algorithm for long-time simulations. Consequently, our primary objective is to devise a higher-order dynamically consistent numerical method that addresses this limitation.

When considering numerical solutions derived from direct discretizations of equations (1) or (1.1), establishing the same unconditional preservation properties of the NSFD scheme is not trivial. These complexities have motivated us to pursue an alternative methodology, built upon an exponential reformulation of the original model. Our starting point is the integro-differential equation (1) under the assumption (2.3). Taking advantage of the positivity of $S(t)$ and of the identity

$$\int_0^\tau A(s)\,\frac{dS}{d\tau}(\tau - s)\,ds = \frac{d}{d\tau}\left(\int_0^\tau A(s)S(\tau - s)\,ds\right) - A(\tau)S_0,$$

we reformulate the equation (1) as follows

$$\frac{S'(\tau)}{S(\tau)} = \beta\left(-\left((N - S_0)A(\tau) + A(\tau)S_0\right) + \frac{d}{d\tau}\left(\int_0^\tau A(s)S(\tau - s)\,ds\right)\right).$$

Then, the integration for $\tau \in [0, t]$ leads to the expression

$$S(t) = S_0 \exp\left(-\beta \int_0^t A(t-s)\,(N - S(s))\; ds\right). \tag{3.1}$$

The implicit Volterra integral equation (3.1) is mathematically equivalent to the age-of-infection model (1) and to (1.1). However, from a numerical perspective, the formulation (3.1) is more advantageous. In fact, the presence of a positive continuous-time exponential operator in the right-hand side of (3.1) constitutes a significant benefit, as its direct discretization results in a positive numerical method.

In this chapter, we discretize equation (3.1) using Direct Quadrature (DQ) methods with Gregory convolution weights, achieving a high order of convergence while retaining the dynamical consistency of the non-standard approach (2.1). In order to do that, we preliminarily provide further insights on integral approximation by Gregory quadrature rules.

3.1 GREGORY QUADRATURE RULES

Consider a uniform mesh $\{t_n\}_{n\in\mathbb{N}_0}$ with $t_n = t_0 + nh$ and $h > 0$. In order to define a discretization to (3.1), let $\{w_{nj}\}$ be the weights associated with the quadrature formula

$$\int_0^{t_n} f(t)\; dt \approx h \sum_{j=0}^{n} w_{nj} f(t_j), \qquad\qquad n \geq n_0 \geq 1.$$

Here, we consider the weights obtained by the $(n_0 - 1)$-th Gregory quadrature rule with $n_0 \geq 1$ quadrature points

$$h\left(\frac{1}{2}f(t_0) + \sum_{j=1}^{n-1} f(t_j) + \frac{1}{2}f(t_n)\right) - h\sum_{i=1}^{n_0-1} c_i \left(\nabla^i f(t_n) + (-\Delta^i) f(t_0)\right), \tag{3.2}$$

where $\Delta f(t) = f(t+h) - f(t)$ and $\nabla f(t) = f(t) - f(t-h)$ denote the forward and the backward difference operators, respectively. When $n_0 = 1$, the

Gregory rule (3.2) reduces to a composite trapezoidal rule, for which the quadrature weights read

$$w_{n0} = w_{nn} = \frac{1}{2}, \qquad w_{nj} = 1, \qquad j = 1, \dots, n-1. \tag{3.3}$$

For $n_0 > 1$, the general $(n_0 - 1)$-th Gregory rule is obtained by adding some corrective terms to the composite trapezoidal rule. These terms are weighted through the coefficients

$$c_i = \sum_{j=1}^{\lfloor (i+1)/2 \rfloor} (-1)^{i-2j+1} \frac{B_{2j} S_i^{(2j-1)}}{(2j)! \prod_{l=2j}^{i} l}, \qquad i = 1, \dots, n_0 - 1,$$

where B_i and $S_j^{(i)}$ are the Bernoulli and first kind Stirling numbers, respectively, defined by

$$\frac{x}{e^x - 1} =: \sum_{j=0}^{+\infty} B_j \frac{x^j}{j!}, \qquad \frac{\log^i(1+x)}{i!} =: \sum_{j=1}^{+\infty} S_j^{(i)} \frac{x^j}{j!}.$$

The Gregory weights are non-negative and exhibit a convolution structure (see, for instance, [97, 98]), i.e. $w_{nk} = \omega_{n-k}$, for $n \geq k$ and $k \geq n_0$. Furthermore (see, for example, [28, Thm. 2.6.10, p. 79]),

$$\sup_{n \geq 0} \max_{0 \leq j < n_0} w_{nj} \leq W < +\infty \qquad \text{and} \qquad \sup_{n \geq 0} \omega_n \leq \Omega < +\infty. \tag{3.4}$$

To represent the weights of Gregory methods with $n_0 > 1$, we define, for $n \geq n_0$, the matrix $\Sigma_{n_0,n} \in \mathbb{R}^{(n-n_0+1) \times n_0}$ and the semi-circulant matrix $\Omega_{n_0,n} \in \mathbb{R}^{(n-n_0+1) \times (n-n_0+1)}$ as follows

$$\Sigma_{n_0,n} = \begin{bmatrix} w_{n_0,0} & \dots & w_{n_0,n_0-1} \\ w_{n_0+1,0} & \dots & w_{n_0+1,n_0-1} \\ w_{n_0+2,0} & \dots & w_{n_0+2,n_0-1} \\ \vdots & & \vdots \\ w_{n,0} & \dots & w_{n,n_0-1} \end{bmatrix}, \quad \Omega_{n_0,n} = \begin{bmatrix} \omega_0 & & & & \\ \omega_1 & \omega_0 & & & \\ \omega_2 & \omega_1 & \omega_0 & & \\ \vdots & & \ddots & \ddots & \\ \omega_{n-n_0} & \dots & \dots & \omega_1 & \omega_0 \end{bmatrix}.$$

In the cases of the first ($n_0 = 2$) and second ($n_0 = 3$) Gregory rules, the explicit form of the matrices $\Sigma_{n_0,n}$ and $\Omega_{n_0,n}$ is reported below.

$$\Sigma_{2,n} = \frac{1}{12}\begin{bmatrix} 5 & 14 \\ 5 & 13 \\ \vdots & \vdots \\ 5 & 13 \end{bmatrix}, \qquad \Omega_{2,n} = \frac{1}{12}\begin{bmatrix} 5 & & & & & \\ 13 & 5 & & & & \\ 12 & 13 & 5 & & & \\ 12 & 12 & 13 & 5 & & \\ \vdots & & \ddots & \ddots & \ddots & \\ 12 & \dots & 12 & 12 & 13 & 5 \end{bmatrix}.$$

$$\Sigma_{3,n} = \frac{1}{24}\begin{bmatrix} 9 & 27 & 27 \\ 9 & 28 & 22 \\ 9 & 28 & 23 \\ \vdots & \vdots & \vdots \\ 9 & 28 & 23 \end{bmatrix}, \qquad \Omega_{3,n} = \frac{1}{24}\begin{bmatrix} 9 & & & & & & \\ 28 & 9 & & & & & \\ 23 & 28 & 9 & & & & \\ 24 & 23 & 28 & 9 & & & \\ 24 & 24 & 23 & 28 & 9 & & \\ \vdots & & \ddots & \ddots & \ddots & \ddots & \\ 24 & \dots & 24 & 24 & 23 & 28 & 9 \end{bmatrix}.$$

3.2 THE DIRECT-QUADRATURE METHOD

Consider a uniform mesh $\{t_n\}_{n\in\mathbb{N}_0}$ with $t_n = nh$ and $h > 0$. The direct discretization of (3.1) by n_0-steps DQ methods with Gregory convolution weights (see, for example, [28]) reads

$$S_n = S_0 \exp\left(-h\beta\left(\sum_{j=0}^{n_0-1} w_{nj}A(t_{n-j})(N - S_j) + \sum_{j=n_0}^{n} \omega_{n-j}A(t_{n-j})(N - S_j)\right)\right), \tag{3.5}$$

where the starting values $S_0, S_1, \dots, S_{n_0-1}$ are given and $S_n \approx S(t_n)$, for $n \geq n_0 \geq 1$. In this context, w_{nj} and ω_j denote the Gregory quadrature weights. Our primary focus lies in the approximation of the function $S(t)$, whose values may be involved in the estimation of the mean infectivity and of the

number of infected individuals, accordingly to the second equation of (1.1) and to (1.3).

For the specific case of $n_0 = 1$, $\omega_0 = 0$ and $\omega_j = 1$, the numerical method (3.5) corresponds to the discrete-time Kermack–McKendrick model introduced by Diekmann in [40]. This motivates us to deepen the analysis of the dynamic behaviour of (3.5) since, as it will be clear later in this chapter, from a numerical point of view it possesses good convergence properties and, in many cases, is easy to implement.

A pseudo-code implementation of the numerical method (3.5) is presented with the Algorithm 2.

Algorithm 2 : Direct Quadrature Scheme for (1)

Inputs : $h, T, \beta, n_0, A(t), [S_0, S_1, \ldots, S_{n_0-1}]$

Outputs : $[t_0, \ldots, t_{\bar{n}}], [S_0, \ldots, S_{\bar{n}}]$

$\bar{n} \leftarrow \lceil T/h \rceil$, $[t_0, t_1, \ldots, t_{n_0-1}] \leftarrow [0, h, \ldots, (n_0 - 1)h]$

for $n_0 \leq n \leq \bar{n}$ **do**

  $t_n \leftarrow (n+1)\, h$

  $ST_{Sum} \leftarrow -h\beta \sum_{j=0}^{n_0-1} w_{nj} A(t_{n-j})(N - S_j)$

  $DQ_{Sum} \leftarrow -h\beta \sum_{j=n_0}^{n-1} \omega_{n-j} A(t_{n-j})(N - S_j)$

  solve the non-linear equation

    $\xi - S_0 e^{-h\beta\omega_0 A(0)(N-\xi)} \cdot e^{ST_{Sum}+DQ_{Sum}} = 0$

  $S_n \leftarrow \xi$

3.2.1 *Qualitative Properties of the Numerical Solution*

In this subsection, we investigate the numerical solution obtained using the DQ method (3.5) and show that it replicates the qualitative properties of the continuous-time solution to (1.1), regardless of the integration step-length.

Theorem 3.1. *Let $\{S_n\}_{n\in\mathbb{N}_0}$ be the solution to the discrete equation (3.5). Assume that $0 < S_j \leq N$ for $j = 0, \ldots, n_0 - 1$. Then, for each $h > 0$,*

- *the sequence $\{S_n\}_{n\in\mathbb{N}_0}$ is positive;*
- *the sequence $\{S_n\}_{n\in\mathbb{N}_0}$ is bounded from above by S_0.*

Proof. At each step and for any fixed $h > 0$, Equation (3.5) implicitly defines S_n, $n \geq n_0$, as the solution of the nonlinear equation $\mathcal{F}_n(x;h) = 0$, where

$$\mathcal{F}_n(x;h) = x - S_0 \exp\left(-h\beta\omega_0 A(0)(N-x)\right) \cdot \exp\left(-h\beta\left(\sum_{j=0}^{n_0-1} w_{nj}A(t_{n-j})(N-S_j) + \sum_{j=n_0}^{n-1} \omega_{n-j}A(t_{n-j})(N-S_j)\right)\right).$$

Independently of n, the non-linear function $\mathcal{F}_n(x;h)$ is concave, $\mathcal{F}_n(0;h) < 0$ and because of the assumption on the starting values, $\mathcal{F}_n(N;h) > 0$. Thus, $\mathcal{F}_n$ has exactly one root in $[0, N]$. Furthermore, this root is less than S_0, which yields the result. □

TRAPEZOIDAL DISCRETIZATION IN SOME REALISTIC CASES In this paragraph, our attention is directed towards specific selections of $A(t)$ in (3.1) that are relevant to practical applications (refer to, for instance, [36, Sec. 2.1] and [2, 56, 86]) and bestow a monotonicity preserving property on the numerical method (3.5). Specifically, we delve into scenarios where the infectivity function $A(t)$ is consistently zero on an initial time interval

$$A(t) = 0, \qquad \text{for } t \leq \tau, \qquad \text{with } \tau \geq 0. \tag{3.6}$$

From a physical perspective, infectivity kernel functions that satisfy (3.6) inherently incorporate strictly positive incubation periods for the disease, along with induced delays in the infection. On the other hand, from an algorithmic viewpoint, $A(0) = 0$ renders the numerical scheme (3.5) explicit, simplifying its analysis and reducing the computational cost at each step.

In such scenarios, we opt to employ in (3.5) the trapezoidal DQ method ($n_0 = 1$) for approximating the continuous-time model. Consequently, the numerical solution not only unconditionally conforms to the fundamental properties outlined in Theorem 3.1 but also exhibits monotonic non-increasing behaviour. The resulting explicit scheme has the form

$$S_n = S_0 \cdot \exp\left(-\frac{h}{2}\beta\left(A(t_n)(N-S_0) + 2\sum_{j=1}^{n-1} A(t_{n-j})(N-S_j)\right)\right), \tag{3.7}$$

for $n > 0$, for which we state the following result.

Theorem 3.2. *Let $S_0 > 0$ and $\{S_n\}_{n\in\mathbb{N}_0}$ be the solution to the discrete equation (3.7). Then, for each $h > 0$, the sequence $\{S_n\}_{n\geq 0}$ is positive, bounded and non-increasing.*

Proof. The positivity and the boundedness of the sequence immediately come from Theorem 3.1. Furthermore, we establish its non-increasing nature by induction, starting from

$$S_1 = S_0 \exp\left(-\frac{h}{2}\beta A(t_1)(N - S_0)\right) \leq S_0.$$

Consider $n > 1$ and assume that $S_j \leq S_{j-1}$ for each $j \leq n-1$. Since from (3.7) we have

$$\begin{aligned}\log\left(\frac{S_n}{S_{n-1}}\right) = &-\frac{h}{2}\beta\left(A(t_{n-1})(N + S_0 - 2S_1)\right)\\ &-\frac{h}{2}\beta\left(2\sum_{j=2}^{n-1} A(t_{n-j})(S_{j-1} - S_j) + A(t_n)(N - S_0)\right) \leq 0,\end{aligned}$$

it is $S_n \leq S_{n-1}$. □

Theorem 3.2 assures that the solution $\{S_n(h)\}_{n\in\mathbb{N}_0}$ to the discrete equation (3.7) is non-increasing for each positive value of h and then it admits a finite limit $S_\infty(h)$, as n goes to $+\infty$. Thus, $S_\infty(h)$ corresponds to the *numerical final size* (see Section 3.3 for further details on the discrete asymptotic dynamics).

We compare the behaviour of the numerical solutions obtained by (3.7) and the following second order trapezoidal discretization of (1.1)

$$\begin{aligned}S_n &= S_0 - h\beta\sum_{j=1}^{n-1} S_j\varphi_j - \frac{h}{2}\beta S_n\varphi_n,\\ \varphi_n &= (N - S_0)A(t_n) + h\beta\sum_{j=1}^{n-1} A(t_{n-j})S_j\varphi_j,\end{aligned} \tag{3.8}$$

for $n > 0$. In (3.8), the enforcement of positiveness and monotonicity of the solution leads to the following constraint on the discretization stepsize

$$h < \frac{2}{\beta N \sup_{t\in\mathbb{R}_0^+} A(t)},$$

which may result in a severe limitation.

3.2.2 *Error Analysis and Convergence*

Aiming to investigate the approximation error of the DQ scheme (3.5), we refer to the properties of the Gregory quadrature weights reported in Section 3.1 and place emphasis on (3.4).

Consider $T > 0$ and $h = T/\bar{n}$, with $\bar{n} \in \mathbb{N}$. The local truncation error of the numerical methods (3.5) is given by

$$\begin{aligned}\delta(h;t_n) = \exp\left(-\beta \int_0^{t_n} A(t_n - s)(N - S(s))\, ds\right) \\ - \exp\left(h\beta\left(\sum_{j=0}^{n_0-1} w_{nj} A(t_{n-j})(S(t_j) - N) + \sum_{j=n_0}^{n} \omega_{n-j} A(t_{n-j})(S(t_j) - N)\right)\right),\end{aligned} \tag{3.9}$$

for $n = 0, \dots, \bar{n}$. It is known that if the kernel function $A(t)$ is sufficiently regular, then $p = n_0 + 1$ is the largest integer so that

$$\max_{0\le n\le \bar{n}} |\delta(h;t_n)| \le ch^p. \tag{3.10}$$

Denote by $e(h;t_n) = S(t_n) - S_n$, $n = 0, \dots, \bar{n}$, the global discretization error. The following convergence result holds.

Theorem 3.3. *Let the given function $A(t)$ be sufficiently smooth on an interval $[0, T]$, with $h = T/\bar{n}$ and $\bar{n} \in \mathbb{N}$. Let $\{S_n\}_{0\le n\le \bar{n}}$ be the approximation of the solution to (1), computed by the DQ method (3.5). Assume that*

- *the starting errors $\eta_j(h) = S(t_j) - S_j$, for $0 \le j < n_0 - 1$, satisfy*

$$|\eta_j(h)| = \mathcal{O}(h^{n_0}); \tag{3.11}$$

- *the kernel function $A(t)$ is smooth enough to assure* (3.10).

Then the method (3.5) *is convergent of order* $p = n_0 + 1$.

Proof. Owing to the expression of the local truncation error $\delta(h; t_n)$ in (3.9), the identity

$$\begin{aligned}\frac{S(t_n) - S_n}{S_0} &= \delta(h; t_n) \\ &+ \exp\left(h\beta\left(\sum_{j=0}^{n_0-1} w_{nj} A(t_{n-j})(S(t_j) - N) + \sum_{j=n_0}^{n} \omega_{n-j} A(t_{n-j})(S(t_j) - N)\right)\right) \\ &- \exp\left(h\beta\left(\sum_{j=0}^{n_0-1} w_{nj} A(t_{n-j})(S_j - N) + \sum_{j=n_0}^{n} \omega_{n-j} A(t_{n-j})(S_j - N)\right)\right),\end{aligned} \tag{3.12}$$

holds true for $n = n_0, \ldots, \bar{n}$. Denote by $\alpha_0 = \beta\omega_0 A(0) S_0$. Then from (3.12), if $h < 1/\alpha_0$,

$$|e(h; t_n)| \leq \frac{S_0 |\delta(h; t_n)|}{1 - h\alpha_0} + h\, \frac{S_0 \beta\ \max_{0\leq t\leq T} A(t)\ \max\{W, \Omega\}}{1 - h\alpha_0} \sum_{j=0}^{n-1} |e(h; t_j)|,$$

for $n = n_0, \ldots, \bar{n}$, with W and Ω defined in (3.4). The Gronwall discrete inequality (see, for example, [63, p. 101]) yields

$$\begin{aligned}|e(h; t_n)| \leq \frac{1}{1 - h\alpha_0} \cdot \exp\left(\frac{\beta S_0 T\ \max_{0\leq t\leq T} A(t)\ \max\{W, \Omega\}}{1 - h\alpha_0}\right) \\ \cdot \left(S_0 \max_{n_0 \leq n \leq M} |\delta(h; t_n)| + h S_0 \beta \max_{0\leq t\leq T} A(t)\ \max\{W, \Omega\} \sum_{j=0}^{n_0-1} |\eta_j(h)|\right),\end{aligned}$$

for $n = n_0, \ldots, \bar{n}$. Since the local error $\delta(h; t_n)$ and the starting errors $\eta_j(h)$ satisfy (3.10) and (3.11), respectively, it follows that

$$\max_{n=n_0,\ldots,\bar{n}} |e(h; t_n)| \leq C h^p,$$

with C positive constant not depending on h. □

Theorem 3.3 naturally applies, with $n_0 = 1$, to the specific case of (3.7), assuring the second order convergence.

3.3 ASYMPTOTIC BEHAVIOUR OF THE NUMERICAL SOLUTION

In this section, we examine the asymptotic behaviour of the solution $S_n(h), n \in \mathbb{N}_0$, to the discrete equation (3.5). Our investigation will be based on (2.3) and on the following assumptions

$$\forall h > 0, \quad \exists\, S_\infty(h) \in (0, S_0] \;:\; S_\infty(h) = \lim_{n\to+\infty} S_n(h), \tag{3.13}$$

$$\forall h > 0, \quad h \sum_{n=0}^{\infty} \omega_n A(t_n) < +\infty. \tag{3.14}$$

As a result of Theorem 3.2, the existence of the discrete final size in (3.13) is assured when (3.6) holds and the trapezoidal weights (3.3) are employed. Moreover, the assumption (3.14) is achieved if $A'(t) \in L^1(\mathbb{R}_0^+)$ (see [76, Lem. 1]), or if $A(t)$ is ultimately monotonic (see [34, p. 208]).

We define the numerical basic reproduction number

$$R_0(h) = h\beta N \sum_{n=0}^{+\infty} \omega_n A(t_n),$$

as the direct discretization (see [28]) of (1.4). The following theorem establishes the connection between $S_\infty(h)$ and $R_0(h)$, thereby presenting the discrete counterpart of the final size relation (1.7).

Theorem 3.4. *Assume that the given function $A(t)$ describing problem (3.1) is sufficiently smooth and that (3.14) holds true. Let $\{S_n\}_{n\geq 0}$ be the solution to the discrete equation (3.5) with positive starting values $S_0, \dots, S_{n_0-1} \leq S_0$. If the condition (3.13) is satisfied, then for each $h > 0$*

$$\log\left(\frac{S_0}{S_\infty(h)}\right) = R_0(h)\left(1 - \frac{S_\infty(h)}{N}\right). \tag{3.15}$$

Proof. For $n \geq n_0$, the DQ scheme (3.5) is equivalent to

$$\log\left(\frac{S_0}{S_n}\right) = h\beta\left(\sum_{j=0}^{n_0-1} w_{nj}A(t_{n-j})(N-S_j) + \sum_{j=n_0}^{n} \omega_{n-j}A(t_{n-j})(N-S_j)\right), \tag{3.16}$$

and therefore

$$\begin{aligned}\log\left(\frac{S_{n-1}}{S_n}\right) =& h\beta\left(\sum_{j=n_0+1}^{n} \omega_{n-j}A(t_{n-j})(S_{j-1}-S_j) + \omega_{n-n_0}A(t_{n-n_0})(N-S_{n_0})\right)\\ &+h\beta\sum_{j=0}^{n_0-1}\left(w_{nj}A(t_{n-j}) - w_{n-1j}A(t_{n-j-1})\right)(N-S_j).\end{aligned}$$

Summing for n ranging from n_0+1 to $+\infty$, we obtain

$$\begin{aligned}\log\left(\frac{S_{n_0}}{S_\infty(h)}\right) =& h(N-S_{n_0})\beta\sum_{n=1}^{+\infty}\omega_n A(t_n)\\ &+h\beta\sum_{n=n_0+1}^{+\infty}\sum_{j=n_0+1}^{n}\omega_{n-j}A(t_{n-j})(S_{j-1}-S_j)\\ &+h\beta\sum_{j=0}^{n_0-1}\left(\sum_{n=n_0+1}^{+\infty}(w_{nj}A(t_{n-j}) - w_{n-1,j}A(t_{n-1-j}))\right)(N-S_j),\end{aligned}$$

hence

$$\begin{aligned}\log\left(\frac{S_{n_0}}{S_\infty(h)}\right) =& h\beta\left((N-S_\infty(h))\sum_{n=0}^{+\infty}\omega_n A(t_n) - (N-S_{n_0})\omega_0 A(0)\right)\\ &-h\beta\left(\sum_{j=0}^{n_0-1} w_{n_0j}A(t_{n_0-j})(N-S_j)\right).\end{aligned} \tag{3.17}$$

Equation (3.16) with $n = n_0$ reads

$$\log\left(\frac{S_0}{S_{n_0}}\right) = h\beta\left(\sum_{j=0}^{n_0-1} w_{n_0j}A(t_{n_0-j})(N-S_j) + (N-S_{n_0})\omega_0 A(0)\right),$$

so that summing it to (3.17) yields

$$\log\left(\frac{S_0}{S_\infty(h)}\right) = h\beta\,(N - S_\infty(h))\sum_{n=0}^{+\infty}\omega_n A(t_n),$$

which completes the proof. □

Thus, accounting for the assumption (2.3), (3.15) can be regarded as the discrete counterpart of (1.7) and, just like (1.7), it possesses a unique solution in $(0, S_0)$ (see also [16]).

3.4 NUMERICAL EXPERIMENTS

Here we provide some numerical simulations to experimentally demonstrate the theoretical outcomes of Section 3.2 and Subsection 3.2.1.

For our experiments, we employ the scheme (3.5) to integrate problem (3.1). Our first example consists of problem (3.1) with

$$A(t) = \frac{1.5}{\sigma\sqrt{2\pi}}\,e^{-\frac{(t-\mu)^2}{2\sigma^2}},\quad \sigma = 0.6,\quad \mu = 0.4,\quad N = 10^2,\quad S_0 = 90,\quad \beta = 10^{-3}, \tag{3.18}$$

for $t \in [0,1]$. We approximate the solution to (3.18) by the DQ method with trapezoidal ($n_0 = 1$, order 2), first ($n_0 = 2$, order 3) and second Gregory ($n_0 = 3$, order 4) quadrature rules. In this case, since $A(t)$ does not meet condition (3.6), the methods are implicit and require at each step the resolution of a nonlinear equation for which a fixed-point iteration process is used. Table 3 and Figure 6 show the behaviour of the numerical error $E(h)$ for different values of the stepsize h and the experimental rate of convergence $\log_{10}(E(h)/E(0.1h))$. The numerical errors are computed against the reference solution obtained by second Gregory rule with $h = 10^{-6}$. It is evident that the experimental order of convergence of DQ methods is coherent with the theoretical one predicted in Theorem 3.3. For the sake of comparison, we also report the errors obtained by integrating (3.18) with the first order NSFD method (2.1) presented in Chapter 2. The work precision diagram of Figure 7 reports the number of function evaluations with respect to the accuracy of the numerical solutions by the four methods under consideration. It shows

APPROXIMATION ERRORS				
h	NSFD	Trap. rule ($n_0 = 1$)	I Gregory ($n_0 = 2$)	II Gregory ($n_0 = 3$)
10^{-1}	$2.48 \cdot 10^{-2}$	$3.34 \cdot 10^{-3}$	$4.38 \cdot 10^{-4}$	$1.98 \cdot 10^{-4}$
10^{-2}	$2.32 \cdot 10^{-3}$	$3.33 \cdot 10^{-5}$	$4.08 \cdot 10^{-7}$	$6.79 \cdot 10^{-9}$
10^{-3}	$2.31 \cdot 10^{-4}$	$3.33 \cdot 10^{-7}$	$4.05 \cdot 10^{-10}$	$6.86 \cdot 10^{-13}$
10^{-4}	$2.31 \cdot 10^{-5}$	$3.33 \cdot 10^{-9}$	$3.94 \cdot 10^{-13}$	\\
EXPERIMENTAL ORDER OF CONVERGENCE				
h	NSFD	Trap. rule	I Gregory	II Gregory
10^{-2}	1.02	2.00	3.03	4.46
10^{-3}	1.00	2.00	3.00	4.00
10^{-4}	1.00	2.00	3.01	\\

Table 3: Approximation errors and experimental rate of convergence for the DQ method (3.5)

better performances in higher order methods. Indeed, even though we are comparing an explicit method with implicit ones, we see that, at the same computational cost, DQ methods exhibit higher accuracy than the NSFD discretization. Furthermore, in achieving specific levels of accuracy, the NSFD scheme proves considerably more demanding than the DQ methods.

Our second experiment investigates the long time behaviour of the numerical solution computed by the DQ framework. Specifically, we integrate problem (3.1) with:

$$A(t) = 2t\, e^{-t}, \quad T = 80, \quad N = 10^5, \quad S_0 = 9 \cdot 10^4, \quad \beta = 10^{-5}. \tag{3.19}$$

In Figure 8, the behaviour of the numerical solution, computed by (3.5) and second Gregory weights, with $h = 10^{-3}$, is reported. In this case, the theoretical value for the final size, obtained by solving the nonlinear Equation (1.7) by the MATLAB routine *fzero* (see [82]), is $S(\infty) = 17171$.

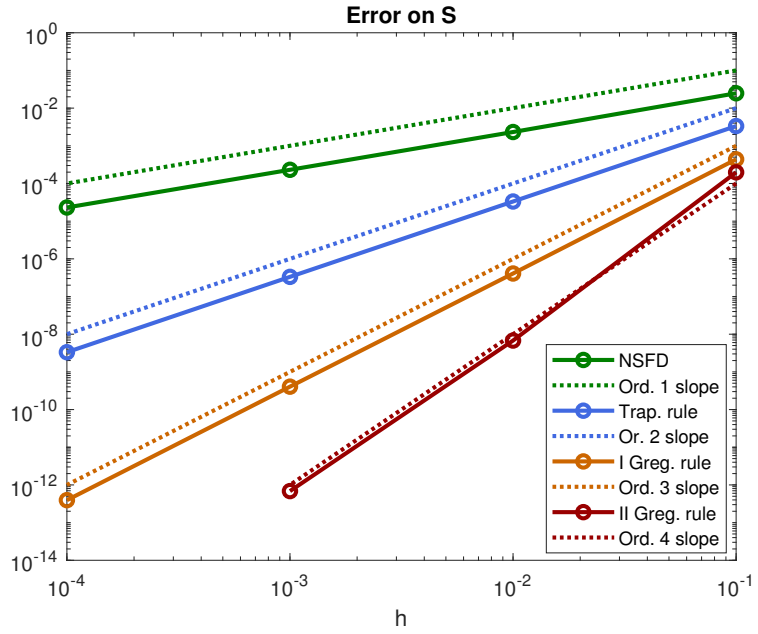

Figure 6: Logarithmic scale plot of the approximation errors and experimental convergence of the DQ method (3.5).

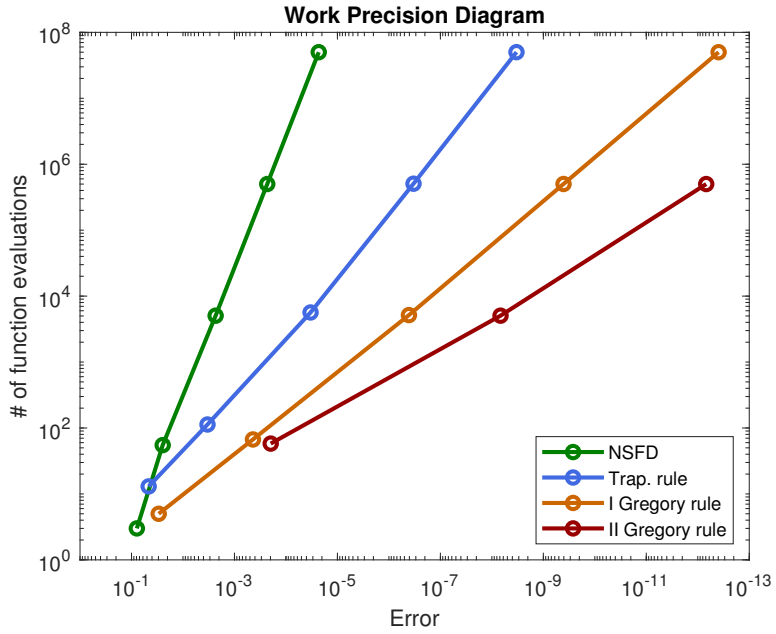

Figure 7: Logarithmic scale plot of the number of function evaluations with respect to the approximation errors for the DQ method (3.5).

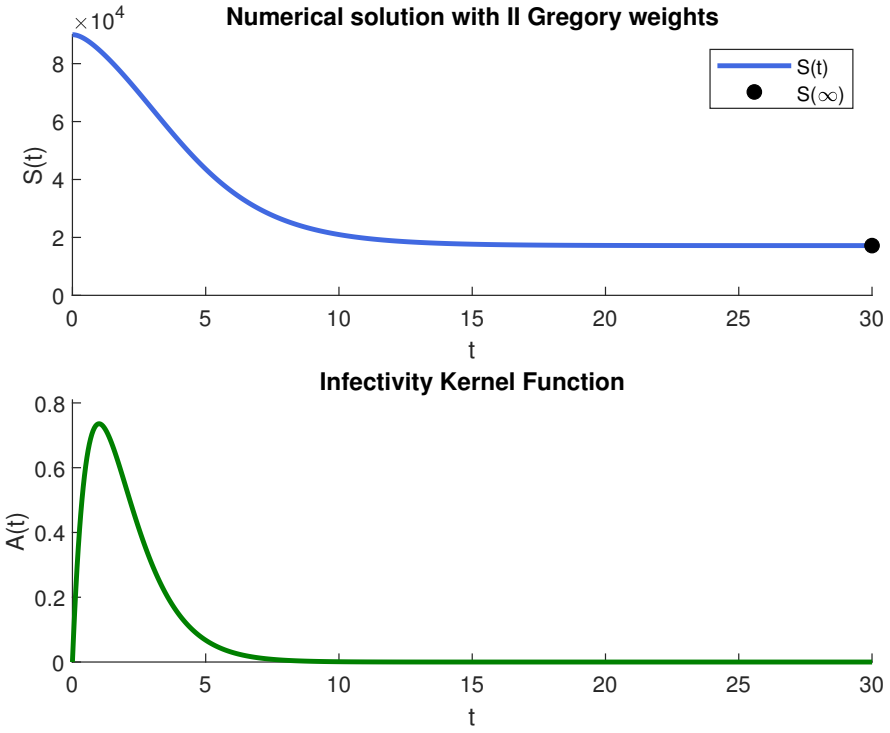

Figure 8: Problem (3.1)-(3.19): infectivity kernel function and zoom on $[0, 30]$ of the numerical solution.

Aiming to investigate the asymptotic discrete dynamics of the solution to (3.5), we introduce the truncated numerical basic reproduction number $\tilde{R}_0(h)$ and the truncated numerical final size $\tilde{S}_\infty(h;T)$ as follows

$$\bar{n} = T/h, \qquad \tilde{R}_0(h) = \beta N h \sum_{n=0}^{\bar{n}} \omega_n A(t_n), \qquad \tilde{S}_\infty(h) = S_{\bar{n}} \tag{3.20}$$

and define the residual on the numerical final size relation (3.15) as

$$r(h;T) = \left| \log\left(\frac{S_0}{\tilde{S}_\infty(h)}\right) - \tilde{R}_0(h)\left(1 - \frac{\tilde{S}_\infty(h)}{N}\right)\right|.$$

The condition (3.6) holds for the infectivity function $A(t)$ describing problem (3.1)-(3.19). As a result, from Theorem 3.2, the numerical solution is unconditionally non-increasing and the existence of the discrete final size $S_\infty(h) = \lim_{n\to+\infty} S_n$ is guaranteed when $n_0 = 1$ and the direct quadrature

DISCRETE ASYMPTOTIC DYNAMICS				
DQ Rule in (3.5)	h	Rel. Err. on $\tilde{R}_0(h;T)$	Rel. Err. on $\tilde{S}_\infty(h;T)$	$r(h;T)$
Trapezoidal	10^{-1}	$8.33 \cdot 10^{-4}$	$2.10 \cdot 10^{-3}$	$3.98 \cdot 10^{-14}$
	10^{-2}	$8.33 \cdot 10^{-6}$	$2.10 \cdot 10^{-5}$	$3.86 \cdot 10^{-14}$
	10^{-3}	$8.33 \cdot 10^{-8}$	$2.10 \cdot 10^{-7}$	$4.17 \cdot 10^{-14}$
I Greg. Rule	10^{-1}	$7.89 \cdot 10^{-5}$	$1.99 \cdot 10^{-4}$	$3.82 \cdot 10^{-14}$
	10^{-2}	$8.29 \cdot 10^{-8}$	$2.09 \cdot 10^{-7}$	$3.80 \cdot 10^{-14}$
	10^{-3}	$8.33 \cdot 10^{-11}$	$2.10 \cdot 10^{-10}$	$3.89 \cdot 10^{-14}$
II Greg. Rule	10^{-1}	$7.13 \cdot 10^{-6}$	$1.80 \cdot 10^{-5}$	$3.82 \cdot 10^{-14}$
	10^{-2}	$7.83 \cdot 10^{-10}$	$1.98 \cdot 10^{-9}$	$3.82 \cdot 10^{-14}$
	10^{-3}	$7.91 \cdot 10^{-14}$	$2.58 \cdot 10^{-13}$	$3.86 \cdot 10^{-14}$

Table 4: Long time behaviour of the numerical solution to (3.1)-(3.19) by the DQ method: numerical truncated R_0 and discrete final size.

method employs the trapezoidal weights (3.3). On the other hand, the existence assumption (3.13) is necessary when $n_0 > 1$, for the cases of the first and second Gregory rules. Our empirical tests comply with this assumption and demonstrate that, for a fixed $h > 0$, the value of $\tilde{S}_\infty(h)$ converges to a finite limit as T increases, regardless of the choice of quadrature weights.

Here, we have used $T = 80$ for computing $\tilde{S}_\infty(h)$ and the effectiveness of this choice is confirmed by the values of $r(h;T)$ reported in Table 4. In particular, Table 4 furnishes, for different values of h, the relative errors for the approximation of R_0 and $S(\infty)$ by (3.20), as well as the corresponding numerical final size residuals. Numerical results validate the outcomes of Theorem 3.4 and also provide insight into unproved theoretical properties. As a matter of fact, it is evident from Table 4 that the the numerical final size converges to its continuous counterpart, as h vanishes, with the same order $p = n_0 + 1$ of the quadrature rule employed in (3.5). In this perspective, the DQ method (3.5) provides a reliable approximation of the continuous-time asymptotic behaviour.

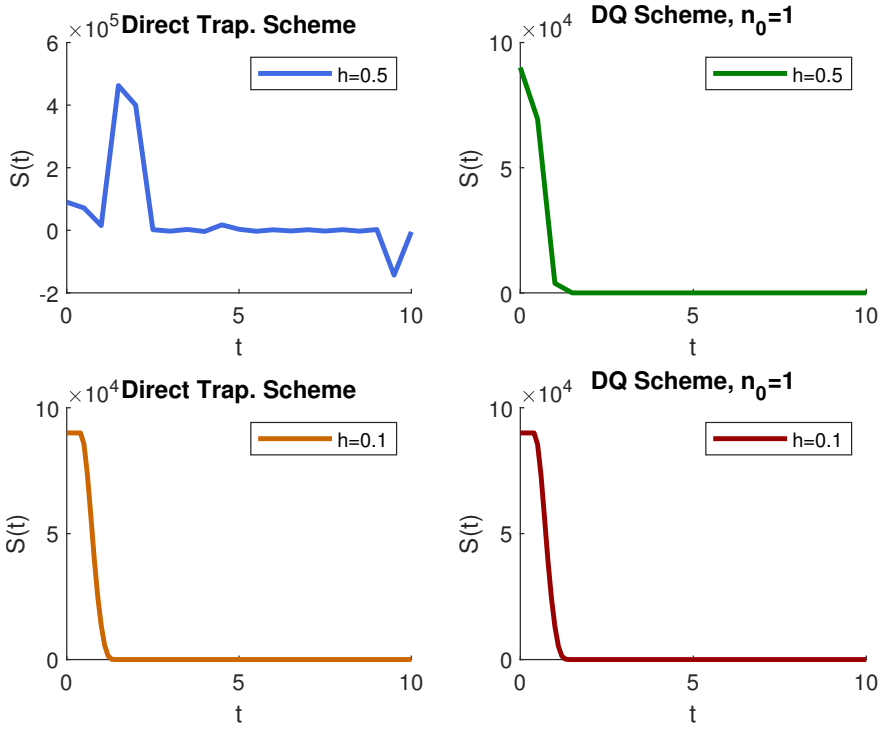

Figure 9: Comparison of the DQ method and the composite trapezoidal discretization for the test problem (3.1)-(3.21).

Motivated by the considerations in [86], we take for our conclusive test

$$t_1 = 0.4 \ \ days,$$
$$t_2 = 2.8 \ \ days,$$
$$t_3 = 3.8 \ \ days,$$
$$t_4 = 7.4 \ \ days,$$

$$A(t) = \begin{cases} \frac{1}{T_I}\ \frac{t-t_1}{t_2-t_1} & if \ \ t_1 \le t \le t_2, \\ \frac{1}{T_I} & if \ \ t_2 \le t \le t_3, \\ \frac{1}{T_I}\ \frac{t_4-t}{t_4-t_3} & if \ \ t_3 \le t \le t_4, \\ 0 & elsewhere. \end{cases} \tag{3.21}$$

The kernel function in (3.21) is well-suited for modeling influenza, as it inherently incorporates the assumptions that no individual in the population is infectious before t_1 days or after t_4 days post-exposure, and that the highest infectivity is reached between t_2 and t_3 days after exposure. The latent period T_L and the infectious period T_I are

$$T_L = \frac{t_1 + t_2}{2} = 1.6 \ \ days, \qquad T_I = \frac{t_4 + t_3 - t_2 - t_1}{2} = 4.0 \ \ days.$$

We integrate problem (3.1)-(3.21) with

$$T = 10, \qquad N = 10^5, \qquad S_0 = 9 \cdot 10^4, \qquad \beta = 10^{-2},$$

by the explicit DQ method (3.7) and the implicit scheme (3.8). Figure 9 displays simulation results using two distinct stepsizes. We remind that, according to Theorem 3.2, the numerical solution computed by the DQ scheme (3.7) with the trapezoidal weights in (3.3) is positive and non-increasing, regardless of the step-length h. Conversely, we observe in Figure 9 that the numerical solution computed by means of the direct trapezoidal scheme (3.8), with $h = 0.5$, exhibits increasing or even negative unrealistic values at certain points.

Part III

ASYMPTOTIC SOLUTIONS OF NON-LINEAR IMPLICIT VOLTERRA DISCRETE EQUATIONS

This part is dedicated to the examination of discrete Volterra equations, which are frequently employed to model phenomena involving memory effects and arise in the discretization of continuous Volterra Integral Equations (VIEs). Motivated by the results of the previous chapters on the approximations of age-of-infection epidemic models, we analyse the boundedness and asymptotic behavior of the solutions to discrete implicit equations of convolution type. Specifically, we investigate discrete models that can often be simplified to non-linear Hammerstein type discrete equations. The theoretical results we provide remain valid even when relaxing the conventional assumptions of Lipschitz-type conditions or of bounded derivatives for the non-linearity. These findings apply to the stability analysis of direct quadrature methods for implicit VIEs and, in a specific case, to the numerical study of the final size of an epidemic modeled by renewal equations.

4 VOLTERRA DISCRETE EQUATIONS: THEORETICAL AND NUMERICAL INSIGHTS

In Chapter 3 we have introduced an unconditionally positive and high order numerical method for approximating the solution to the age-of-infection epidemic model (1). Based on the DQ discretization of the exponential reformulation (3.1), it outperforms the NSFD method (2.1) presented in Chapter 2 in terms of accuracy and overall computational cost. However, the more involved structure of the discrete equation underlying the DQ method (3.5) makes the asymptotic analysis of the numerical solutions less straightforward. The necessity arises of a more in-depth investigation, with particular emphasis on two key aspects. Firstly, apart from the specific scenario discussed in Subsection 3.2.1, it becomes imperative to establish the discrete final size's existence for any selection of quadrature weights. On the other hand, as the numerical tests in Section 3.4 demonstrate the empirical convergence of the discrete final size to its continuous counterpart, a corresponding theoretical result is needed asses the convergence of the asymptotic numerical solution.

Motivated by these considerations, we carry out a comprehensive analysis of non-linear implicit Volterra discrete equations, of which the DQ method (3.5) serves as a specific instance.

4.1 IMPLICIT VOLTERRA DISCRETE EQUATIONS

Volterra discrete equations find relevant applications in numerous mathematical models where memory effects assume a pivotal role (cf. [27] and the references therein). Owing to their inherent ability to interlink empirical data and theoretical models [1, 44, 66, 85], they emerge as a compelling tool for describing several real life phenomena. The analysis of Volterra discrete equations traces its origins to [43] and has been subject of great attention over

the years, as evident from [4, 21, 32, 40, 45, 52, 81, 89, 94]. Despite the variety of approaches, the principal focus resides in investigating the boundedness and asymptotic behaviour of the solution.

Our main focus will be on implicit equations of the form

$$f(x_n) = g_n + \sum_{j=0}^{n} k_{n-j} x_j, \qquad n \in \mathbb{N}, \qquad x_0 \text{ given}, \tag{4.1}$$

under the assumptions:

A) $f : A \subseteq \mathbb{R} \to B \subseteq \mathbb{R}$ strictly increasing and continuous on A and the derivative f' exists on A;

B) $k_n \geq 0$, for all $n \in \mathbb{N}_0$;

C) $\lim_{n\to+\infty} g_n = g_\infty < +\infty$;

D) $K = \sum_{n=0}^{+\infty} k_n < \infty$;

E) there exists a solution $\{x_n\}_{n\in\mathbb{N}_0}$ to (4.1).

Equations of the form (4.1) can be regarded as equivalent to non-linear discrete equations of the Hammerstein type

$$y_n = g_n + \sum_{j=0}^{n} k_{n-j} \varphi(y_j), \qquad n \in \mathbb{N}, \qquad x_0 \text{ given}. \tag{4.2}$$

In fact, equation (4.1) can be transformed into the Hammerstein form (4.2) with $y_n = f(x_n)$, and $\varphi = f^{-1}$. For such cases, existing results detail the behaviour of solutions when the non-linearity possesses bounded derivatives. Conversely, the theory is less developed in more general cases and is primarily focused on specific problem analyses. Here, we examine the asymptotic behaviour of solutions to implicit equations in the general form (4.1) and then extend the consequent findings to (4.2).

The upcoming outcome serves as the preamble for all forthcoming discussions throughout the remainder of this section.

Lemma 4.1. *Consider the discrete equation (4.1), and assume that the solution* $\{x_n\}_{n\geq 0}$ *is bounded. Denote by* $\bar{\bar{x}} = \limsup_{n\to+\infty} x_n$ *and* $\bar{x} = \liminf_{n\to+\infty} x_n$. *Then*

$$f(\bar{\bar{x}}) \leq g_\infty + K\bar{\bar{x}}, \tag{4.3}$$

$$f(\bar{x}) \geq g_\infty + K\bar{x}. \tag{4.4}$$

Proof. Let $m \geq n$ be an arbitrary positive integer, from (4.1) it follows that

$$f(x_n) \leq g_n + \sum_{j=0}^{m-1} k_{n-j}x_j + \sup_{j\geq m} x_j \sum_{j=0}^{n-m} k_j. \tag{4.5}$$

Owing to the assumption D), the non-negative sequence $\{k_n\}_{n\in\mathbb{N}_0}$ vanishes as n tends to infinity, implying

$$\limsup_{n\to+\infty} \sum_{j=0}^{n} k_{n-j}x_j = \limsup_{n\to+\infty} \sum_{j=m}^{n} k_{n-j}x_j \leq K \sup_{j\geq m} x_j.$$

Therefore, back to (4.5), we have

$$\limsup_{n\to+\infty} f(x_n) \leq g_\infty + K \sup_{j\geq m} x_j.$$

Since f is a continuous strictly increasing function it is $\limsup_{n\to+\infty} f(x_n) = f(\limsup_{n\to+\infty} x_n)$, and passing to the limit for $m \to +\infty$, we obtain (4.3). By similar arguments, one may prove that (4.4) holds true for the limit inferior $\bar{x}$. □

As a consequence of Lemma 4.1, if the limit x_∞ exists, as $n \to +\infty$, for the solution $\{x_n\}_{n\in\mathbb{N}_0}$ to (4.1), then the relation $f(x_\infty) = g_\infty + Kx_\infty$ is valid. In other words, if the limit x_∞ exists, it constitutes a zero of the non-linear function

$$\Phi(x) = f(x) - g_\infty - Kx. \tag{4.6}$$

In fact, the inequalities (4.3) and (4.4) for the limit superior and inferior of $\{x_n\}_{n\in\mathbb{N}_0}$, respectively, yield

$$\Phi(\bar{x}) \geq 0 \qquad \text{and} \qquad \Phi(\bar{\bar{x}}) \leq 0, \tag{4.7}$$

so that, when $\bar{x} = \bar{\bar{x}} = x_\infty$, $\Phi(x_\infty) = 0$.

Theorem 4.2. *Consider the discrete equation (4.1). Suppose that the non-linear function $\Phi(x)$ in (4.6) has a unique zero x_∞ in $\mathbb{R}$, with $\Phi'(x_\infty) > 0$. Then, for any bounded solution $\{x_n\}_{n\geq 0}$, it is*

$$\lim_{n\to+\infty} x_n = x_\infty.$$

Proof. From $\Phi'(x_\infty) > 0$, the fact that $\Phi(x)$ has a unique zero x_∞ and (4.7), we have $\bar{\bar{x}} \leq x_\infty \leq \bar{x}$ and therefore $\bar{x} = \bar{\bar{x}} = x_\infty$. □

In some cases of interest the function $\Phi(x)$, defined in (4.6), may have more than one zero in $\mathbb{R}$ (for example if $\lim_{x\to\infty} \frac{f(x)}{x} = 0$) and, for one of them, it is possible to find an isolation interval which contains also the sequence solution of (4.1). In this case we can state a corresponding result, whose proof is identical to that of Theorem 4.2 and therefore will be omitted.

Theorem 4.3. *Consider equation (4.1) and assume that, for the given functions, there exist X_{min} and X_{max}, with $X_{min} < X_{max}$, such that, for each $n > 0$, $X_{min} \leq x_n \leq X_{max}$. If the non-linear function $\Phi(x)$, defined in (4.6), has a unique zero $x_\infty \in [X_{min}, X_{max}]$, with $\Phi'(x_\infty) > 0$, then*

$$\lim_{n\to+\infty} x_n = x_\infty.$$

An investigation upon the significance of hypotheses B) and C) leads to a non-convergence result, when $\{k_n\}_{n\geq 0}$ is a non-positive sequence and a limit to $\{g_n\}_{n\geq 0}$ does not exist. We outline that, when $k_n \leq 0$, for all $n \in \mathbb{N}_0$, the inequalities (4.7) become

$$\Phi(\bar{x}) \leq 0, \qquad \text{and} \qquad \Phi(\bar{\bar{x}}) \geq 0.$$

Theorem 4.4. *Consider the discrete equation (4.1) and assume that $k_n \leq 0$, for any $n \geq 0$. If $\{g_n\}_{n\geq 0}$ is bounded and has no limit, then also $\{x_n\}_{n\geq 0}$ has no limit.*

Proof. We prove the result by contradiction. Assume that $\lim_{n\to+\infty} x_n = \bar{x} = \bar{\bar{x}}$. Let $\bar{g} = \liminf_{n\to+\infty} g_n$ and $\bar{\bar{g}} = \limsup_{n\to+\infty} g_n$. Then $\bar{g} \geq f(\bar{x}) - K\bar{x}$ and $\bar{\bar{g}} \leq f(\bar{\bar{x}}) - K\bar{\bar{x}}$. Since $\bar{x} = \bar{\bar{x}}$, it follows that $\bar{g} = \bar{\bar{g}}$, which is absurd. □

4.1.1 *Existence and Uniqueness of a Solution*

Here, we present some conditions that ensure the existence of a unique solution to the non-linear implicit Volterra discrete equation (4.1). In order to do that, we introduce the function

$$\Phi_n(x) = f(x) - g_n - \sum_{j=0}^{n-1} k_{n-j} x_j - k_0 x, \qquad n \in \mathbb{N}, \tag{4.8}$$

and outline that the sequence $\{x_n\}_{n\in\mathbb{N}_0}$ satisfies (4.1) if and only if $\Phi_n(x_n) = 0$ holds true for any value of $n > 0$.

Theorem 4.5. *Consider the function (4.8) and assume that there exist X_{min} and X_{max}, with $-\infty < X_{min} < X_{max} < +\infty$, such that, for each $n > 0$,*

$$f(X_{min}) - X_{min} \sum_{j=0}^{n} k_j < g_n < f(X_{max}) - X_{max} \sum_{j=0}^{n} k_j. \tag{4.9}$$

If $x_0 \in [X_{min}, X_{max}]$, the nonlinear equation $\Phi_n(x) = 0$ has, for $n > 0$, at least one root in $[X_{min}, X_{max}]$. Furthermore, if f'' has constant sign in $[X_{min}, X_{max}]$, then the root $x_n \in [X_{min}, X_{max}]$ is unique.

Proof. We prove the existence by induction. For $n = 1$, $\Phi_1(x) = f(x) - g_1 - k_1 x_0 - k_0 x$ and the statement is true since, from (4.9),

$$\Phi_1(X_{min}) < k_1(X_{min} - x_0) \leq 0, \quad \text{and} \quad \Phi_1(X_{max}) > k_1(X_{max} - x_0) \geq 0.$$

Assume that $n > 1$ and that $x_j \in [X_{min}, X_{max}]$ is a root of $\Phi_j(x) = 0$, for $j = 1, \ldots, n-1$. Consider $\Phi_n(x)$ and observe that due to induction hypothesis,

$$\Phi_n(X_{min}) = f(X_{min}) - g_n - \sum_{j=0}^{n-1} k_{n-j} x_j - k_0 X_{min} \leq f(X_{min}) - g_n - X_{min} \sum_{j=0}^{n} k_j,$$

$$\Phi_n(X_{max}) = f(X_{max}) - g_n - \sum_{j=0}^{n-1} k_{n-j} x_j - k_0 X_{max} \geq f(X_{max}) - g_n - X_{max} \sum_{j=0}^{n} k_j,$$

Then, from (4.9), it follows that

$$\Phi_n(X_{min}) < 0, \qquad \text{and} \qquad \Phi_n(X_{max}) > 0. \tag{4.10}$$

Therefore the existence is proved. As for the uniqueness, we suppose that f'' has a constant sign in $[X_{min}, X_{max}]$ and proceed by contradiction. Let, for $n \geq 1$, $X_{min} \leq \tilde{x}_n < \hat{x}_n \leq X_{max}$ be two different roots of $\Phi_n(x) = 0$. Conditions (4.10) then imply that Φ_n admits at least one inflection point in $[\tilde{x}_n, \hat{x}_n]$, which is absurd since $\Phi_n'' = f''$. □

The sufficient conditions (4.9), for the existence of a solution to (4.1), can also be used to assure that $\Phi(x)$, defined in (4.6), has a zero $x_\infty \in [X_{min}, X_{max}]$, with positive derivative. As a matter of fact, passing to the limit for $n \to +\infty$ in (4.9) leads to

$$f(X_{min}) - K X_{min} \leq g_\infty \leq f(X_{max}) - K X_{max}.$$

So, if at least one of the previous inequalities is strict, and the second derivative of f has constant sign in $[X_{min}, X_{max}]$, then this zero is also unique. Thus $\Phi'(x_\infty) > 0$ and the asymptotic behaviour of $\{x_n\}_{n \geq 0}$ is described by Theorem 4.3.

Remark. *The results obtained in this section, on the behaviour of the solution $\{x_n\}_{n \geq 0}$ to (4.1), can be transferred to the solution $\{y_n\}_{n \geq 0}$ of the general Hammerstein type discrete equation (4.2). Since the derivative of the non-linear function $\varphi(y)$ is not necessarily bounded, the results in this section expand the actual knowledge about the asymptotic properties of solutions to Hammerstein discrete Volterra equations.*

4.2 IMPLICIT VOLTERRA DISCRETE SYSTEMS

All the results of the previous section can be generalized to d-dimensional discrete systems. From now on, the inequalities involving vectors are considered component wise. We address implicit systems of the form

$$F(X^n) = G^n + \sum_{j=0}^{n} K^{n-j} X^j, \qquad n \in \mathbb{N}, \qquad X^0 \text{ given}, \tag{4.11}$$

where $d > 1$, X^n and G^n are real d-dimensional vectors, $K^n \in \mathbb{R}^{d\times d}$ and

$$F \;:\; X = [X_1, \ldots, X_d]^T \in \mathbb{R}^d \quad \longrightarrow \quad F(X) = [f_1(X_1), \ldots, f_d(X_d)]^T \in \mathbb{R}^d.$$

Our investigation is based on the assumptions:

A*) $f_i : A \subseteq \mathbb{R} \to B \subseteq \mathbb{R}$ strictly increasing and continuous on A. Moreover, the derivative f_i' exists on A, for $i = 1, \ldots, d$;

B*) $K^n \geq 0$, for all $n \in \mathbb{N}_0$;

C*) $\lim_{n\to+\infty} G^n = G^\infty < +\infty$;

D*) $\hat{K} = \sum_{n=0}^{+\infty} K^n < \infty$;

E*) there exists a solution $\{X^n\}_{n\in\mathbb{N}_0}$ to (4.11).

Let $X_{min} \in \mathbb{R}^d$ and $X_{max} \in \mathbb{R}^d$ be two vectors such that $-\infty < X_{min} < X_{max} < +\infty$, the result below describes the generalization of Theorem 4.3.

Theorem 4.6. *Consider the discrete system (4.11) and assume that the solution $\{X^n\}_{n\in\mathbb{N}_0}$ satisfies*

$$X_{min} \leq X^n \leq X_{max}, \qquad n \geq 0.$$

Define the non-linear function

$$\Phi(X) = F(X) - G^\infty - \hat{K}X, \tag{4.12}$$

and assume that it has a unique zero X^∞ *with* $X_{min} \leq X^\infty \leq X_{max}$. *Furthermore, assume that*

$$\Phi(X_{min}) \leq 0 \qquad \textit{and} \qquad \Phi(X_{max}) \geq 0, \tag{4.13}$$

where, for each component of the vector function $\Phi(X)$, *the equal sign cannot happen at the same time. Then*

$$\lim_{n\to+\infty} X^n = X^\infty.$$

Proof. Denote $X^n = [X_1^n, \ldots, X_d^n]^T$, for $n \in \mathbb{N}_0$. Let $\bar{X}_i = \liminf_{n\to\infty} X_i^n$ and $\bar{\bar{X}}_i = \limsup_{n\to\infty} X_i^n$, for $i = 1, \ldots, d$. Proceeding component-wise on (4.11), we get

$$F(\bar{X}) \geq G^\infty + \hat{K}\bar{X} \qquad \text{and} \qquad F(\bar{\bar{X}}) \leq G^\infty + \hat{K}\bar{\bar{X}}.$$

Thus, referring to (4.12),

$$\Phi(\bar{X}) \geq 0 \qquad \text{and} \qquad \Phi(\bar{\bar{X}}) \leq 0.$$

Set $\alpha^0 = \bar{X}$, and $\beta^0 = \bar{\bar{X}}$. Construct two vector sequences through the following iterative formulas, $k = 0, 1, \ldots,$

$$F(\alpha^{k+1}) = G^\infty + \hat{K}\alpha^k \qquad \text{and} \qquad F(\beta^{k+1}) = G^\infty + \hat{K}\beta^k.$$

By (4.13) it is easy to see that $X_{min} \leq \alpha^k,\ \beta^k \leq X_{max}$, and that $\{\alpha^k\}_{k\geq 0}$ is decreasing and $\{\beta^k\}_{k\geq 0}$ is increasing. Hence,

$$\lim_{n\to+\infty} \alpha^n = \alpha \leq \bar{X} \qquad \text{and} \qquad \lim_{n\to+\infty} \beta^n = \beta \geq \bar{\bar{X}},$$

with $\Phi(\alpha) = 0$ and $\Phi(\beta) = 0$. Since, for assumption, $\Phi(X)$ has a unique zero, $X^\infty = \alpha = \beta$. Thus $\bar{\bar{X}} \leq X^\infty \leq \bar{X}$ implies that $\bar{X} = \bar{\bar{X}} = X^\infty$, which completes the proof. □

4.3 FROM DISCRETE EQUATIONS TO NUMERICAL ANALYSIS

The study of discrete equations is also valuable not only for its intrinsic significance but also because it gives insight into the behaviour of numerical methods used to approximate continuous problems. This relation enables us to employ theoretical outcomes from the previous section to explore the degree to which the dynamical and asymptotic behaviour of numerical solutions mirrors that of the continuous problem.

From now on, we focus only on results dealing with the non-linear function $\Phi(x)$ defined in (4.6) to have a unique zero with positive derivative.

4.3.1 *Continuous Volterra Integral Equations*

As already pointed out, the theoretical findings on the discrete operator (4.1) are general enough to encompass the numerical approximations of implicit Volterra Integral Equations (VIEs) of the form

$$f(x(t)) = g(t) + \int_0^t k(t-s)x(s)\,ds, \qquad t \in \mathbb{R}_0^+. \tag{4.14}$$

These equations arise, for example, in the study of the existence of continuous solutions of non-linear VIEs of the first type and frequently in some applications such as percolation theory, shock wave dynamics [27] or in age-of-infection epidemiological models [20, 36]. When $f(x)$ is invertible, equation (4.14) turns into a non-linear Hammerstein VIE of the form

$$y(t) = g(t) + \int_0^t k(t-s)\varphi(y(s))\,ds, \qquad t \in \mathbb{R}_0^+, \tag{4.15}$$

with $\varphi(y) = f^{-1}(y)$, for which the theory on continuous and numerical problem is well known in case of Lipschitz non-linearities. We mainly focus on implicit VIEs represented by (4.14), as the results derived for these equations can be straightforwardly transferred to Hammerstein-type equations.

Our analysis will be carried out by supposing that the continuous counterparts to the properties A)-E) hold true. Specifically, we assume that:

Ā) $f : A \subseteq \mathbb{R} \to B \subseteq \mathbb{R}$ strictly increasing and continuous on A and the derivative f' exists on A;

B̄) $k(t) \geq 0$, for all $t \in \mathbb{R}_0^+$;

C̄) g continuous on $\mathbb{R}_0^+$ and $\lim_{t\to+\infty} g(t) = g_\infty < +\infty$;

D̄) $K = \displaystyle\int_0^{+\infty} k(t)\, dt < \infty$;

Ē) there exists a continuous solution $x(t)$ to (4.14).

Regarding the assumption Ē), the local existence of $x(t) \in C(\mathbb{R}_0^+)$ solution to (4.14), and therefore of $y(t) \in C(\mathbb{R}_0^+)$ solution to (4.15), can be established by resorting to [29, Thm. 3.2.2]. From here and [29, Thm. 3.3.1], the continuation, for $t \geq 0$, of any bounded solution follows.

Then, the following result holds, whose proof parallels the one for the discrete equation reported in the previous section.

Theorem 4.7. *Consider the Volterra integral equation* (4.14) *and assume that its solution satisfies*

$$X_{min} \leq x(t) \leq X_{max}, \qquad t \in \mathbb{R}_0^+,$$

with $-\infty < X_{min} < X_{max} < +\infty$. *Let* $k(t)$ *be a uniformly continuous function on* $\mathbb{R}_0^+$ *for which* $\lim_{t\to+\infty} k(t) = 0$. *Define the non-linear function*

$$\Phi(x) = f(x) - g_\infty - Kx \tag{4.16}$$

and assume that it has a unique zero x_∞ *in* $[X_{min}, X_{max}]$, *with* $\Phi'(x_\infty) > 0$. *Then*

$$\lim_{t\to+\infty} x(t) = x_\infty < +\infty.$$

Observe that the existence of a unique zero of the non-linear function $\Phi(x)$ in (4.16) is guaranteed if

$$f(X_{min}) - KX_{min} < g_\infty < f(X_{max}) - KX_{max},$$

and if the second derivative f'' does not change sign in $[X_{min}, X_{max}]$.

4.3.2 *Numerical Approximations of Implicit VIEs*

Let $t_n = nh$, for $n \in \mathbb{N}_0$, with $h > 0$. Under the assumptions Ā)-Ē), we discretize the integral terms in (4.14) and (4.15) by the n_0-steps DQ method with Gregory convolution weights, as follows

$$f(x_n) = g_n + h \sum_{j=n_0}^{n} \omega_{n-j} k(t_{n-j}) x_j, \qquad n \geq n_0, \tag{4.17}$$

$$y_n = g_n + h \sum_{j=n_0}^{n} \omega_{n-j} k(t_{n-j}) \varphi(y_j), \qquad n \geq n_0. \tag{4.18}$$

Here, the starting values $x_0, x_1, \ldots, x_{n_0-1}$ are given, $x_n \approx x(t_n)$, $y_n \approx y(t_n)$, for $n \geq n_0$ and

$$g_n = g(t_n) + h \sum_{j=0}^{n_0-1} w_{nj} k(t_{n-j}) x_j = g(t_n) + h \sum_{j=0}^{n_0-1} w_{nj} k(t_{n-j}) \varphi(y_j).$$

The convolution and starting weights ω_n and w_{nj}, respectively, are positive, bounded and satisfy the condition (3.4) (we refer to Section 3.1 and to [28, 97, 98] for further details on Gregory quadrature rules).

With the following preliminary result the existence of the numerical solution, intended as a unique solution to the discrete VIEs (4.17) and (4.18), is investigated.

Lemma 4.8. *Consider the numerical methods* (4.17) *and* (4.18). *Then, for sufficiently small values of h, these methods possess a unique solution.*

Proof. For the sake of brevity, here we consider only the case of equation (4.17). Thus, proceeding in a similar way, the statement may be proved for equation (4.18) too. Consider, for $n \geq n_0$, the function

$$\Phi_n(h, x) = f(x) - g_n - h \sum_{j=n_0}^{n-1} \omega_{n-j} k(t_{n-j}) x_j - h\omega_0 k(0) x. \tag{4.19}$$

Since $\Phi_n(0,x) = f(x) - g_n$, it follows that $\Phi_n(0, f^{-1}(g_n)) = 0$. Furthermore,

$$\frac{\partial \Phi_n(h,x)}{\partial x} = f'(x) - h\omega_0 k(0) \qquad \text{and} \qquad \frac{\partial \Phi_n(0,x)}{\partial x} = f'(x) \neq 0.$$

Therefore, owing to the implicit function theorem, for sufficiently small $h > 0$, there exists a unique $x(h)$ such that $\Phi_n(h, x(h)) = 0$. This means that equation (4.17) has a unique solution (i.e. the numerical solution). □

Similar arguments of those in Theorem 4.5 lead, under additional assumptions, to the existence and uniqueness of a bounded numerical solution for any given $h > 0$, as guaranteed by the following result.

Theorem 4.9. *Consider the function $\Phi_n(h,x)$ in (4.19) and assume that there exist X_{min} and X_{max}, with $-\infty < X_{min} < X_{max} < +\infty$, such that, for $n > 0$,*

$$f(X_{min}) - X_{min} h \sum_{j=0}^{n-n_0} \omega_j k(t_j) < g_n < f(X_{max}) - X_{max} h \sum_{j=0}^{n-n_0} \omega_j k(t_j). \quad (4.20)$$

If $x_0, \dots, x_{n_0-1} \in [X_{min}, X_{max}]$, the non–linear equation $\Phi_n(h,x) = 0$, has at least one root in $[X_{min}, X_{max}]$. Furthermore, if f'' has constant sign in $[X_{min}, X_{max}]$, then the root $x_n \in [X_{min}, X_{max}]$ is unique.

Remark. *The sufficient condition (4.20) can be replaced by the following, more stringent but easier to check, assumptions:*

- *if $X_{min} > 0$,*

$$f(X_{min}) < g_n < f(X_{max}) - X_{max} K(h); \quad (4.21)$$

- *if $X_{min} < 0$ and $X_{max} > 0$,*

$$f(X_{min}) - X_{min} K(h) < g_n < f(X_{max}) - X_{max} K(h);$$

- *if $X_{max} < 0$,*

$$f(X_{min}) - X_{min} K(h) < g_n < f(X_{max}).$$

ERROR ANALYSIS AND CONVERGENCE Consider $T > 0$ and $\bar{n} \in \mathbb{N}$ such that $h = T/\bar{n}$. It is notorious (see, for instance, [28]) that if the kernel $k(t)$ and the forcing function $g(t)$ describing problems (4.14)-(4.15) are sufficiently regular on $[0, T]$, then for the local truncation error

$$\begin{aligned}\delta(h; t_n) = &\int_0^{t_n} k(t_n - s)x(s)\, ds \\ &- h\left(\sum_{j=0}^{n_0-1} w_{nj}k(t_{n-j})x(t_j) + \sum_{j=n_0}^{n} \omega_{n-j}k(t_{n-j})x(t_j)\right),\end{aligned} \tag{4.22}$$

the integer $n_0 + 1$ is the largest one for which

$$\max_{0\le n\le M} |\delta(h; t_n)| \le ch^p. \tag{4.23}$$

The following convergence result can be proved by standard analysis.

Theorem 4.10. *Let $x(t)$ and $\{x_n\}_{n\in N_0}$ be, respectively, the continuous-time solution of (4.14) on $[0, T]$ and its approximation obtained by (4.17), with $h = T/\bar{n}$. Assume that (4.23) holds, and that:*

- *the starting errors $\eta_j = x(t_j) - x_j$, for $0 \le j \le n_0 - 1$, satisfy*

$$|\eta_j| = \mathcal{O}(h^{n_0}); \tag{4.24}$$

- *$f \in C^1([\mu, \nu])$ and $f^* = \min_{x\in[\mu,\nu]} f'(x) > 0$, where μ and ν are such that $\mu \le x(t) \le \nu$, for $t \in [0, T]$ and $\mu \le x_n \le \nu$, for $n = 0, 1, \ldots, \bar{n}$.*

Then the method (4.17) is convergent of order $p = n_0 + 1$.

Proof. The global discretization error is $e(h; t_j) = \eta_j$ for $j = 0, \ldots, n_0 - 1$ and

$$e(h; t_n) = x(t_n) - x_n, \qquad \text{for } n = n_0, \ldots, \bar{n}.$$

From (4.14), (4.17) and the mean value theorem it follows that for each $n_0 \leq n \leq \bar{n}$ there exists $\mu \leq \min\{x_n, x(t_n)\} < \theta_n < \max\{x_n, x(t_n)\} \leq \nu$, such that

$$f'(\theta_n)|e(h;t_n)| \leq |\delta(h;t_n)| + W^*k^*h\sum_{j=0}^{n-1}|e(h;t_j)| + h\omega_0 k(0)\ |e(h;t_n)|,$$

where $W^* = \max\{W, \Omega\}$ and $k^* = \max_{0\leq t\leq T} k(t)$. Let $\alpha_0 = \omega_0 k(0)$. Thus, for each positive $h < f^*/\alpha_0$, it holds

$$|e(h;t_n)| \leq \frac{|\delta(h;t_n)|}{f^* - h\alpha_0} + \frac{W^*k^*}{f^* - h\alpha_0}\, h\sum_{j=0}^{n-1}|e(h;t_j)|, \qquad n = n_0, \ldots, \bar{n}.$$

The Gronwall discrete inequality (see, for example, [63, p. 101]) yields

$$|e(h;t_n)| \leq \left(\frac{\max_{n_0\leq n\leq\bar{n}}|\delta(h;t_n)|}{f^* - h\alpha_0} + \frac{W^*k^*}{f^* - h\alpha_0}\, h\sum_{j=0}^{n_0-1}|\eta_j|\right)\exp\left(\frac{TW^*k^*}{f^* - h\alpha_0}\right).$$

Since the local error $\delta(h;t_n)$ and the starting errors η_j, $j = 0, \ldots, n_0 - 1$, satisfy (4.23) and (4.24), respectively, it turns out that

$$\max_{0\leq n\leq\bar{n}}|e(h;t_n)| \leq Ch^{n_0+1},$$

with C a positive constant not depending on h. □

Proceeding as in the proof of Theorem 4.10, one may prove the order p convergence of the approximation of the solution to (4.15) computed by (4.18).

4.3.3 *Existence of the Limit and Asymptotic Convergence*

When k_n in (4.1) and (4.2) is replaced by $h\omega_n k(t_n)$, the numerical methods (4.17) and (4.18) are encompassed within the general framework of discrete Volterra equations. As a consequence, the theoretical findings of Section 4.1 offer supplementary insights into the approximation of solutions to continuous implicit VIEs of the form (4.14) and to continuous Hammerstein VIEs of the form (4.15).

In this case, the assumption D) reads

$$K(h) = h \sum_{n=0}^{+\infty} \omega_n k(t_n) < \infty, \qquad \text{for all } h > 0 \tag{4.25}$$

and, in analogy to (4.6), we consistently define the function

$$\Phi(h, x) = f(x) - g_\infty - K(h)x. \tag{4.26}$$

The following result, which is essentially a reformulation of Theorem 4.3, provides conditions for the numerical solution to admit a limit as the number of time steps goes to infinity. From a wider perspective, it represents a stability result, as the property of existence of a limit at infinity of the continuous-time solution is inherited by its approximation.

Theorem 4.11. *Consider, for $h > 0$, the numerical method (4.17). Assume that there exist X_{min} and X_{max}, with $-\infty < X_{min} < X_{max} < +\infty$, such that, for $n > 0$, $X_{min} \leq x_n \leq X_{max}$. If the non-linear function $\Phi(h, x)$, defined in (4.26), has a unique zero $x_\infty(h) \in [X_{min}, X_{max}]$, with $\frac{\partial \Phi}{\partial x}(h, x_\infty(h)) > 0$, then*

$$\lim_{n \to +\infty} x_n = x_\infty(h).$$

A bridge between the integral problem (4.14) and its numerical discretization (4.17) is possible when

$$k(t) \text{ is definitely decreasing} \qquad \text{or} \qquad k'(t) \in L^1[0, +\infty), \tag{4.27}$$

then the assumption D̄) implies (4.25) (see for example [77, Lem. 1]). In these cases,

$$\lim_{h \to 0} h \sum_{n=0}^{+\infty} \omega_n k(t_n) = \int_0^{+\infty} k(t)\, dt,$$

and then

$$\lim_{h \to 0} \Phi(h, x) = \Phi(x).$$

Furthermore, also the items in Remark 4.3.2 become easier to verify, for sufficiently small h. For example, condition (4.21) is accomplished when the forcing term $g(t)$ in (4.14) satisfies

$$f(X_{\min}) < g(t) < f(X_{max}) - KX_{max},$$

with K given in $\bar{\text{D}}$).

Theorem 4.11 gives sufficient conditions for the existence of a limit $x_\infty(h)$ of the numerical solution x_n, as $n \to +\infty$. Now we investigate about the behaviour, as $h \to 0$, of the numerical asymptotic solution $x_\infty(h)$ and its connection with the asymptotic solution of the continuous problem. The following theorem represents a general result on continuity of the fixed points with respect to parameters (see [60] for a discussion on the continuous dependence of solutions to non-linear equations with respect to parameters).

Theorem 4.12. *Consider a closed bounded subset D of $\mathbb{R}^d$ and a function*

$$\Phi : [0, +\infty) \times D \to \mathbb{R}^d, \tag{4.28}$$

satisfying:

- *$\Phi(h, w)$ is continuous for each $(h, w) \in [0, +\infty) \times D$;*
- *the equation $\Phi(h, w) = 0$ has at least one solution $\hat{w}(h) \in D$, $\forall h \in [0, +\infty)$;*
- *the equation $\Phi(h, w) = 0$ has a unique solution for $h = 0$, namely $\hat{w} = \hat{w}(0) \in D$.*

Then $\lim_{h\to 0} \hat{w}(h) = \hat{w}$.

Proof. In the following, we denote the vector function in (4.28) as follows

$$\Phi(h, w) = \begin{bmatrix} \varphi_1(h, w_1, \dots, w_d) \\ \varphi_2(h, w_1, \dots, w_d) \\ \vdots \\ \varphi_d(h, w_1, \dots, w_d) \end{bmatrix}.$$

Let $\hat{w}(h)$ be a solution to $\Phi(h, w(h)) = 0$ in D, which exists due to the second assumption. Since $\hat{w}(h) \in D$, there exist, in D,

$$\bar{l} = \liminf_{h\to 0} \hat{w}(h) = \begin{bmatrix} \bar{l}_1 \\ \vdots \\ \bar{l}_d \end{bmatrix} \qquad \text{and} \qquad \bar{\bar{l}} = \limsup_{h\to 0} \hat{w}(h) = \begin{bmatrix} \bar{\bar{l}}_1 \\ \vdots \\ \bar{\bar{l}}_d \end{bmatrix},$$

with $\bar{l}_i = \liminf_{h\to 0} \hat{w}_i(h)$ and $\bar{\bar{l}}_i = \limsup_{h\to 0} \hat{w}_i(h)$, $i = 1, \ldots, d$.
Consider $\hat{w}_1(h)$, since $\liminf_{h\to 0} \hat{w}_1(h) = \bar{l}_1$, for a property of limit inferior there exists a vanishing sequence $\{h_n\}_{n\in\mathbb{N}_0}$, such that $\lim_{n\to+\infty} \hat{w}_1(h_n) = \bar{l}_1$. Consider now the sequence $\{\hat{w}_2(h_n)\}_{n\in\mathbb{N}_0}$ made by the second component of $\hat{w}(h)$ evaluated at h_n. This sequence is bounded since $\hat{w}_2(h) \in D$, then for the Bolzano-Weierstrass Theorem, $\{\hat{w}_2(h_n)\}_{n\in\mathbb{N}_0}$ has a convergent subsequence $\{\hat{w}_2(h_{n_k})\}_{k\in\mathbb{N}_0}$ to $\tilde{w}_2$. We turn our attention to the third component sequence $\{\hat{w}_3(h_{n_k})\}_{n\in\mathbb{N}_0}$. This is still bounded and so it has a convergent subsequence, say $\{\hat{w}_3(h_{n_{k_j}})\}_{j\in\mathbb{N}_0}$, to $\tilde{w}_3$. Continue in this manner until we get all component sequences converging. Take that subsequence, thus

$$\tilde{w} = \lim_{i\to+\infty} \hat{w}\left(h_{n_{k_{j_{\ldots i}}}}\right) = \begin{bmatrix} \bar{l}_1 \\ \tilde{w}_2 \\ \vdots \\ \tilde{w}_d \end{bmatrix},$$

with $\lim_{i\to+\infty} h_{n_{k_{j_{\ldots i}}}} = 0$. From the continuity of Φ it is $\Phi(0, \tilde{w}) = 0$ and then, from the last assumption, $\tilde{w} = \hat{w}$. In particular it is $\bar{l}_1 = \hat{w}_1$.
When, instead of limit inferior we consider $\limsup_{h\to 0} \hat{w}_1(h) = \bar{\bar{l}}_1$, we adopt the same strategy of constructing cascading sequences for which all components of the solution converge. In particular $\bar{\bar{l}}_1 = \hat{w}_1$. Thus, $\lim_{h\to 0} \hat{w}_1(h)$ exists and it is equal to $\hat{w}_1$.
Now, turning to $\hat{w}_2(h)$ and observing that an analogous procedure can be applied to this second component, it results that also $\lim_{h\to 0} \hat{w}_2(h)$ exists and it is equal to $\hat{w}_2$. The repetition of this procedure for all the d solution components produces the desired result. □

Theorem 4.12 can be applied to the function $\Phi(h, x)$ in (4.26) (with $d = 1$ and $D = [X_{min}, X_{max}]$). Therefore, all the outcomes of this section allow to conclude with the following convergence result.

Theorem 4.13. *Assuming that the hypotheses of Theorem 4.11 hold, and that the kernel $k(t)$ satisfies one of the conditions (4.27), then*

$$\lim_{h \to 0} x_\infty(h) = x_\infty. \tag{4.29}$$

The convergence as $h \to 0$ is an obvious property that a numerical method must satisfy while integrating over a limited range, but it is not at all guaranteed and, in general, difficult to prove for the asymptotic solution. From this viewpoint, Theorem 4.13 reveals crucial proving that the numerical error at infinity, intended as the error in approximating the asymptotic limit, vanishes as h diminishes. Moreover, by employing the result of Theorem 4.29, it is possible to describe the asymptotics of the numerical solution to a broad range of non-linear problems (which do not necessarily have to satisfy Lipschitz conditions).

Taking into account the preliminary analysis on implicit discrete systems carried out in Section 4.2 and the fact that Theorem 4.12 applies to a d-dimensional non-linear system, all the results of this section can be generalized to systems.

4.3.4 *Numerical Experiments*

Our objective in this section is to provide experimental evidence to the theoretical results of the preceding sections. To achieve this goal, we introduce two test problems of the form (4.14).

Our first experiment corresponds to problem (4.14) with

$$f(x(t)) = x^3(t), \qquad k(t) = e^{-2t} \tag{4.30}$$

and $g(t)$ such that $x(t) = 1 + e^{-t} + t^2 e^{5-t^2}$. In this case

$$\Phi(x) = \frac{1}{2}\left(2x^3 - x - 1\right), \qquad K = \frac{1}{2}, \qquad g_\infty = \frac{1}{2}, \qquad 1 \leq x(t) \leq 56,$$

and $x_\infty = 1$ is the only zero of the function $\Phi(x)$ lying in the interval $[1, 56]$. The DQ numerical solutions computed by the scheme (4.17) with trapezoidal, first and second Gregory weights, are reported in Tables 5 and 6. More specifically, Table 5 shows the norm of errors $E(h)$ and the experimental rate of convergence $\log_{10}(E(h)/E(0.1h))$. We observe that the numerical solutions exhibit the expected convergence behaviour, with an order ranging from 2 to 4, in agreement with Theorem 4.10.

	APPROXIMATION ERRORS			EXP. ORDER OF CONVERGENCE		
h	Trap. rule	I Gregory	II Gregory	Trap. rule	I Gregory	II Gregory
10^{-1}	$1.51 \cdot 10^{-2}$	$2.50 \cdot 10^{-3}$	$1.30 \cdot 10^{-3}$	\\	\\	\\
10^{-2}	$1.51 \cdot 10^{-4}$	$2.76 \cdot 10^{-6}$	$9.08 \cdot 10^{-8}$	1.95	2.95	4.14
10^{-3}	$1.51 \cdot 10^{-6}$	$2.79 \cdot 10^{-9}$	$9.57 \cdot 10^{-12}$	2.00	2.99	3.98
10^{-4}	$1.51 \cdot 10^{-8}$	$2.80 \cdot 10^{-12}$	$8.13 \cdot 10^{-15}$	2.00	3.00	3.07

Table 5: Approximation errors and experimental rate of convergence for the DQ method (4.17) on the example (4.14)-(4.30).

In order to study the asymptotic behaviour of the numerical solution, we compute $x_{\bar{n}}(h)$ for some values of h and $\bar{n} = 30/h$, and we use it as an approximation to the numerical final state $x_\infty(h)$. This choice for $\bar{n}$ is based on the fact that the exact solution $x(t)$ approximates, for $t \geq 30$, the limit of the exact solution x_∞ with an error less than 10^{-13}. Simulations reported in Table 6 and Figure 10 show that, when $h \to 0$, the errors in approximating $\Phi(x)$ in (4.16) by $\Phi_h(x) = \Phi(h, x)$ in (4.26), and x_∞ by $x_{\bar{n}}(h)$ decrease at the same rate of convergence as the DQ method used.

Consider now problem (4.14) with

$$f(x(t)) = \sinh(x(t)), \quad k(t) = -\frac{5}{(3t+2)^3}, \quad g(t) = \cos^2\left(\frac{t}{\pi}\right) + \frac{t}{2t+5}, \tag{4.31}$$

and its discretization by (4.17). The properties (3.4) of the convolution weights allow us to state that, for each finite $h > 0$, the hypotheses of Theorem 4.4 are verified. Therefore, we expect that, independently of the method and of the value of h, the numerical solution x_n of (4.14)-(4.31) does not admit a limit for $n \to \infty$. In Figure 11 we see that the numerical solution $\{x_n\}_{n \in \mathbb{N}_0}$ com-

	$\|\Phi(x) - \Phi_h(x)\|_\infty$			$\|x_\infty - x_{\bar{n}}\|$		
h	Trap. rule	I Gregory	II Gregory	Trap. rule	I Gregory	II Gregory
10^{-1}	$9.33 \cdot 10^{-2}$	$8.68 \cdot 10^{-3}$	$1.26 \cdot 10^{-3}$	$6.66 \cdot 10^{-4}$	$6.20 \cdot 10^{-5}$	$7.23 \cdot 10^{-6}$
10^{-2}	$9.33 \cdot 10^{-4}$	$9.27 \cdot 10^{-6}$	$9.08 \cdot 10^{-8}$	$6.67 \cdot 10^{-6}$	$6.62 \cdot 10^{-8}$	$8.31 \cdot 10^{-10}$
10^{-3}	$9.33 \cdot 10^{-6}$	$9.33 \cdot 10^{-9}$	$9.57 \cdot 10^{-12}$	$6.67 \cdot 10^{-8}$	$6.67 \cdot 10^{-11}$	$1.77 \cdot 10^{-13}$
10^{-4}	$9.33 \cdot 10^{-8}$	$9.33 \cdot 10^{-12}$	$9.60 \cdot 10^{-16}$	$6.67 \cdot 10^{-10}$	$1.59 \cdot 10^{-13}$	$9.24 \cdot 10^{-14}$

Table 6: Asymptotic errors and final state convergence for the DQ method (4.17) on the example (4.14)-(4.30).

puted by Trapezoidal and II Gregory rules for $h = 2$ and $h = 10^{-2}$, behaves in agreement with the theoretical results.

4.4 THE AGE-OF-INFECTION CASE STUDY

In this section we show how Theorem 4.11 can be employed to answer a question left open in Chapter 3 for the DQ approximations of the solution to the age-of-infection model (1). Here, the existence of a numerical final size approximating the asymptotic number of susceptible individuals $S(\infty)$, is addressed. Furthermore, we prove its convergence towards the continuous final size as the integration stepsize h tends to 0.

The starting point of our asymptotic investigation is twofold. Firstly, we consider the implicit continuous VIE

$$\log S(t) = \log S_0 - \beta \int_0^t A(t-s)(N - S(s))\, ds, \tag{4.32}$$

obtained from (3.1) by standard manipulations. On the other hand, we define

$$\Phi(x) = \log x - \log S_0 + \beta \left(\int_0^{+\infty} A(s)\, ds \right) (N - x),$$

and delve into the non-linear equation $\Phi(x) = 0$ that, owing to (1.7), $S(\infty)$ satisfies when (2.3) holds.

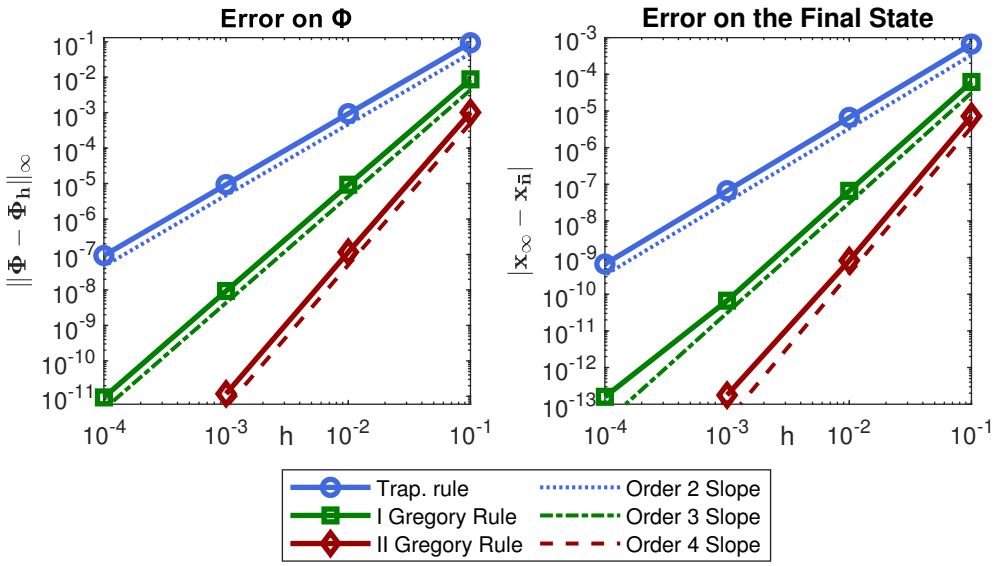

Figure 10: Logarithmic plot of the errors at infinity for the DQ method (4.17) on the example (4.14)-(4.30).

The numerical discretization of equation (4.32) by the n_0-steps DQ method (4.17) results in

$$\log S_n = g_n - h\beta \sum_{j=n_0}^{n} \omega_{n-j} A(t_{n-j})(N - S_j), \qquad n \geq n_0, \tag{4.33}$$

where the starting values $S_0, S_1, \ldots, S_{n_0-1}$ are given and $S_n \approx S(t_n)$, for $n \geq n_0 \geq 1$. Here

$$g_n = \log S_0 - h\beta \sum_{j=0}^{n_0-1} w_{nj} A(t_{n-j})(N - S_j),$$

and w_{nj} and ω_j are the non-negative quadrature weights satisfying (3.4). Since the numerical method (4.33) is equivalent to (3.5), the results of Chapter 3 apply. Therefore, the solution $\{S_n\}_{n\in\mathbb{N}_0}$ to (4.33) is unconditionally positive

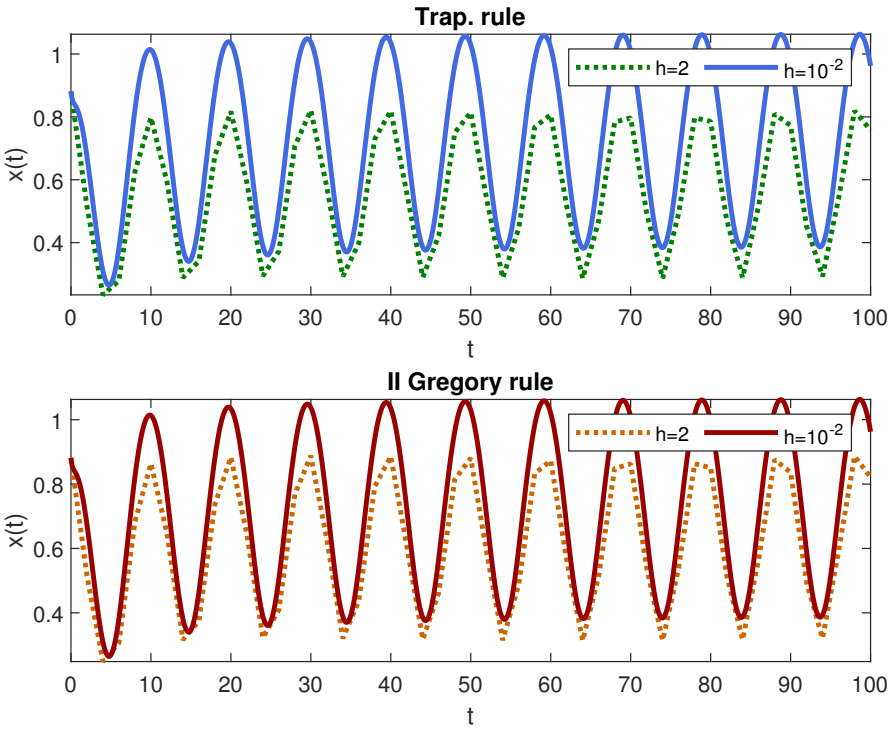

Figure 11: Numerical solutions of example (4.14)-(4.31) computed by the DQ scheme (4.17) with Trapezoidal and II Gregory weights.

and bounded from above by S_0. Furthermore, under the assumption (3.14), the non–linear function

$$\Phi(h, x) = \log x - \log S_0 + h\beta \sum_{n=0}^{+\infty} \omega_n A(t_n)(N - x), \tag{4.34}$$

corresponding to (4.26) has a unique zero in $(0, S_0]$. In fact, this solution lies in the compact interval $[\bar{S}, S_0]$, with

$$\bar{S} = S_0 \exp\left(-h\beta N \left(W n_0 \max_{0 \le t \le t_{n_0}} A(t) + \sum_{n=0}^{+\infty} \omega_n A(t_n)\right)\right) > 0,$$

where W is defined in (3.4). Thus, all the assumptions of Theorem 4.11 are accomplished with $X_{min} = \bar{S}$ and $X_{max} = S_0$. Therefore,

$$\lim_{n \to \infty} S_n = S_\infty(h),$$

which is the numerical approximation of the final size of the epidemic described by equation (1).

These observations complement the analysis of Chapter 3 and effectively address the previously unresolved questions. We refer to (4.34) as the *numerical final size relation*. When the infectivity function $A(t)$ satisfies one of the conditions outlined in (4.27), Theorem 4.13 ensures the convergence of the numerical final size $S_\infty(h)$ to $S(\infty)$, as $h \to 0$. It's noteworthy that the convergence as h vanishes is an inherent requirement for a numerical method when integrating within a bounded interval. However, such convergence is not generally guaranteed and is particularly challenging to establish in the context of asymptotic solutions. As a result, taking into account the theoretical findings of Chapter 3 and the comparison with the NSFD strategy, it can be firmly stated that direct quadrature-based methods constitute an attractive and promising tool for the accurate simulation of an epidemic. As a matter of fact, the relatively reduced computational costs and the ability to unconditionally mimic the qualitative and asymptotic properties of the continuous model, make these schemes effective for even long-time simulations.

Part IV

UNCONDITIONALLY POSITIVE LONG-TIME BEHAVIOUR PRESERVING NUMERICAL METHODS FOR MULTI-DIMENSIONAL AGE-OF-INFECTION MODELS

In this section, we extend the discretization approaches from the previous chapters to address more complex variants of the original Kermack and McKendrick model and deepen the theoretical analysis of the resulting numerical schemes. Specifically, we propose in Chapter 5 a high-order DQ scheme for the system of IDEs (1.16) representing the age-of-infection model with static heterogeneity. In Chapter 6 we present a comprehensive NSFD numerical framework for the general renewal equations system (1.20), as a tool to simulate different infection scenarios. In both cases, we establish the unconditional positivity of the numerical solution. Our focus is on the asymptotic discrete dynamics, which constitutes the core of our findings and major contributions. As a matter of fact, we prove the existence of the asymptotic limit as the number of time steps approaches infinity and the convergence of the numerical final size to the continuous final size as the step-length vanishes.

5 DQ DISCRETIZATION OF THE HETEROGENEOUSLY MIXED AGE-OF-INFECTION MODEL

In this chapter we present a direct quadrature numerical method to approximate the solution to the non-linear integro-differential system (1.16), arising in age-of-infection models accounting for demographically closed and heterogeneously mixed host populations. Thus, we refer to Section 1.3 for the theoretical details on the model and for the epidemiological interpretation of the involved parameters.

Proceeding as in the scalar case of Chapter 3, we base our numerical discretization on an implicit reformulation of the Volterra integral equations in (1.16). Our starting point is the relation

$$\frac{d}{d\tau}\log\left(S_i(\tau)\right) = -a_i \sum_{j=1}^{d} \frac{p_{ij}}{N_j}\varphi_{0j}(\tau) + a_i \sum_{j=1}^{d} \frac{p_{ij}}{N_j} \int_0^\tau A_j(s)\, \frac{dS_j}{d\tau}(\tau - s)\, ds, \quad (5.1)$$

derived from (1.16) by straightforward manipulations. Here, we normalize the number of susceptible individuals at time $t \geq 0$ of each group introducing the unknown functions

$$Z_i(t) := \frac{S_i(t)}{S_i^0}, \qquad \text{so that} \quad Z_i^0 = Z_i(0) = 1, \qquad \text{for } 1 \leq i \leq d. \quad (5.2)$$

Therefore, because of the identity

$$\int_0^t \int_0^\tau A_j(s)\, \frac{dZ_j}{d\tau}(\tau - s)\, ds\, d\tau = -\int_0^t A_j(t-s)(1 - Z_j(s))\, ds,$$

the integration on $[0,t]$ of both members of (5.1) yields the following nonlinear implicit Volterra system equivalent to (1.16)

$$\log(Z(t)) = G(t) - P\int_0^t A(t-s)(e - Z(s))\,ds. \tag{5.3}$$

In the following, we will refer either to (1.16) or to (5.3) as needed. Here $e = [1,\dots,1]^T \in \mathbb{R}^d$ is the unitary vector and for $t \in \mathbb{R}_0^+$,

$$Z(t) = \begin{bmatrix} Z_1(t) \\ Z_2(t) \\ \dots \\ Z_d(t) \end{bmatrix} \in \mathbb{R}^d, \qquad P = \begin{bmatrix} a_1 p_{11} S_1^0/N_1 & \dots & a_1 p_{1d} S_d^0/N_d \\ a_2 p_{21} S_1^0/N_1 & \dots & a_2 p_{2d} S_d^0/N_d \\ \dots & \dots & \dots \\ a_d p_{d1} S_1^0/N_1 & \dots & a_d p_{dd} S_d^0/N_d \end{bmatrix} \in \mathbb{R}^{d\times d},$$
$$G(t) = \begin{bmatrix} G_1(t) \\ G_2(t) \\ \dots \\ G_d(t) \end{bmatrix} \in \mathbb{R}^d, \qquad A(t) = \begin{bmatrix} A_1(t) & 0 & \dots & 0 & 0 \\ 0 & A_2(t) & \dots & 0 & 0 \\ \dots & \dots & \dots & \dots & \dots \\ 0 & 0 & \dots & 0 & A_d(t) \end{bmatrix} \in \mathbb{R}^{d\times d}, \tag{5.4}$$

where the components of the known forcing function read

$$G_i(t) = -a_i \sum_{j=1}^d \frac{p_{ij}}{N_j} \int_0^t \varphi_{0j}(s)\,ds \le 0, \qquad i = 1,\dots,d. \tag{5.5}$$

Notice that, since $\varphi_{0i}(t) \in L^1(\mathbb{R}_0^+)$ for $1 \le i \le d$, there exists the limit $G(\infty) = \lim_{t\to+\infty} G(t)$, given by

$$G_i(\infty) = -a_i \sum_{j=1}^d \frac{p_{ij}}{N_j} \int_0^{+\infty} \varphi_{0j}(s)\,ds \le G_i(t), \qquad i = 1,\dots,d. \tag{5.6}$$

In this chapter, as throughout the rest of the thesis, all vector inequalities have to be interpreted component-wise. From (5.2) and the theoretical findings of [23] it follows that the solution to (5.3) is positive, non-increasing and

bounded from above ($0 < Z(t) \leq 1$, for all $t \in \mathbb{R}_0^+$). Furthermore, from (1.18), the final size of the epidemic

$$Z(\infty) = \lim_{t \to +\infty} Z(t) \in (0,1]^d, \tag{5.7}$$

satisfies the d-dimensional non-linear final size relation

$$\Phi(Z(\infty)) = \log(Z(\infty)) - G(\infty) + P \int_0^{+\infty} A(s)ds \; (e - Z(\infty)) = 0, \tag{5.8}$$

with $G(\infty) = [G_1(\infty), \ldots, G_d(\infty)]^T \in \mathbb{R}^d$, whose components are defined in (5.6). The final size relation (5.8) simplifies to a scalar equation in case of proportionate mixing. As a matter of fact, if the condition (1.17) holds true and $a_i > 0$, then

$$Z_i(\infty) = \sigma^{a_i}, \qquad i = 1, \ldots, d,$$

where σ solves the scalar non-linear equation (1.19).

5.1 THE DIRECT QUADRATURE METHOD

Consider, for positive values of the stepsize h, the uniform mesh $\{t_n = nh, \; n = 0, 1, 2, \ldots\}$. The numerical discretization of equation (5.3) by the n_0-step DQ method with Gregory convolution weights (see [28]) then reads

$$\log(Z^n) = G^n - hP \sum_{k=n_0}^{n} \omega_{n-k} A(t_{n-k})(e - Z^k), \tag{5.9}$$

where, for $n \geq n_0 \geq 1$, $Z^n = Z^n(h) = [Z_1^n(h), \ldots, Z_d^n(h)]^T \approx Z(t_n)$, the starting values $Z^0, Z^1, \ldots, Z^{n_0-1} \in \mathbb{R}^d$ are given and

$$G^n = G(t_n) - hP \sum_{k=0}^{n_0-1} w_{nk} A(t_{n-k})(e - Z^k), \tag{5.10}$$

with P, $A(t)$ and $G(t)$ defined in (5.4) and (5.5), respectively. The quadrature and starting weights in (5.9) and in (5.10) are positive and satisfy the relation (3.4). We refer to Section 3.1 and to the references therein for further details on Gregory quadrature rules. A pseudo-code implementation of the numerical method (5.9) is presented with the Algorithm 3.

Algorithm 3 : Direct Quadrature Scheme for (1.16)

Inputs : $h, T, n_0, P, A(t), G(t)$

Outputs : $[t_0, \dots, t_{\bar{n}}], \{Z^0, \dots, Z^{\bar{n}}\}$

$\bar{n} \leftarrow \lceil T/h \rceil$, $[t_0, t_1, \dots, t_{n_0-1}] \leftarrow [0, h, \dots, (n_0-1)h]$

for $n_0 \leq n \leq \bar{n}$ **do**

  $t_n \leftarrow (n+1)\, h$

  $ST_{Sum} \leftarrow -hP \sum_{k=0}^{n_0-1} w_{nk} A(t_{n-k})(e - Z^k)$

  $DQ_{Sum} \leftarrow -hP \sum_{k=n_0}^{n} \omega_{n-k} A(t_{n-k})(e - Z^k)$

  $G^n \leftarrow G(t_n) + ST_{Sum}$

  solve the non-linear system

    $\log(\xi) - G^n - DQ_{Sum} = 0$

  $Z^n \leftarrow \xi$

The numerical method (5.9) is a generalization of the DQ scheme (3.5) to more complex infection scenarios (multiple groups for which the condition (2.3) does not necessarily hold). Therefore, since the discrete-time Kermack–McKendrick model in [40] corresponds to a specific instance of (3.5), it may be derived from (5.9) as well. From a mathematical standpoint, the analysis of the implicit Volterra discrete system (5.9) poses additional challenges, and a more comprehensive examination is warranted to extend the outcomes established in Chapter 3 for the scalar case.

5.1.1 *Existence and Uniqueness of a Positive Numerical Solution*

The numerical method (5.9) represents, at each step, a non-linear algebraic system with unknowns Z_i^n, $i = 1, \dots, d$. In order to prove the existence of a

unique solution to it, we establish the following preliminary result for non–linear systems of the form

$$\Gamma_i(x_i) = \sum_{j=1}^{d} \gamma_{ij}(x_j), \qquad i = 1, \dots, d. \tag{5.11}$$

Theorem 5.1. *Let $\Gamma_i : [q_i^*, q_i^{**}] \to \mathbb{R}$, and $\gamma_{ij} : [q_j^*, q_j^{**}] \to \mathbb{R}$, $1 \le i, j \le d$, be continuous functions and consider*

$$D = \{x = [x_1, \dots, x_d]^T \in \mathbb{R}^d : q_i^* \le x_i \le q_i^{**},\ i = 1, \dots, d\}.$$

Assume that for all $1 \le i, j \le d$:

- *$\Gamma_i(\xi) > 0$, and $\Gamma_i'(\xi) < 0$, for $\xi \in [q_i^*, q_i^{**})$;*
- *$\gamma_{ij}(\xi) > 0$, and $\gamma_{ij}'(\xi) < 0$, for $\xi \in [q_j^*, q_j^{**})$;*
- *$\frac{\Gamma_j(\xi)}{\gamma_{ij}(\xi)}$ is strictly decreasing on $[q_j^*, q_j^{**})$;*
- *$\psi : x \in D \to [\psi_1(x), \dots, \psi_d(x)]^T \in D$, defined as $\psi_i(x) = \Gamma_i^{-1}\left(\sum_{j=1}^{d} \gamma_{ij}(x_j)\right)$, for $1 \le i \le d$, is a continuous self-mapping.*

Then the solution to system (5.11) exists in D and it is unique.

Proof. The existence of a solution in D immediately comes from Brouwer's fixed point theorem applied to the continuous function $\psi : D \to D$. As for the uniqueness, the result in [51, Theorem 2.1] can be easily adapted. □

From now on, we assume that

$$\forall h > 0, \qquad \tilde{A}_j(h) = h \sum_{n=0}^{+\infty} \omega_n A_j(t_n) < +\infty, \qquad j = 1, \dots, d \tag{5.12}$$

and define the diagonal matrix

$$\tilde{A}(h) = \begin{bmatrix} \tilde{A}_1(h) & 0 & \dots & 0 \\ 0 & \tilde{A}_2(h) & \dots & 0 \\ \dots & \dots & \dots & \dots \\ 0 & 0 & \dots & \tilde{A}_d(h) \end{bmatrix} \in \mathbb{R}^{d \times d}. \tag{5.13}$$

Sufficient conditions for (5.13) are, for example, $A_j(t)$ ultimately monotonic (see [34, p. 208]) or $A_j'(t) \in L^1(\mathbb{R}^+)$ for each $1 \leq j \leq d$ (see [76, Lem.1]).

Here we apply Theorem 5.1 to the scheme (5.9) to prove the existence, for each $n \geq n_0$ and $h > 0$, of a unique numerical solution Z^n which unconditionally retains the positivity and boundedness properties of the continuous-time solution.

Theorem 5.2. *Assume that the starting values satisfy $0 < Z^k \leq 1$, for $k = 0, 1, \ldots, n_0 - 1$. Then, for each $h > 0$, the discrete system (5.9) admits, for any $n \geq n_0$, a unique solution Z^n. Furthermore*

1. *$\bar{Z}(h) \leq Z^n \leq 1$, for $n \geq n_0$, with $\bar{Z}(h) = [\bar{Z}_1(h), \ldots, \bar{Z}_d(h)]^T$ defined by*

$$\bar{Z}(h) = \exp\left(G(\infty) - P\left(t_{n_0}\bar{w}\max_{0\leq t\leq t_{n_0}} A(t) + \tilde{A}(h)\right)e\right), \tag{5.14}$$

   where $G(\infty)$ and $\tilde{A}(h)$ are defined in (5.6) and in (5.13), respectively.

2. *if $n_0 = 1$ (Trapezoidal rule) and $A_j(0) = 0$, $1 \leq j \leq d$, then the sequence $\{Z^n\}_{n\geq n_0}$ is non-increasing.*

Proof. Assume that a solution Z^n to (5.9) exists for each n, since

$$Z^n = \exp\left(G^n - hP\sum_{k=n_0}^{n} \omega_{n-k}A(t_{n-k})(e - Z^k)\right),$$

Z^n is positive. Furthermore from (5.10), (5.5) and (5.6)

$$G^n - hP\sum_{k=n_0}^{n} \omega_{n-k}A(t_{n-k})(e - Z^k) \geq G(\infty) - P\left(t_{n_0}\bar{w}\max_{0\leq t\leq t_{n_0}} A(t) + \tilde{A}(h)\right)e,$$

so Z^n is bounded from below by $\bar{Z}(h)$ given in (5.14). For each $n \geq n_0$, equation (5.9) implicitly defines Z^n as the solution to a non-linear system of the form (5.11) with $\Gamma_i(\xi) = \log(1/\xi)$, and

$$\gamma_{ij}(\xi) = \varepsilon_{ij}^n + ha_i\frac{p_{ij}}{N_j}S_j^0\omega_0 A_j(0)(1 - \xi),$$

where

$$\varepsilon_{ij}^n = a_i \frac{p_{ij}}{N_j} \left(hS_j^0 \left(\sum_{k=0}^{n_0-1} w_{nk} A_j(t_{n-k})(1 - Z_j^k) + \sum_{k=n_0}^{n-1} \omega_{n-k} A_j(t_{n-k})(1 - Z_j^k) \right) \right) + a_i \frac{p_{ij}}{N_j} \int_0^{t_n} \varphi_{0j}(s)\, ds.$$

Therefore,

$$\left(\frac{\Gamma_j(\xi)}{\gamma_{ij}(\xi)} \right)' = \frac{1}{(\gamma_{ij}(\xi))^2} \left(ha_i \frac{p_{ij}}{N_j} S_j^0 \omega_0 A_j(0) \left(1 + \log\left(\frac{1}{\xi}\right) - \frac{1}{\xi} \right) - \frac{\varepsilon_{ij}^n}{\xi} \right).$$

Let

$$D(h) = \{x = [x_1, \ldots, x_d]^T \in \mathbb{R}^d : \bar{Z}(h) \leq x \leq 1\}, \tag{5.15}$$

and define, for $n \geq n_0$, and $1 \leq i \leq d$, $\psi_i(x) = \Gamma_i^{-1}\left(\sum_{j=1}^d \gamma_{ij}(x_j)\right)$.
We prove the existence and the uniqueness of a solution in $D(h)$ by using Theorem 5.1. As a matter of fact, for each $n \geq n_0$, it holds:

- $\Gamma_i(\xi) = -\log(\xi) > 0$, and $\Gamma_i'(\xi) = -\frac{1}{\xi} < 0$, for $\bar{Z}_i(h) \leq \xi < 1$;
- $\gamma_{ij}'(\xi) = -ha_i \frac{p_{ij}}{N_j} S_j^0 \omega_0 A_j(0) < 0$, for $\bar{Z}_j(h) \leq \xi < 1$;
- $1 + \log(1/\xi) \leq 1/\xi$, for $\bar{Z}_j(h) \leq \xi < 1$,
- $\psi = [\psi_1, \ldots, \psi_d]^T : D(h) \to D(h)$, is a continuous self-mapping.

In order to prove that $\gamma_{ij}(\xi) > 0$ and $\left(\Gamma_j(\xi)/\gamma_{ij}(\xi)\right)' < 0$ we need that $\varepsilon_{ij}^n \geq 0$, so we proceed by induction. When $n = n_0$, since $\varepsilon_{ij}^{n_0} \geq 0$, the assertion is verified. Consider now $n > n_0$ and suppose that for each $m < n$, $\varepsilon_{ij}^m \geq 0$ and thus, by Theorem 5.1, a unique $Z^m \in D(h)$, solution to (5.9), exists. It follows that $\varepsilon_{ij}^n \geq 0$ and, once again, all the assumptions of Theorem 5.1 are satisfied. So the first part of Theorem 5.2 is proved.
Regarding the item 2 we notice that in this case equation (5.9) reads

$$\log(Z^n) = G(t_n) - hP \sum_{k=1}^{n-1} A(t_{n-k})(e - Z^k),$$

and for $n = 1$, $Z^1 = \exp(G(h)) \leq 1 = Z_i^0$, since, for (5.5), $G(h) < 0$. Let $n > 1$ and suppose the assertion true for each $m < n$. We get

$$\log\left(\frac{Z^{n-1}}{Z^n}\right) = hP\left(A(t_{n-1})(e - Z^1) + \sum_{k=2}^{n-1} A(t_{n-k})(Z^{k-1} - Z^k)\right) + G(t_{n-1}) - G(t_n) \geq 0.$$

Then $Z^n \leq Z^{n-1}$, for all n. □

Remark. *Infectivity kernel functions $A(t)$, as defined in (5.4), which are identically zero on an initial time interval are well-suited for modeling realistic infections. As a matter of fact, initially null kernels naturally account for positive incubation periods (see, for example, [2, 56, 83]) and for the time delay between the introduction of restrictive measures and the observation of their effects. Furthermore, the condition $A_j(0) = 0$ for all $1 \leq j \leq d$ renders the numerical scheme (5.9) explicitly solvable, resulting in a computationally less demanding algorithm.*

5.1.2 *Error Analysis and Convergence*

Consider, for $T > 0$, the equispaced mesh points $t_n = nh$, for $n = 0, 1, \ldots, \bar{n}$, with $\bar{n} \in \mathbb{N}$ and $T = \bar{n}h$. We denote by $\eta^k = Z(t_k) - Z^k \in \mathbb{R}^d$, for $0 \leq k < n_0$, the starting errors and by

$$\delta(h; t_n) = \int_0^{t_n} A(t_n - s)(e - Z(s))\, ds - h\left(\sum_{k=0}^{n_0-1} w_{nk} A(t_{n-k})(e - Z(t_k)) + \sum_{k=n_0}^{n} \omega_{n-k} A(t_{n-k})(e - Z(t_k))\right),$$

for $0 \leq n \leq \bar{n}$, the local truncation error of the discretization (5.9). It is known (see, for instance, [28]) that if the kernel function $A(t)$ in (5.4) is sufficiently regular, then $p = n_0 + 1$ is the largest integer so that

$$\max_{0 \leq n \leq \bar{n}} \|\delta(h; t_n)\| \leq ch^p. \tag{5.16}$$

A quite standard analysis leads to the following convergence result.

Theorem 5.3. *Let $Z(t)$ be the solution to (5.3) for $t \in [0,T]$, with $T > 0$ and let $\{Z^n\}_{0\le n\le \bar n}$ be its approximation computed by (5.9) with $h = T/\bar n$ and $\bar n > 0$. Assume that*

- *the starting errors η^k, for $0 \le k < n_0$, satisfy*

$$\|\eta^k(h)\| = \mathcal{O}(h^{n_0}); \tag{5.17}$$

- *the kernel function $A(t)$ defined in (5.4) is smooth enough to ensure (5.16).*

Then the method (5.9) is convergent of order $p = n_0 + 1$.

Proof. Let $E(h;t_n) = Z(t_n) - Z^n$, for $n_0 \le n \le \bar n$, be the global approximation error of (5.9). Thus $E(h;t_k) = \eta^k$ for $k = 0,\dots,n_0-1$. Evaluating (5.3) at t_n, for $n = n_0,\dots,\bar n$ and subtracting (5.9)-(5.10), yields

$$\begin{aligned}\log(Z(t_n)) - \log(Z^n) = &- P\delta(h;t_n) - Ph\sum_{k=0}^{n_0-1} w_{nk}A(t_{n-k})\eta^k \\ &- Ph\sum_{k=n_0}^{n}\omega_{n-k}A(t_{n-k})E(h;t_k).\end{aligned}$$

Since $0 < Z(t_n), Z^n \le 1$, from the mean value theorem, there exist d positive constants $\theta^1,\dots,\theta^d \ge 1$ such that

$$\log(Z(t_n)) - \log(Z^n) = \operatorname{diag}(\theta^i)\ E(h;t_n), \qquad n = n_0,\dots,\bar n.$$

It follows that $\|E(h;t_n)\| \le \|\log(Z(t_n)) - \log(Z^n)\|$. Consider, recalling the boundedness property (3.4) of the weights,

$$w^* = \max\{\bar w,\Omega\}, \qquad A^* = \max_{0\le t\le T}\|A(t)\|, \qquad \alpha_0 = \omega_0\|P\|\|A(0)\|.$$

Then, for a sufficiently small stepsize h, it holds

$$\|E(h;t_n)\| \le \frac{\|P\|\|\delta(h;t_n)\|}{1-h\alpha_0} + \frac{\|P\|w^*A^*}{1-h\alpha_0}\,h\sum_{k=0}^{n-1}\|E(h;t_k)\|, \quad n = n_0,\dots,\bar n.$$

The Gronwall discrete inequality (see, for example, [63, p. 101]) yields

$$\|E(h;t_n)\| \leq \|P\| \left(\max_{n_0 \leq n \leq \bar{n}} \frac{\|\delta(h;t_n)\|}{1-h\alpha_0} + \frac{w^* A^*}{1-h\alpha_0} h \sum_{k=0}^{n_0-1} \|\eta^k\| \right) \exp\left(\frac{Tw^* A^* \|P\|}{1-h\alpha_0} \right),$$

for $n = n_0, \ldots, \bar{n}$. Since the local error $\delta(h;t_n)$ and the starting errors $\eta^k(h)$ satisfy (5.16) and (5.17), respectively, it turns out that

$$\max_{0 \leq n \leq \bar{n}} \|E(h;t_n)\| \leq Ch^{n_0+1},$$

with C a positive constant not depending on h. □

5.2 ASYMPTOTIC PROPERTIES OF THE NUMERICAL SOLUTION

In this section, we delve into the analysis of the asymptotic behaviour of the numerical solution to (5.9) and clarify its relation to the final size of the epidemic $Z(\infty)$, defined in (5.7). Specifically, we demonstrate that, for each $h > 0$, the sequence $\{Z^n\}_{n \in \mathbb{N}}$ converges, as n approaches infinity, to the root of the non-linear system

$$\tilde{\Phi}(x,h) := \log(x) - G(\infty) + P\tilde{A}(h)(e-x) = 0, \tag{5.18}$$

where $G(\infty)$ and $\tilde{A}(h)$ are given in (5.6) and (5.13), respectively.

The initial step to attain the aforementioned result is to prove the existence of a unique root for (5.18). Then, we show that the DQ approximation of the solution to (5.3), computed by (5.9), admits an asymptotic limit as $n \to +\infty$, which corresponds to the unique root of (5.18).

Theorem 5.4. *Consider $D(h)$ as defined in (5.15). For each $h > 0$, the non-linear system (5.18) has a unique solution $Z^\infty(h) \in D(h)$.*

Proof. Equation (5.18) fits the form of (5.11) with $\Gamma_i(\xi) = \log(1/\xi)$ and

$$\gamma_{ij}(\xi) = a_i \frac{p_{ij}}{N_j} \left(S_j^0 (1-\xi) \tilde{A}_j(h) + \int_0^{+\infty} \varphi_{0j}(s)\, ds \right).$$

Then Theorem 5.1 yields the result. □

With the exception of the specific case analyzed in Theorem 5.2–item 2, the general monotonicity of the numerical solution cannot be proved. Consequently, our objective here is to assess the existence of the limit for the sequence $\{Z^n\}_{n\geq n_0}$. To do that, we restate the results of Section 4.2 for implicit discrete Volterra systems of the form

$$F(x^n) = v^n + \sum_{j=0}^{n} K^{n-j} x^j, \tag{5.19}$$

where $F : \mathbb{R}^d \to \mathbb{R}^d$, $F(x) = [F_1(x_1), \ldots, F_d(x_d)]^T$ and for each $0 \leq j \leq n$, $v^n, x^j \in \mathbb{R}^d$ and $K^j \in \mathbb{R}^{d\times d}$. Define the non-linear function $\bar{\Phi} : \mathbb{R}^d \to \mathbb{R}^d$, as follows

$$\bar{\Phi}(x) = F(x) - v^\infty - Kx. \tag{5.20}$$

Theorem 5.5. *Consider system (5.19). Assume that for each $1 \leq j \leq d$,*

- *$F_j : B_j \subseteq \mathbb{R} \to \mathbb{R}$ is strictly increasing, continuous and differentiable on B_j;*
- *$K^j \geq 0$ and $K = \sum_{n=0}^{+\infty} K^n < +\infty$;*
- *$\lim_{n\to+\infty} v^n = v^\infty < +\infty$;*
- *a solution $\{\xi^n\}_{n\geq 0}$ to (5.19) exists, with $\mu \leq \xi^n \leq \nu$, for all $n \geq 0$.*
- *there exists a unique $\mu \leq \xi^\infty \leq \nu$ such that $\bar{\Phi}(\xi^\infty) = 0$, with $\bar{\Phi}(x)$ in (5.20);*
- *$\bar{\Phi}(\mu) \leq 0$, and $\bar{\Phi}(\nu) \geq 0$, where the equal sign cannot happen at the same time.*

Then $\lim_{n\to+\infty} \xi^n = \xi^\infty$.

The following result applies Theorem 5.5 to the discrete system (5.9), which represents the numerical method.

Theorem 5.6. *Let, for $h > 0$, $\{Z^n\}_{n\geq n_0}$ be the approximation of the solution to (5.3) computed by (5.9). Let $Z^\infty(h) \in D(h)$ be the unique root of $\tilde{\Phi}(x, h) = 0$, with $D(h)$ in (5.15) and $\tilde{\Phi}$ in (5.18). Then there exists $\lim_{n\to\infty} Z^n$ and*

$$Z^\infty(h) = \lim_{n\to\infty} Z^n.$$

Proof. The DQ numerical method (5.9) falls into the general form (5.19) with

$$F(x) = \log(x), \qquad K^{n-j} = \begin{cases} hPw_{nj}A(t_{n-j}), & \text{for } 0 \le j < n_0, \\ hP\omega_{n-j}A(t_{n-j}), & \text{for } n_0 \le j \le n. \end{cases}$$
$$x_j = Z_j,$$
$$v^n = G(t_n) - hP\left(\sum_{k=0}^{n_0-1} w_{nk}A(t_{n-k}) + \sum_{k=n_0}^{n} \omega_{n-k}A(t_{n-k})\right)e.$$

With this choice, $\tilde{\Phi}(x,h)$ in (5.18) coincides with $\bar{\Phi}(x,h)$ in (5.20) for all fixed $h > 0$. Hence, from Theorem 5.4, $Z^\infty(h)$ is the only zero of $\tilde{\Phi}(x,h)$ on $D(h)$. So we set $\mu = \bar{Z}(h)$ and $\nu = Z^0 = 1$, then

$$\tilde{\Phi}(Z^0,h) = -G(\infty) \ge 0,$$
$$\tilde{\Phi}(\bar{Z}(h),h) = -P\left(t_{n_0}\bar{w}\max_{0\le t\le t_{n_0}} A(t) + \tilde{A}(h)\bar{Z}(h)\right) \le 0,$$

all the hypotheses of Theorem 5.5 are fulfilled and we get the result. □

Theorem 5.6 states that independently of the step length, the numerical solution Z^n converges, when $n \to +\infty$, to the root $Z^\infty(h)$ of (5.18) that represents the discrete counterpart to the final size relation (5.8). For this reason, we refer to (5.18) as the *numerical final size relation* and to $Z^\infty(h)$ as the *numerical final size*.

5.2.1 *Convergence of the Numerical Final Size*

Theorem (5.3) ensures the high-order convergence of the DQ discretization (5.9) in case of integration over bounded time intervals. Our objective is to prove that the numerical solution can accurately replicate and efficiently approximate the asymptotic behaviour of $Z(t)$. Stated differently, we aim to demonstrate that the discrete final size $Z^\infty(h)$ converges to the continuous final size $Z(\infty)$ as h vanishes. This is shown in the theorem below. We assume that

$$\lim_{h\to 0} \tilde{A}(h) = \int_0^{+\infty} A(s)\, ds, \tag{5.21}$$

with the matrix $\tilde{A}(h)$ defined in (5.13).

Theorem 5.7. *Let $Z(t)$ be the solution on $\mathbb{R}_0^+$ to (5.3) and $Z(\infty) = \lim_{t\to+\infty} Z(t)$. Let $\{Z^n\}_{n\geq 0} = \{Z^n(h)\}_{n\geq 0}$ be its approximation computed by (5.9). Suppose that (5.21) holds true. Then*

$$\lim_{h\to 0}\lim_{n\to+\infty} Z^n(h) = Z(\infty).$$

Proof. Owing to the final size relation (5.8), the equality $\Phi(Z(\infty)) = 0$ holds true for the non-linear function

$$\Phi : x \in \mathbb{R}^d \longrightarrow \log(x) - G(\infty) + P\int_0^{+\infty} A(s)ds\ (e - x) \in \mathbb{R}^d.$$

Due to the hypotheses, $\lim_{h\to 0}\tilde{\Phi}(x,h) = \Phi(x)$ and the numerical final size relation (5.18) tends to the continuous one (5.8) as h goes to zero. Furthermore, from Theorem 5.4 and Theorem 5.6, $\lim_{n\to+\infty} Z^n(h) = Z^\infty(h)$ is the only root in $D(h)$ of $\tilde{\Phi}(x,h) = 0$. Consider

$$\bar{Z}_i^\infty = \liminf_{h\to 0} Z_i^\infty(h) \qquad \text{and} \qquad \bar{\bar{Z}}_i^\infty = \limsup_{h\to 0} Z_i^\infty(h) \qquad \text{for} \quad i = 1,\dots,d.$$

Properties of limit inferior ensure the existence of a vanishing sequence $\{h_n\}_{n\geq 0}$ such that

$$\lim_{n\to+\infty} Z_1^\infty(h_n) = \bar{Z}_1^\infty.$$

Due to Bolzano-Weierstrass theorem, the bounded sequence $\{Z_2^\infty(h_n)\}_{n\in\mathbb{N}_0}$ admits a subsequence $\{Z_2^\infty(h_{n_k})\}_{k\in\mathbb{N}_0}$ such that $\lim_{k\to+\infty} Z_2^\infty(h_{n_k}) = Z_2^*$. Then we proceed by considering the bounded sequence $\{Z_3^\infty(h_{n_k})\}_{k\in\mathbb{N}_0}$ and a convergent subsequence of it $Z_3^\infty(h_{n_{k_l}}) \overset{l\to\infty}{\longrightarrow} Z_3^*$. Proceeding in this way it is possible to obtain all component sequences converging. Thus there exists a sequence $h_{n_{k_{l\dots r}}} \overset{r\to\infty}{\longrightarrow} 0$, such that

$$Z^* = \lim_{r\to+\infty} Z^\infty\left(h_{n_{k_{l\dots r}}}\right) = [\bar{Z}_1^\infty, Z_2^*, \dots, Z_d^*]^T.$$

Hence, given the continuity with respect to both x and h of $\tilde{\Phi}(x,h)$, we can conclude that $Z^* = Z(\infty)$ and $\bar{Z}_1^\infty = Z_1(\infty)$. In a similar fashion it is possible to prove that $\bar{\bar{Z}}_1^\infty = Z_1(\infty)$ and consequently that $\lim_{h\to 0} Z_1^\infty(h) = Z_1(\infty)$. Repeating the procedure for the remaining $d-1$ components then completes the proof. □

The numerical method (5.9) unconditionally retains the asymptotic properties of the continuous–time solution to the model (5.3). Furthermore, the theoretical findings outlined in this section demonstrate that as h tends to zero, the asymptotic numerical solution converges to its continuous counterpart. We stress the importance of this result, since the convergence of the asymptotic solution is not guaranteed and in general challenging to prove, for still accurate standard numerical techniques.

The commutative diagram in Figure 12 sums up all these outcomes.

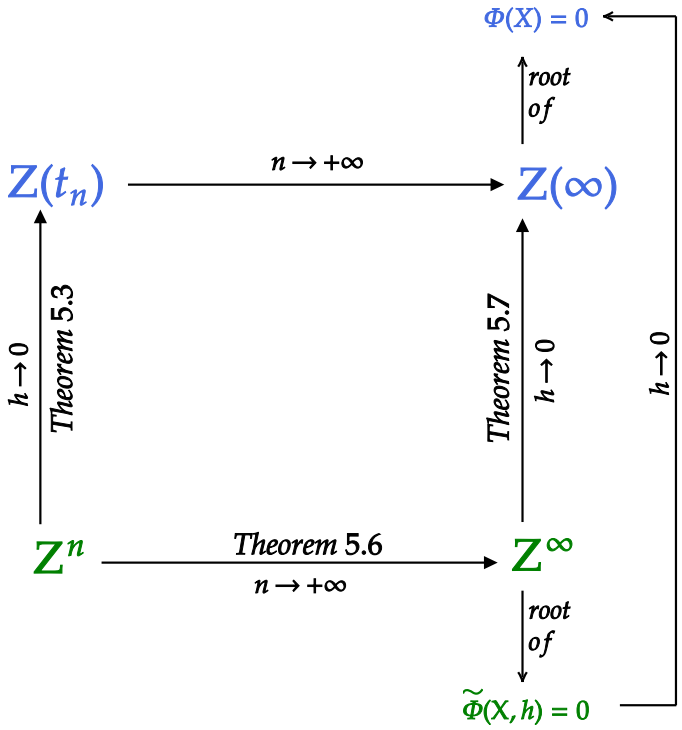

Figure 12: Convergence results for the the DQ approximation of the age-of-infection model with static heterogeneity. Here, the blue colour represents the continuous-time level, while the green colour denotes the discrete one.

5.2.2 *The Proportionate Mixing Case*

The d-dimensional final size relation (5.8) simplifies to the scalar non-linear equation (1.19) in case of proportionate mixing. Here we show that the asymptotic limiting system of the DQ solution exhibits a similar property.

Assume that $a_i > 0$ and consider $\Lambda_i = G_i(\infty)/a_i$, for $i = 1, \dots, d$, with $G_i(\infty)$ defined in (5.6). The numerical final size relation (5.18) then reads

$$\frac{1}{a_i} \log\left(Z_i^\infty(h)\right) = -\Lambda_i - \sum_{j=1}^{d} \frac{p_{ij}}{N_j} S_j^0 \tilde{A}_j(h)(1 - Z_j^\infty(h)), \qquad i = 1, \dots, d,$$

where $\tilde{A}_j(h)$, $1 \leq j \leq d$, is given by (5.12). In case of proportionate mixing, (1.17) holds true and

$$\Lambda_i = -\sum_{j=1}^{d} \frac{p_{ij}}{N_j} \int_0^t \varphi_{0j}(s)\, ds = \Lambda, \qquad i = 1, \dots, d.$$

Therefore, independently of step length, $Z_i^\infty(h) = \sigma(h)^{a_i}$, for all $i = 1, \dots, d$, where $\sigma(h)$ solves the scalar equation

$$\log(\sigma(h)) + \sum_{j=1}^{d} \frac{p_j}{N_j} \left(\int_0^{+\infty} \varphi_{0j}(s)\, ds + S_j^0 \tilde{A}_j(h)(1 - \sigma(h)^{a_j}) \right) = 0. \tag{5.22}$$

Equation (5.22) represents the direct discretization of (1.19) and the results of this section can be employed to prove that under the assumption (5.21), $\lim_{h \to 0} \sigma(h) = \sigma$ as well.

5.3 NUMERICAL EXPERIMENTS

In this section, we present two experiments aimed at validating the theoretical findings of the preceding sections, alongside a simulation delineating the dynamics of a typical influenza outbreak.

Our first example consists of system (5.3) with $d = 4$,

$$S^0 = \begin{bmatrix} 1000 \\ 500 \\ 300 \\ 200 \end{bmatrix}, \qquad A(t) = \begin{bmatrix} 5(1+t^2)^{-1} & 0 & 0 & 0 \\ 0 & e^{-2t} & 0 & 0 \\ 0 & 0 & te^{-0.2t} & 0 \\ 0 & 0 & 0 & (0.2+t)^{-2} \end{bmatrix}, \tag{5.23}$$

$$N_i = \frac{6}{5i} \cdot 10^3, \qquad a_i = \frac{i}{3}, \qquad p_{ij} = \frac{1}{4}, \qquad \varphi_{0j}(t) = (N_j - S_j^0)A_j(t),$$

for $1 \leq i, j \leq 4$, whose solution is approximated by the method (5.9) with different choices of the weights (see Section 3.1). The maximum errors $E(h)$ at the end point of the integration interval $[0, 1]$ and the experimental rate of convergence

$$\hat{p} = \log_{10}\left(\frac{E(h)}{E(h/10)}\right),$$

are listed in Table 7. Here, the errors are computed by using, as a reference solution, the one obtained by II Gregory rule and $h = 10^{-5}$. From Table 7 and Figure 13 it is clear that the experimental order agrees with the theoretical one established in Theorem 5.3.

	APPROXIMATION ERRORS			EXP. ORDER OF CONVERGENCE		
h	Trap. ($n_0 = 1$)	I Greg. ($n_0 = 2$)	II Greg. ($n_0 = 3$)	Trap. ($n_0 = 1$)	I Greg. ($n_0 = 2$)	II Greg. ($n_0 = 3$)
10^{-1}	$3.15 \cdot 10^{-2}$	$1.48 \cdot 10^{-2}$	$9.07 \cdot 10^{-3}$	\\	\\	\\
10^{-2}	$3.34 \cdot 10^{-4}$	$2.59 \cdot 10^{-5}$	$3.23 \cdot 10^{-6}$	1.98	2.76	3.45
10^{-3}	$3.34 \cdot 10^{-6}$	$2.76 \cdot 10^{-8}$	$3.83 \cdot 10^{-10}$	2.00	2.97	3.93
10^{-4}	$3.34 \cdot 10^{-8}$	$2.78 \cdot 10^{-11}$	$3.99 \cdot 10^{-14}$	2.00	3.00	3.98

Table 7: Approximation errors and experimental rate of convergence for the DQ method (5.9)

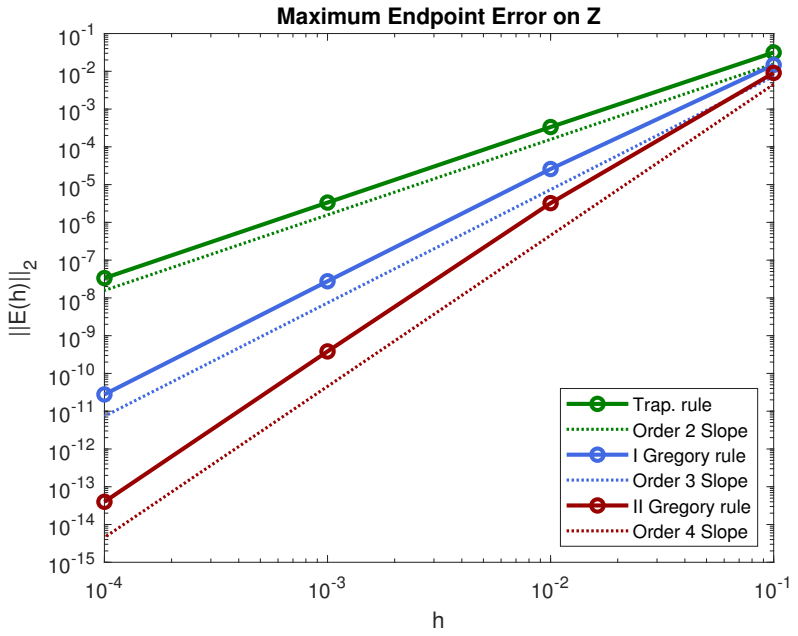

Figure 13: Logarithmic scale plot of the approximation errors and experimental convergence of the DQ method (5.9).

To assess the numerical method's reliability and confirm the preservation of the distinctive characteristics of the continuous model, we examine problem (5.3) with for $1 \leq i, j \leq 3$,

$$\begin{aligned} &N_1 = 1000, \\ &N_2 = 2000, \\ &N_3 = 3000, \end{aligned} \quad S^0 = \begin{bmatrix} 900 \\ 1800 \\ 2700 \end{bmatrix}, \quad A(t) = \begin{bmatrix} 2e^{-2t} & 0 & 0 \\ 0 & \sqrt{\frac{2}{\pi}} e^{-t^2/2} & 0 \\ 0 & 0 & 2te^{-t^2} \end{bmatrix} \tag{5.24}$$

$$a_i = \frac{0.6}{i}, \quad p_{ij} = \frac{1}{3}, \quad \varphi_{0j}(t) = (N_j - S_j^0) A_j(t), \quad 1 \leq i, j \leq 3.$$

The numerical solution over the interval $[0, 30]$, computed using the DQ scheme (5.9) with second Gregory weights, is depicted in Figure 14. There, we report the continuous final size $Z(\infty)$ as well, obtained by using the fzero MATLAB routine [82] for the equation (1.19), within the context of the proportionate mixing case. From Figure 14 it is clear that the positivity, the boundedness and the qualitative long-time behaviour of the continuous solution are retained. Our tests show that for fixed $h > 0$, the value of Z^n con-

verges to a finite value, as n grows, for any choice of the quadrature weights. To quantitatively investigate the asymptotic behaviour of the DQ numerical solution, we integrate the problem (5.3)-(5.24) on a large time interval $[0, T]$, with $T >> 0$. Then we define the truncated numerical final size $\tilde{Z}^{\infty}(h;T)$ and the truncated sum $\tilde{A}^{\bar{n}}(h;T)$ of (5.13) as follows

$$\tilde{Z}^{\infty}(h;T) = Z^{\bar{n}}(h) \in \mathbb{R}^d \quad \text{and} \quad \tilde{A}^{\bar{n}}(h;T) = h \sum_{n=0}^{\bar{n}} \omega_n A(t_n) \in \mathbb{R}^{d\times d}, \tag{5.25}$$

where $\bar{n}$ is the positive integer for which $\bar{n}h = T$. Furthermore we consider the residual on the numerical final size relation (5.18)

$$r(h;T) = \left\| \log(\tilde{Z}^{\infty}(h;T)) - G(\infty) + P\tilde{A}^{\bar{n}}(h;T)(e - \tilde{Z}^{\infty}(h;T)) \right\|_2,$$

as a measure of the goodness of the choice of T.

We conduct our experiment by setting $T = 100$ for computing $\tilde{Z}^{\infty}(h;T)$, and the effectiveness of this choice is confirmed by the values of $r(h;T)$. Table 8 shows the residuals of the numerical final size and the asymptotic approximation errors $\|Z(\infty) - Z^{\bar{n}}(h)\|_2$, which tend to zero as h vanishes. The numerical outcomes agree with the theoretical result of Theorem 5.6 and illustrate a convergence of the numerical final size to the continuous one with an experimental rate of $n_0 + 1$.

5.3.1 *Age Structured Simulation of Influenza in Italy*

Age-structured models are founded on the idea that the social behaviour and the contact pattern of host individuals may vary with the age, resulting in different responses to the infection. A common assumption in this context is that the disease spread occurs within a relatively short time frame, during which the heterogeneity can be considered static. In this setting, we select the parameters in (5.3) to model the evolution of an influenza outbreak in Italy. From demographic data in [55], we derive the age-structured partition of Italian population in 2018 reported in Table 9. Moreover, the contact matrix $[p_{ij}]_{1\le i,j\le 5}$ is determined from [49, Table S1] by reorganizing the age-specific groups and calculating the relative frequency of contact for each group. Finally, the contact rates a_i, $1 \le i \le 5$, are computed by solving the balance

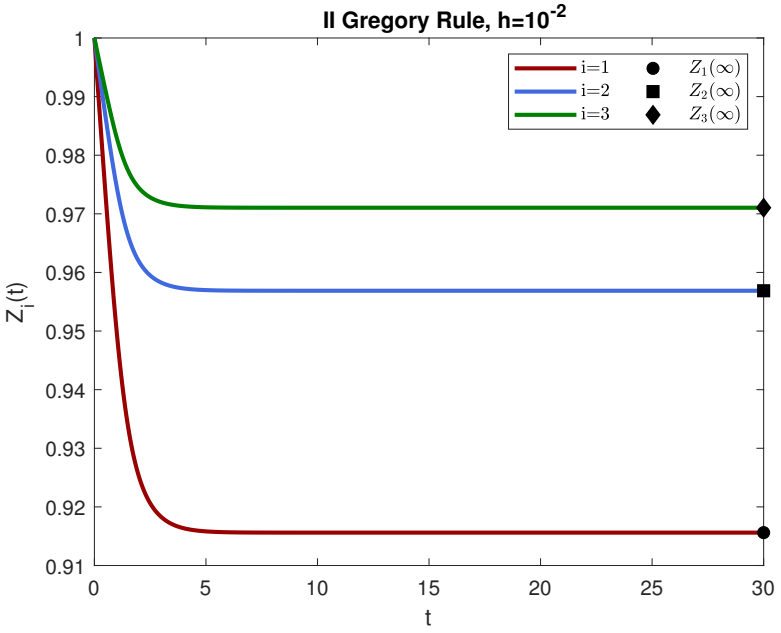

Figure 14: Problem (5.3)-(5.24): results of simulation on $[0, 30]$.

relation (1.15) with the fsolve MATLAB routine (see [82]) with tolerances of 10^{-15}.

Epidemic models arising from VIEs and renewal equations provide a precise description of the non-instantaneous nature of the contagion process by incorporating delays. We base our investigation on the assumptions that no member of the population is infectious before t_1 days or after t_4 days post-exposure and maximum infectivity occurs between t_2 and t_3 days after exposure. To incorporate these considerations, we choose, for $j = 1, 2 \dots 5$, the trapezium kernel functions

$$\begin{aligned} &t_1 = 1.0 \ \text{ days}, \\ &t_2 = 2.0 \ \text{ days}, \\ &t_3 = 2.4 \ \text{ days}, \\ &t_4 = 3.0 \ \text{ days}, \end{aligned} \qquad A_j(t) = \begin{cases} \frac{1}{T_I} \ \frac{t-t_1}{t_2-t_1} & \text{if } \ t_1 \le t \le t_2, \\ \frac{1}{T_I} & \text{if } \ t_2 \le t \le t_3, \\ \frac{1}{T_I} \ \frac{t_4-t}{t_4-t_3} & \text{if } \ t_3 \le t \le t_4, \\ 0 & \text{elsewhere}, \end{cases} \tag{5.26}$$

as suitable to model a common flu (see, for instance, [86]).

DISCRETE ASYMPTOTIC DYNAMICS				
DQ Rule in (5.9)	h	$\|Z(\infty) - Z^{\bar{n}}(h)\|_2$	$r(h;10^2)$	Exp. Conv. Rate
Trapezoidal	10^{0}	$6.24 \cdot 10^{-3}$	$6.13 \cdot 10^{-17}$	\\
	10^{-1}	$6.57 \cdot 10^{-5}$	$1.60 \cdot 10^{-16}$	1.98
	10^{-2}	$6.57 \cdot 10^{-7}$	$1.39 \cdot 10^{-16}$	2.00
	10^{-3}	$6.57 \cdot 10^{-9}$	$2.12 \cdot 10^{-16}$	2.00
I Greg. Rule	10^{0}	$2.72 \cdot 10^{-3}$	$8.06 \cdot 10^{-17}$	\\
	10^{-1}	$6.83 \cdot 10^{-6}$	$2.89 \cdot 10^{-16}$	2.60
	10^{-2}	$7.46 \cdot 10^{-9}$	$1.17 \cdot 10^{-17}$	2.96
	10^{-3}	$7.52 \cdot 10^{-12}$	$5.93 \cdot 10^{-16}$	3.00
II Greg. Rule	10^{-1}	$1.70 \cdot 10^{-3}$	$5.40 \cdot 10^{-17}$	\\
	10^{-2}	$1.10 \cdot 10^{-6}$	$1.55 \cdot 10^{-16}$	3.19
	10^{-3}	$1.25 \cdot 10^{-10}$	$3.20 \cdot 10^{-16}$	3.95

Table 8: Long time behaviour of the numerical solution to (5.3)-(5.24) by the DQ method: numerical final size convergence.

Here, in agreement with recent influenza literature (see [31, 70, 95] and references therein), the latent period T_L and the infectious period T_I are

$$T_L = \frac{t_1 + t_2}{2} = 1.5 \ \ days, \qquad T_I = \frac{t_4 + t_3 - t_2 - t_1}{2} = 1.2 \ \ days.$$

From a computational standpoint, the shape of the functions in (5.26) and the condition $A_j(0) = 0$, for all $1 \leq j \leq 5$, render the numerical method (5.9) explicit. We assume that the 99% of the individuals in each group are susceptibles and that all initial infectives in each group have infection-age zero, at the disease outbreak. Specifically, we set

$$S_j^0 = 0.99 N_j, \qquad \text{and} \qquad \varphi_{0j} = (N_j - S_j^0) A_j(t), \qquad \text{for } j = 1, \ldots, 5.$$

We simulate problem (5.3)-(5.26)-Table 9 on $[0, 60]$ by second Gregory rule and $h = 10^{-3}$. The results, showed with Figure 15, illustrate the variation of susceptibles $S_i(t) = S_i^0 Z_i(t)$, $1 \leq i \leq 5$.

DEMOGRAPHIC AND CONTACT DATA FOR ITALY							
i	Age Groups	N_i	p_{i1}	p_{i2}	p_{i3}	p_{i4}	p_{i5}
1	$00-19$ years	10745563	0.5782	0.1861	0.1762	0.0476	0.0118
2	$20-39$ years	13113139	0.1583	0.3939	0.3260	0.1072	0.0146
3	$40-59$ years	18445702	0.1652	0.3595	0.3217	0.1288	0.0248
4	$60-79$ years	13215981	0.0999	0.2645	0.2882	0.2832	0.0641
5	≥ 80 years	4296288	0.1201	0.1746	0.2677	0.3097	0.1279
Contact rates $a_1 = 2.557,\ a_2 = 2.464,\ a_3 = 1.589,\ a_4 = 0.991,\ a_5 = 0.631$							
Total Population size $= 59816673,$ $\sum_{j=1}^{5} p_{ij} = 1$ for each $1 \leq i \leq 5.$							

Table 9: Age structure partition and contact patterns of 2018 Italian population.

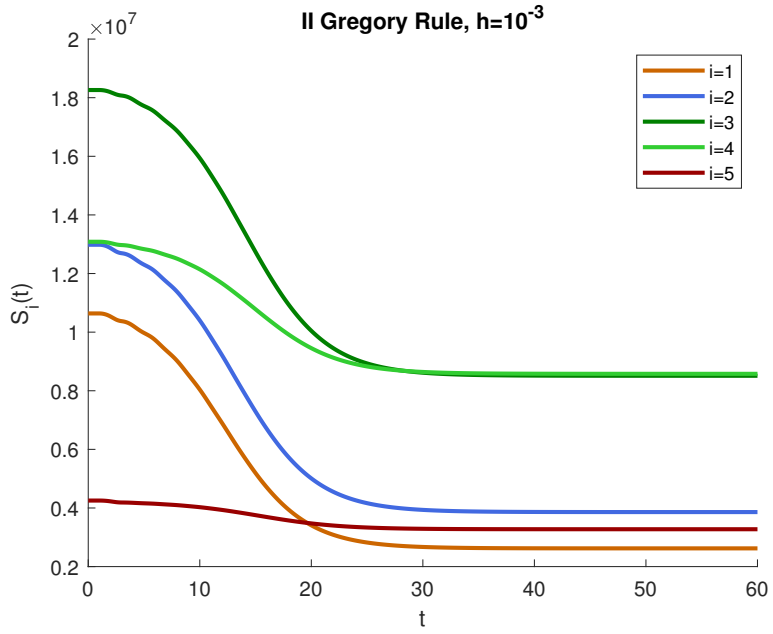

Figure 15: Age structured simulation of influenza in Italy, problem (1.16)-(5.26)-Table 9.

It is evident that, since we are not in the case of proportionate mixing, analyzing the asymptotic behaviour through the non-linear system (5.8) could potentially incur higher computational costs compared to conducting long

time simulations using (5.9). For $h = 10^{-2}$ and $T = 10^2$, we compute the truncated numerical final size defined in (5.25)

$$\tilde{Z}^{\infty}(h;T) = \begin{bmatrix} 0.246 \\ 0.297 \\ 0.466 \\ 0.656 \\ 0.770 \end{bmatrix}, \qquad \text{and} \qquad \tilde{S}^{\infty}(h;T) := S^0 \circ \tilde{Z}^{\infty}(h;T) = \begin{bmatrix} 2621706 \\ 3860315 \\ 8511097 \\ 8577571 \\ 3274802 \end{bmatrix},$$

with a residual of order of 10^{-12} (here, $\circ$ denotes the component-wise product).

6 NON-LOCAL DISCRETIZATION OF A CLASS OF RENEWAL TYPE EPIDEMIC MODELS

In this chapter, we introduce a numerical method that employs a non-local discretization technique to address the general renewal-type system (1.20), which encompasses the class of age-of-infection epidemic models. Our objective is to develop numerical schemes capable of replicating specific qualitative properties of the continuous system, regardless of the step size. To achieve this goal, we combine implicit and explicit approximations of the convoluted functions. Then we delve into the discrete asymptotic dynamics, showing its adherence to the continuous one. Thus, our analysis is built upon the assumptions outlined in Section 1.4.

6.1 THE NON-LOCAL FINITE DIFFERENCE SCHEME

Consider, for positive values of the step length h, a uniform mesh $\{t_n = nh,\ n = 0,1,\ldots\}$. Our approach for approximating the continuous solution to the non-linear integro-differential system (1.20) involves the following Non-Local Finite Difference (NLFD) scheme

$$\begin{aligned} S_i^{n+1} &= S_i^n - h\beta_i S_i^{n+1} V_i^n, \\ \varphi_i^{n+1} &= \varphi_{i0}(t_{n+1}) + h\beta_i \sum_{j=0}^{n} A_i(t_{n+1-j}) S_i^{j+1} V_i^j, \\ P^{n+1} &= P_0(t_{n+1}) + h \sum_{j=0}^{n} B(t_{n+1-j}) \sum_{r=1}^{M} c_r \varphi_r^j, \end{aligned} \tag{6.1}$$

for $n = 0,1,\ldots$, where

$$V_i^n = \sum_{r=1}^{M} \beta_{ir} \varphi_r^n + \alpha_i P^n, \qquad i = 1,\ldots,M.$$

Here, the starting values $S_i^0 = S_i(0)$, $\varphi_i^0 = \varphi_{i0}(0)$, $i = 1, \dots, M$ and $P^0 = P_0(0)$ are given. Furthermore, $S_i^n \approx S_i(t_n)$, $\varphi_i^n \approx \varphi_i(t_n)$, for $i = 1, \dots, M$, and $P^n \approx P(t_n)$, for $n \geq 0$. We designate the scheme (6.1) as non-standard owing to its non-local approximation of the integral operator in (1.20). Furthermore, since the NSFD method (2.1) is derived from (6.1) with the positions specified in I, the theoretical results of the subsequent sections extend to more general scenarios the investigation carried out in Chapter 2. A pseudo-code implementation of the numerical method (6.1) is reported with the Algorithm 4.

Algorithm 4 : Non-standard Finite Difference Method for (1.20)

Inputs : $h, T, M, \{S_i^0\}_{i=1}^M, \{\varphi_{i0}(t)\}_{i=1}^M, P_0(t), \{A_i(t)\}_{i=1}^M, B(t), \{\beta_i\}_{i=1}^M, \{\beta_{ir}\}_{i,r=1}^M, \{\alpha_i\}_{i=1}^M, \{c_i\}_{i=1}^M$

Outputs : $[t_0, \dots, t_{\bar{n}}], \{[S_i^0, \dots, S_i^{\bar{n}}]\}_{i=1}^M, \{[\varphi_i^0, \dots, \varphi_i^{\bar{n}}]\}_{i=1}^M, [P^0, \dots, P^{\bar{n}}]$

$\bar{n} \leftarrow \lceil T/h \rceil$
$t_0 \leftarrow 0$, $P^0 \leftarrow P_0(0)$
for $1 \leq i \leq M$ **do**
  $\varphi_i^0 \leftarrow \varphi_i(0)$
for $1 \leq i \leq M$ **do**
  $V_i^0 \leftarrow \sum_{r=1}^M \beta_{ir} \varphi_r^0 + \alpha_i P^0$
for $0 \leq n \leq \bar{n} - 1$ **do**
  $t_{n+1} \leftarrow (n+1)\, h$
  for $1 \leq i \leq M$ **do**
    $S_i^{n+1} \leftarrow \frac{S_i^n}{1 + h\beta_i V_i^n}$
    $\varphi_i^{n+1} \leftarrow \varphi_{i0}(t_{n+1}) + h\beta_i \sum_{j=0}^n A_i(t_{n+1-j}) S_i^{j+1} V_i^j$
    $P^{n+1} \leftarrow P_0(t_{n+1}) + h \sum_{j=0}^n B(t_{n+1-j}) \sum_{r=1}^M c_r \varphi_r^j$
    $V_i^{n+1} \leftarrow \sum_{r=1}^M \beta_{ir} \varphi_r^{n+1} + \alpha_i P^{n+1}$

6.1.1 *Non Negativity, Monotonicity and Boundedness Preservation*

Within this subsection we investigate the qualitative properties of the approximation of the solution to (1.20), obtained by (6.1). The following result, concerning non-negativity and monotonicity of the numerical solution, holds true.

Theorem 6.1. *Consider the discrete system (6.1) under the Assumptions A. Then, independently of $h > 0$, the solution sequences $\{S_i^n\}_{n\in\mathbb{N}_0}$, $\{\varphi_i^n\}_{n\in\mathbb{N}_0}$, $i = 1,\dots,M$ and $\{P^n\}_{n\in\mathbb{N}_0}$, are non-negative. Furthermore, the sequence $\{S_i^n\}_{n\in\mathbb{N}_0}$, $i = 1,\dots,M$, is positive and non-increasing.*

Proof. By inductive arguments we demonstrate that the assertions $S_i^n > 0$, $\varphi_i^n \geq 0$ and $P^n \geq 0$, hold for all $n \in \mathbb{N}_0$, $h > 0$ and $1 \leq i \leq M$. For the base case, $n = 0$, the result immediately comes from the non-negativity of the starting values and from $V_i^0 = \sum_{r=1}^{M} \beta_{ir}\varphi_r^0 + \alpha_i P^0 \geq 0$, $i = 1,\dots,M$. Consider $n \geq 1$ and assume that the properties are true for each $0 \leq j \leq n-1$. It follows that $V_i^j \geq 0$, for $0 \leq j \leq n-1$, therefore it is

$$S_i^n = \frac{S_i^{n-1}}{1 + h\beta_i V_i^{n-1}} > 0, \qquad i = 1,\dots,M \tag{6.2}$$

and then, from (6.1), also $\varphi_i^n \geq 0$, $i = 1,\dots,M$ and $P^n \geq 0$. Furthermore, from (6.2), $S_i^n \leq S_i^{n-1}$, for all $n \geq 1$ and $i = 1,\dots,M$, which completes the proof. □

The existence of a bound for the numerical solution, independent of the stepsize value, is provided by the following result.

Theorem 6.2. *Consider the discrete system (6.1) under the assumptions Assumptions A and B. Then, independently of $h > 0$, the solution sequences $\{S_i^n\}_{n\in\mathbb{N}_0}$, $\{\varphi_i^n\}_{n\in\mathbb{N}_0}$, $i = 1,\dots,M$ and $\{P^n\}_{n\in\mathbb{N}_0}$, are bounded.*

Proof. From Theorem 6.1, $\{S_i^n\}_{n\in\mathbb{N}_0}$ is a non-increasing sequence, thus it is bounded from above by S_i^0, $i = 1,\dots,M$. Consider φ_i^n, from the first equation and the second equation of (6.1), it is

$$\varphi_i^n \leq \varphi_{0,max} + A_{max}(S_i^0 - S_i^{n+1}) \leq \varphi_{0,max} + A_{max}S_i^0,$$

for $i = 1,\dots,M$ and $n \geq 0$. Finally, the inequality

$$P^n \leq P_{0,max} + \bar{B}\sum_{r=1}^{M} c_r \left(\varphi_{0,max} + A_{max}S_r^0\right),$$

directly follows from the assumptions and the third equation in (6.1). □

As previously discussed in Section 1.4, the continuous-time solution to (1.20) is non-negative and bounded from above. Therefore, the results of this section show that the proposed numerical method retains these properties unconditionally with respect to the discretization step-length.

6.1.2 *Error Analysis and Convergence*

To investigate the convergence of the numerical method (6.1), we assume that the known functions are continuously differentiable over the interval $[0, T]$, where $T < +\infty$. Our primary objective is to analyze the behaviour of the local truncation error, as defined in [63]. For the sake of this discussion, we narrow our focus to the case where $M = 1$, since extending the analysis to $M > 1$ is straightforward. In this particular scenario, the local truncation error of the discretization in (6.1) can be expressed as follows

$$\delta^n(h) = \int_0^{t_n} \begin{bmatrix} -\beta_1 S_1(\tau) V_1(\tau) \\ \beta_1 S_1(\tau) V_1(\tau) A_1(t_n - \tau) \\ c_1 B(t_n - \tau) \varphi_1(\tau) \end{bmatrix} d\tau - h \sum_{j=0}^{n-1} \begin{bmatrix} -\beta_1 S_1(t_{j+1}) V_1(t_j) \\ \beta_1 S_1(t_{j+1}) V_1(t_j) A_1(t_{n-j}) \\ c_1 B(t_{n-j}) \varphi_1(t_j) \end{bmatrix}, \tag{6.3}$$

where $n = 0, \ldots, \bar{n}$ and $T = \bar{n}h$. From the mean value theorem (see, for instance [61, Sec. 1.3]), there exist $\theta_j \in (0, 1)$, $j = 0, \ldots, n-1$, such that

$$\begin{aligned} &\int_0^{t_n} \begin{bmatrix} -\beta_1 S_1(\tau) V_1(\tau) \\ \beta_1 S_1(\tau) V_1(\tau) A_1(t_n - \tau) \\ c_1 B(t_n - \tau) \varphi_1(\tau) \end{bmatrix} d\tau \\ &= \sum_{j=0}^{n-1} \int_{t_j}^{t_{j+1}} \begin{bmatrix} -\beta_1 (S_1(\tau + h) - h S'(\tau + \theta_j h)) V_1(\tau) \\ \beta_1 (S_1(\tau + h) - h S'(\tau + \theta_j h)) V_1(\tau) A_1(t_n - \tau) \\ c_1 B(t_n - \tau) \varphi_1(\tau) \end{bmatrix} d\tau. \end{aligned}$$

Moreover, owing to the convergence properties of the rectangular quadrature rule (see, for example, [34]), for each $0 \leq j \leq n-1$, the norm

$$\left\| \int_{t_j}^{t_{j+1}} \begin{bmatrix} -\beta_1 S_1(\tau+h) V_1(\tau) \\ \beta_1 S_1(\tau+h) V_1(\tau) A_1(t_n-\tau) \\ c_1 B(t_n-\tau)\varphi_1(\tau) \end{bmatrix} d\tau - h \begin{bmatrix} -\beta_1 S_1(t_{j+1}) V_1(t_j) \\ \beta_1 S_1(t_{j+1}) V_1(t_j) A_1(t_{n-j}) \\ c_1 B(t_{n-j})\varphi_1(t_j) \end{bmatrix} \right\|,$$

is bounded from above by the product Ch^2, with $C > 0$, independent of h. Therefore, from (6.3), it follows that

$$\|\delta^n(h)\| \leq \bar{n} C h^2 + h \sum_{j=0}^{\bar{n}-1} \int_{t_j}^{t_{j+1}} \left\| \begin{bmatrix} -\beta_1 S'(\tau+\theta_j h) V_1(\tau) \\ \beta_1 S'(\tau+\theta_j h) V_1(\tau) A_1(t_n-\tau) \end{bmatrix} \right\| d\tau,$$

for each $n = 0, \ldots, \bar{n}$. Hence

$$\max_{0 \leq n \leq \bar{n}} \|\delta^n(h)\| \leq \tilde{C} h, \tag{6.4}$$

being $\tilde{C}$ a positive constant not depending on h.

With the following theorem we analyse the behaviour of the global error

$$E^n(h) = \left[\ldots, \quad S_i(t_n) - S_i^n, \quad \ldots, \quad \varphi_i(t_n) - \varphi_i^n, \quad \ldots, \quad P(t_n) - P^n \right]^T \in \mathbb{R}^{2M+1},$$

arising in approximating the continuous-time solution to (1.20) by (6.1) and provide conditions for the linear convergence of the numerical method.

Theorem 6.3. *Assume that the given functions $A_i(t)$, $i = 1, \ldots, M$ and $B(t)$, describing problem (1.20), are continuously differentiable on an interval $[0, T]$. Let $\{S_i^n\}_{n \in \mathbb{N}_0}$, $\{\varphi_i^n\}_{n \in \mathbb{N}_0}$, $\{P^n\}_{n \in \mathbb{N}_0}$ be the approximations of the solution to (1.20), defined by (6.1) with $h = T/\bar{n}$ and $\bar{n}$ positive integer. Then*

$$\lim_{h \to 0} \max_{0 \leq n \leq \bar{n}} \|E^n(h)\| = 0.$$

Furthermore, the order of convergence is 1.

Proof. Here, we confine our proof to the case of $M = 1$ since, by the same arguments, the result readily extends to $M > 1$. When $M = 1$, the continuous system (1.20) reads

$$\begin{aligned}\begin{bmatrix} S_1(t_n) \\ \varphi_1(t_n) \\ P(t_n) \end{bmatrix} &= \begin{bmatrix} S_1(0) \\ \varphi_{10}(t_n) \\ P_0(t_n) \end{bmatrix} + \int_0^{t_n} \begin{bmatrix} -\beta_1 S_1(\tau) V_1(\tau) \\ \beta_1 S_1(\tau) V_1(\tau) A_1(t_n - \tau) \\ c_1 B(t_n - \tau) \varphi_1(\tau) \end{bmatrix} d\tau \\ &= \begin{bmatrix} S_1(0) \\ \varphi_{10}(t_n) \\ P_0(t_n) \end{bmatrix} + h \sum_{j=0}^{n-1} \begin{bmatrix} -\beta_1 S_1(t_{j+1}) V_1(t_j) \\ \beta_1 S_1(t_{j+1}) V_1(t_j) A_1(t_{n-j}) \\ c_1 B(t_{n-j}) \varphi_1(t_j) \end{bmatrix} + \delta^n(h),\end{aligned}$$

for $n = 0, \ldots, \bar{n}$, with $\delta^n(h)$ defined in (6.3). Subtracting (6.1) from the relation above leads to the global error

$$E^n(h) = \delta^n(h) + h \sum_{j=0}^{n-1} \begin{bmatrix} -\beta_1 & 0 & 0 \\ 0 & \beta_1 A_1(t_{n-j}) & 0 \\ 0 & 0 & c_1 B(t_{n-j}) \end{bmatrix} \begin{bmatrix} S_1(t_{j+1}) V_1(t_j) - S_1^{j+1} V_1^j \\ S_1(t_{j+1}) V_1(t_j) - S_1^{j+1} V_1^j \\ \varphi_1(t_j) - \varphi_1^j \end{bmatrix}, \tag{6.5}$$

for $n = 0, \ldots, \bar{n}$. Furthermore, for each $j = 0, \ldots, n-1$,

$$\begin{aligned}|S_1(t_{j+1}) V_1(t_j) - S_1^{j+1} V_1^j| &= |S_1(t_{j+1})(V_1(t_j) - V_1^j) + V_1^j (S_1(t_{j+1}) - S_1^{j+1})| \\ &\leq K(\|E^j(h)\| + \|E^{j+1}(h)\|),\end{aligned}$$

hence, from (6.5),

$$\|E^n(h)\| \leq \|\delta^n(h)\| + h\tilde{K} \sum_{j=0}^{n-1} (\|E^j(h)\| + \|E^{j+1}(h)\|),$$

with K and $\tilde{K}$ positive constants depending on the parameters and the known functions of problem (1.20) but not on h. Therefore, for a sufficiently small h,

$$\|E^n(h)\| \leq \frac{\|\delta^n(h)\|}{1 - h\tilde{K}} + h \frac{2\tilde{K}}{1 - h\tilde{K}} \sum_{j=0}^{n-1} \|E^j(h)\|, \qquad n = 0, \ldots, \bar{n}.$$

Finally, the Gronwall discrete inequality yields (see, for instance [63, p.101]),

$$\|E^n(h)\| \leq \left(\frac{\max_{0\leq n\leq \bar{n}} \|\delta^n(h)\|}{1-h\tilde{K}} + h\,\frac{2\tilde{K}(S_1^0+\varphi_1^0+P^0)}{1-h\tilde{K}} \right) \exp\left(\frac{2\tilde{K}T}{1-h\tilde{K}}\right),$$

for $n = 0, \ldots, \bar{n}$. Then, from (6.4), the result follows. □

6.2 ASYMPTOTIC BEHAVIOUR OF THE NUMERICAL SOLUTION

To investigate the asymptotic behaviour of the numerical solution to system (6.1), we establish some preliminary theoretical results.

Lemma 6.4. *Consider the discrete system* (6.1), *for* $i = 1, \ldots, M$, *it is*

$$\sum_{n=0}^{+\infty} V_i^n = \alpha_i \sum_{n=0}^{+\infty} P_0(t_n) + \sum_{r=1}^{M} \left(\beta_{ir} + \alpha_i c_r h \sum_{n=1}^{+\infty} B(t_n)\right) \left(S_r^0 \left(1 - \frac{S_r^\infty(h)}{S_r^0}\right) \sum_{n=1}^{+\infty} A_r(t_n)\right) + \sum_{r=1}^{M} \left(\beta_{ir} + \alpha_i c_r h \sum_{n=1}^{+\infty} B(t_n)\right) \left(\sum_{n=0}^{+\infty} \varphi_{0r}(t_n)\right).$$

Proof. Summing from 0 to ∞ in the last equation of (6.1), interchanging the order of summation and adding to both members $P(0) = P^0$, it is

$$\sum_{n=0}^{+\infty} P^n = \sum_{n=0}^{+\infty} P_0(t_n) + \sum_{r=1}^{M} c_r h \sum_{n=1}^{+\infty} B(t_n) \sum_{n=0}^{+\infty} \varphi_r^n.$$

The same can be done for the second equation of (6.1), where taking into account that, from the first of (6.1) it is $h\beta_r \sum_{j=0}^{+\infty} S_r^{j+1} V_r^j = S_r^0 - S_r^\infty(h)$, we have

$$\sum_{n=0}^{+\infty} \varphi_r^n = (S_r^0 - S_r^\infty(h)) \sum_{n=1}^{+\infty} A_r(t_n) + \sum_{n=0}^{+\infty} \varphi_{0r}(t_n), \tag{6.6}$$

for any $r = 1, \dots, M$. Combining the previous expressions with

$$\sum_{n=0}^{+\infty} V_i^n = \alpha_i \sum_{n=0}^{+\infty} P^n + \sum_{r=1}^{M} \beta_{ir} \sum_{n=0}^{+\infty} \varphi_r^n, \qquad i = 1, \dots, M,$$

we get the result. □

Theorem 6.5. *Consider equation (6.1) with Assumptions A, B and C, then there exists* $0 < \bar{V} < +\infty$, *such that* $h \sum_{n=0}^{+\infty} V_r^n < \bar{V}$.

Proof. The result comes from 6.4 since, for $i = 1, \dots, M$, it is

$$h \sum_{n=0}^{+\infty} V_i^n \leq \alpha_i \bar{P}_0 + \left(\max_{r=1,\dots,M} \beta_{ir} + \bar{B}\alpha_i \max_{r=1,\dots,M} c_r \right) \left(\bar{A} \sum_{r=1}^{M} S_r^0 + M\bar{\varphi}_0 \right),$$

which completes the proof. □

6.2.1 *Numerical Final State and Asymptotic Convergence*

The results of Section 6.1 establish the dynamical consistency of the scheme (6.1), whose solution unconditionally retains the basic properties of the model (1.20). Our objective here is to prove that the asymptotic behaviour of the numerical solution $\{S_i^n\}_{n \in \mathbb{N}_0}$, $\{\varphi_i^n\}_{n \in \mathbb{N}_0}$, exactly replicates its continuous counterpart.

Firstly we point out that, from Assumptions C and (6.6),

$$h \sum_{n=0}^{+\infty} \varphi_i^n \leq (S_i^0 - S_i^\infty(h))\bar{A} + \bar{\varphi}_0 < +\infty, \qquad i = 1, \dots, M, \tag{6.7}$$

hence, in compliance with the theoretical observations of Section 1.4, we have $\lim_{n \to +\infty} \varphi_i^n = 0$, for each $h > 0$ and $1 \leq i \leq M$.

Referring to Theorem 6.1, the numerical scheme (6.1) exhibits a monotonicity-preserving property for the sequence $\{S_i^n\}_{n \in \mathbb{N}_0}$, ensuring the existence of the

discrete final state $S_i^\infty(h) = \lim_{n\to\infty} S_i^n$, $i = 1, \dots, M$, regardless of the value of $h > 0$. Furthermore, from the first equation of (6.1) it is

$$S_i^{n+1} = \frac{S_i^0}{\prod_{j=0}^n (1 + h\beta_i V_i^j)}, \qquad n \in \mathbb{N}_0,$$

therefore the asymptotic numerical solution $S_i^\infty(h)$ satisfies the relation

$$\log\left(\frac{S_i^0}{S_i^\infty(h)}\right) = \sum_{n=0}^{+\infty} \log\left(1 + h\beta_i V_i^n\right), \qquad i = 1, \dots, M. \tag{6.8}$$

In Chapter 1.4 we proved that the limit of the continuous solution is as a root of the non-linear system $R_i(x) = 0$, $i = 1, \dots, M$, where $R_i : \mathbb{R}^M \to \mathbb{R}$ is defined in (1.22), under the assumption that a solution to this system exists. Aiming to investigate the discrete equivalent of this property we introduce

$$U_i(h) = \frac{\sum_{n=0}^{+\infty} \log\left(1 + h\beta_i V_i^n\right)}{h\beta_i \sum_{n=0}^{+\infty} V_i^n}, \qquad i = 1, \dots, M \tag{6.9}$$

and for $h > 0$, $x = [x_1, \dots, x_M]^T$, and $i = 1, \dots, M$,

$$\begin{aligned} R_i(x,h) = &\log\left(\frac{S_i^0}{x_i}\right) - \beta_i \alpha_i U_i(h) h \sum_{n=0}^{+\infty} P_0(t_n) - \beta_i U_i(h) \sum_{r=1}^{M} \left(\beta_{ir} + \alpha_i c_r h \sum_{n=1}^{+\infty} B(t_n)\right) \\ &\cdot \left(S_r^0 \left(1 - \frac{x_r}{S_r^0}\right) h \sum_{n=1}^{+\infty} A_r(t_n) + h \sum_{n=0}^{+\infty} \varphi_{0r}(t_n)\right). \end{aligned} \tag{6.10}$$

Because of (6.9), the relation (6.8) is equivalent to

$$\log \frac{S_i^0}{S_i^\infty(h)} - U_i(h) \left(h\beta_i \sum_{n=0}^{+\infty} V_i^n\right) = 0, \qquad i = 1, \dots, M.$$

Hence, upon substituting the expression for $\sum_{n=0}^{+\infty} V_i^n$ from Lemma 6.4 into it, it becomes evident that for any given positive h, the asymptotic numerical solution $S_i^\infty(h)$, $i = 1, \dots, M$, is a root of the non-linear system of equations

$$R_i(x(h), h) = 0, \qquad i = 1, \dots, M, \tag{6.11}$$

if a solution to (6.11) exists.

To show that the behaviour of $S_i^\infty(h)$ mirrors the one of the asymptotic continuous-time solution, we firstly prove that (6.11) admits a unique solution for $h > 0$. To do that, we consider a general non-linear algebraic system,

$$\Gamma_i(x_1, \dots, x_M) = 0, \qquad i = 1, \dots, M, \tag{6.12}$$

for which the following result holds.

Theorem 6.6. *Consider $D_i = (a_i, b_i]$, for $i = 1, \dots, M$ and denote by $D = \prod_{i=1}^M D_i$. Let $\Gamma_i : D \to \mathbb{R}$, $i = 1, \dots, M$, be a twice continuously differentiable function and assume that, for each $i = 1, \dots, M$ and any fixed $(x_1, \dots, x_{i-1}, x_{i+1}, \dots, x_M) \in \prod_{j=1, j\neq i}^M D_j$,*

A) *the univariate function $\Gamma_i(x_1, \dots, x_{i-1}, \zeta, x_{i+1}, \dots, x_M)$ admits at least one zero lying in D_i;*

B) *$\lim_{\zeta \to a_i^+} \Gamma_i(\dots, x_{i-1}, \zeta, x_{i+1}, \dots) > 0$ and $\Gamma_i(\dots, x_{i-1}, b_i, x_{i+1}, \dots) < 0$;*

C) *$\partial_{x_j} \Gamma_i(x) > 0$, for all $x \in D$ and $j \in \{1, \dots, M\} \setminus \{i\}$;*

D) *$\partial^2_{x_j x_k} \Gamma_i(x) \geq 0$, for all $x \in D$ and $j, k \in \{1, \dots, M\}$.*

Then, the system (6.12) has a unique solution in D.

Proof. We proceed by induction on M. Choose $M = 2$. Let $x_1 \in D_1$, then from A), B) and D), $\Gamma_2(x_1, \zeta)$ has a unique zero $\xi_2 = \xi_2(x_1) \in D_2$, with $\partial_{x_2} \Gamma_2(x_1, \xi_2) < 0$. Therefore, taking in account the arbitrariness of x_1 in D_1, from the implicit function theorem, $\forall x \in D_1$, there exists a unique $z(x) \in D_2$ such that $u_2(x) := \Gamma_2(x, z(x)) \equiv 0$. Since $u_2'(x) \equiv 0$ and $u_2''(x) \equiv 0$, using assumption C) and the fact that A), B) and D) imply $\partial_{x_2} \Gamma_2(x, z(x)) < 0$, we conclude that $z'(x) > 0$ and $z''(x) \geq 0$. Now, we exploit the function $z(x)$ to build a solution to system (6.12) with $M = 2$.

For an arbitrary $\alpha_0 \in D_1$, let $\alpha_1 \in D_1$ be the unique root of the function $\Gamma_1(\zeta, z(\alpha_0))$. If $\alpha_1 = \alpha_0$, then $(\alpha_0, z(\alpha_0))$ is a solution to (6.12) with $M = 2$. Otherwise we can suppose, with no loss of generality, that $\alpha_0 < \alpha_1$. It follows that $z(\alpha_0) < z(\alpha_1)$ and, from C), $0 = \Gamma_1(\alpha_1, z(\alpha_0)) < \Gamma_1(\alpha_1, z(\alpha_1))$. Thus $\Gamma_1(\zeta, z(\alpha_1))$ has a unique zero $\alpha_2 \in D_1$, for which $\alpha_0 < \alpha_1 < \alpha_2$. Similar arguments lead to an increasing sequence $\{\alpha_n\}_{n\in\mathbb{N}} \subset D_1$, such that

$$\Gamma_1(\alpha_{n+1}, z(\alpha_n)) = 0, \qquad \text{for all } n \in \mathbb{N},$$

$$\alpha = \lim_{n\to+\infty} \alpha_n, \qquad \text{and} \qquad \Gamma_1(\alpha, z(\alpha)) = \Gamma_2(\alpha, z(\alpha)) = 0.$$

Hence, $(\alpha, z(\alpha)) \in D$ is a solution to system (6.12), with $M = 2$.
To prove its uniqueness, we consider another solution $(\beta, \gamma) \in D$ and define the function $u_1 : x \in D_1 \to \Gamma_1(x, z(x))$. Since $\Gamma_2(\beta, \gamma) = 0$, it follows that $\gamma = z(\beta)$ and $u_1(\beta) = 0 = u_1(\alpha)$. Since u_1 is convex and, from B), it admits a unique zero $\beta = \alpha$, then the solution to (6.12) for $M = 2$ is unique.
Now assume that the result holds for any $M-1$ dimensional system satisfying A)–D). Consider $M > 2$, proceeding as in the previous case, for each $(x_1, \ldots, x_{M-1}) \in \prod_{j=1}^{M-1} D_j$, there exists a unique function $z(x_1, \ldots, x_{M-1})$ such that

$$\Gamma_M(x_1, \ldots, x_{M-1}, z(x_1, \ldots, x_{M-1})) = 0,$$

$$\partial_{x_i} z(x_1, \ldots, x_{M-1}) > 0 \quad \text{and} \quad \partial^2_{x_i^2} z(x_1, \ldots, x_{M-1}) \geq 0, \quad i = 1, \ldots, M-1. \tag{6.13}$$

Define, for $i = 1, \ldots, M-1$, the functions

$$u_i(x_1, \ldots, x_{M-1}) = \Gamma_i(x_1, \ldots, x_{M-1}, z(x_1, \ldots, x_{M-1})). \tag{6.14}$$

Now we want to prove that assumptions A)-D) are true for the $M-1$ dimensional system

$$u_i(x_1, \ldots, x_{M-1}) = 0, \qquad i = 1, \ldots, M-1, \tag{6.15}$$

which is equivalent to (6.12). Regarding the assumption A), we need to prove that, for each fixed $(x_1, \dots, x_{i-1}, x_{i+1}, \dots, x_{M-1}) \in \prod_{j=1, j\neq i}^{M-1} D_j$, the function

$$u_i(x_1, \dots, x_{i-1}, \zeta, x_{i+1}, \dots, x_{M-1})$$

has at least one zero in D_i, $i = 1, \dots, M-1$. For the theorem assumptions, given $\alpha_0 \in D_i$, there exists a unique $\alpha_1 \in D_i$, such that

$$\Gamma_i(x_1, \dots, x_{i-1}, \alpha_1, x_{i+1}, \dots, x_{M-1}, z(x_1, \dots, x_{i-1}, \alpha_0, x_{i+1}, \dots, x_{M-1})) = 0.$$

If $\alpha_0 = \alpha_1$, we get the result. Otherwise, proceeding as in the $M = 2$ case, we construct a monotone sequence $\{\alpha_n\}_{n\in\mathbb{N}}$ such that

$$\alpha = \lim_{n\to+\infty} \alpha_n \in D_i \qquad \text{and} \qquad u_i(x_1, \dots, x_{i-1}, \alpha, x_{i-1}, \dots, x_{M-1}) = 0.$$

Furthermore, B), C) and D) immediately follow from the hypotheses of the theorem, from (6.13) and from (6.14). Therefore, induction hypotheses assure that there exists a unique $\lambda \in \prod_{i=1}^{M-1} D_i$, root of the system (6.15). It follows that $(\lambda, z(\lambda))$ is a solution to the original system (6.12).
Finally, if (η, θ) is another solution of (6.12), with $\eta \in \prod_{i=1}^{M-1} D_i$ and $\theta \in D_M$, then $\theta = z(\eta)$. Thus η solves (6.15) and the uniqueness of its solution, that we have just proved, yields $\eta = \lambda$, which completes the proof. □

In order to prove that Theorem 6.6 applies to the non-linear system (6.11) for $h > 0$, we consider $\Gamma_i(x) = R_i(x, h)$, where $R_i(x, h)$ is defined in (6.10) and set $D_i = (0, S_i^0]$ for $i = 1, \dots, M$. We address, for $h > 0$ and $i = 1, \dots, M$, the twice continuously differentiable function $R_i(x_1, \dots, x_{i-1}, \zeta, x_{i+1}, \dots, x_M, h)$, with $0 < \zeta \leq S_i^0$ and $0 < x_j \leq S_j^0$ fixed, for $j \in \{1, \dots, M\} \setminus \{i\}$. Since

$$\begin{aligned} &\lim_{\zeta\to 0^+} R_i(x_1, \dots, x_{i-1}, \zeta, x_{i+1}, \dots, x_M, h) = +\infty, \\ &\qquad R_i(x_1, \dots, x_{i-1}, S_i^0, x_{i+1}, \dots, x_M, h) \leq 0, \qquad\qquad i = 1, \dots, M, \end{aligned}$$

there exists a positive $S_i^\infty(h) \leq S_i^0$, such that

$$R_i(x_1, \dots, x_{i-1}, S_i^\infty(h), x_{i+1}, \dots, x_M, h) = 0, \qquad\qquad i = 1, \dots, M.$$

Moreover, for each $i, j = 1, \ldots, M$, with $i \neq j$, it is

$$\partial_{x_j} R_i(x,h) > 0, \qquad \partial^2_{x_j^2} R_i(x,h) = 0 \qquad \text{and} \qquad \partial^2_{x_i^2} R_i(x,h) = 1/x_i^2.$$

As a result, all the hypotheses of Theorem 6.6 are fulfilled. This implies that, for each $h > 0$, the system (6.11) has a unique solution $S^\infty(h) = [S_1^\infty(h), \ldots, S_M^\infty(h)]^T$ with $0 < S_i^\infty(h) \leq S_i^0$, for $i = 1, \ldots, M$. This solution represents the asymptotic numerical solution $\lim_{n\to\infty} S^n(h)$ and, from this perspective, we may refer to the non-linear system (6.11) as the numerical final state relation.

Regarding the continuous-time system (1.20), the observations of Section 1.4 indicate that if a solution exists for the non-linear system

$$R_i(x) = 0, \qquad i = 1, \ldots, M, \tag{6.16}$$

with $R_i(x)$ defined in (1.22), then the asymptotic analytical solution

$$S_i(\infty) = \lim_{t\to+\infty} S_i(t), \qquad i = 1, \ldots, M,$$

is indeed one of its roots. Thus, Theorem 6.6 may be applied to establish the asymptotic state $S(\infty) = [S_1(\infty), \ldots, S_M(\infty)]^T$ as the unique solution belonging to $\prod_{i=1}^M (0, S_i^0]$, of the continuous final state relation (6.16). We explore, as the step-length h vanishes, the asymptotic properties of the numerical solution computed by (6.1) and delve into its connection with $S(\infty)$ and the associated algebraic limiting system.

We base our investigation on the assumptions that for each $h > 0$,

$$\begin{aligned}
&\lim_{h\to 0} h \sum_{n=1}^{+\infty} A_i(t_n) = \int_0^{+\infty} A_i(t)\, dt, \qquad && \lim_{h\to 0} h \sum_{n=1}^{+\infty} B(t_n) = \int_0^{+\infty} B(t)\, dt, \\
&\lim_{h\to 0} h \sum_{n=1}^{+\infty} \varphi_{0i}(t_n) = \int_0^{+\infty} \varphi_{0i}(t)\, dt, && i = 1, \ldots, M.
\end{aligned} \tag{6.17}$$

The mathematical conditions outlined in (6.17) hold true under various scenarios. For instance, they are satisfied when the involved functions exhibit ul-

timate non-increasing behaviour or when their derivatives belong to $L^1[0,+\infty)$ (as detailed in [71] and related references).

The following lemma establishes a preliminary result.

Lemma 6.7. *Consider equation (6.1) with Assumptions A, B and C, then, for $U_i(h)$ defined in (6.9), it is*

$$\lim_{h\to 0} U_i(h) = 1, \qquad i = 1,\dots,M. \tag{6.18}$$

Proof. From its definition and Lemma 6.4 it follows that for $n \in \mathbb{N}_0$, the term V_i^n, $i = 1,\dots,M$, is bounded by a constant independent of h. This implies that $\lim_{h\to 0} hV_i^n = 0$, uniformly with respect to n. In this situation, we are allowed to proceed as in the proof of Theorem 2.7 to get (6.18). □

The following result addresses the convergence, as h tends to zero, of the asymptotic numerical solution to the continuous one.

Theorem 6.8. *Consider a bounded subset D of $\mathbb{R}^M$ and a function*

$$\Phi : D \times [0,+\infty) \to \mathbb{R}^M,$$

satisfying:

- *$\Phi(w,h)$, continuous for each $(w,h) \in D \times [0,+\infty)$;*
- *equation $\Phi(w,h) = 0$, has at least one solution $\bar{w}(h) \in D$, $\forall h \in [0,+\infty)$;*
- *equation $\Phi(w,h) = 0$ has a unique solution for $h = 0$, namely $\bar{w} = \bar{w}(0) \in D$.*

Then $\lim_{h\to 0} \bar{w}(h) = \bar{w}$.

Proof. An extension of the arguments of Theorem 4.12's proof to the case of functions defined on open sets yields the result. □

Consider $D = \prod_{i=1}^M (0, S_i^0]$ and the vector function

$$R \;:\; (x,h) \in D \times \mathbb{R}_0^+ \;\longrightarrow\; [R_1(x,h),\dots,R_M(x,h)]^T \in \mathbb{R}^M,$$

with $R_i(x)$, $i = 1,\dots,M$, defined in (1.22). The hypotheses of Theorem 6.8 are valid for the system $R(x,h) = 0$. Furthermore, owing to the assumptions

(6.17) and the result of Lemma 6.7, the system corresponding to $h = 0$ is given by (6.16). Therefore, Theorem 6.8 establishes a connection between the asymptotic numerical solution $S_i^\infty(h)$, $i = 1, \dots, M$ and the solution $S_i(\infty)$, $i = 1, \dots, M$ of the non-linear system (6.16), thus emphasizing that the limit of $S_i^\infty(h)$, $i = 1, \dots, M$, for $h \to 0$ exists and

$$\lim_{h\to 0} \lim_{n\to+\infty} S_i^n(h) = \lim_{h\to 0} S_i^\infty(h) = S_i(\infty), \qquad i = 1, \dots, M. \tag{6.19}$$

The outcome above constitutes the primary accomplishment of the non-local method in (6.1), which is established as an efficient tool to simulate the long-term dynamics of the system (1.20).

6.3 NUMERICAL EXPERIMENTS

As highlighted in Section 1.4, the continuous-time system (1.20) serves as a comprehensive theoretical framework encompassing various epidemic models documented in the literature. We focus on four specific cases of particular interest, which, owing to their connection with the age-of-infection models outlined in Chapter 1, serve as crucial test cases in our analysis. Within this context, the final state $S(\infty)$ and the discrete final state $S^\infty(h)$ represent the continuous and the numerical final size of the epidemic, respectively. Furthermore, the non-linear systems (6.16) and (6.11) correspond to the final size relation of the continuous solution to (1.20) and to its approximation computed by (6.1), respectively. Sections 6.1 and 6.2 analyse how the qualitative properties of epidemic models are preserved when the system is integrated by the numerical scheme (6.1). As a matter of fact, Theorems 6.1 and 6.2 guarantee that the numerical solution remains both non-negative and bounded for any positive stepsize h, thereby ensuring a reliable simulation of the epidemic using the method (6.1). The analysis of the preceding section is applicable to demonstrate that the asymptotic behaviour is also preserved, as the numerical final size converges to the epidemic's final size as h approaches zero. This convergence is experimentally verified and showed with figures and tables, illustrating the results of our numerical simulations for each test model under consideration.

THE AGE-OF-INFECTION MODEL Our first case study involves the original Kermack and McKendrick model (1), derived from (1.20) under the identifications of the parameters in I. In this case, the final size of the epidemic $S(\infty)$ is the unique root of the non-linear equation (1.7) which, if (2.3) holds true, reduces to

$$\log \frac{S^0}{x} - R_0 \left(1 - \frac{x}{N}\right) = 0, \tag{6.20}$$

where R_0 is the basic reproduction number defined in (1.4) (we refer to [9, 25] for more general discussions on R_0 and its numerical computation). Thus, when the identifications in I hold, the non-linear system (6.16) corresponds to the equation (6.20). Furthermore, in this case, the non-local discretization (6.1) coincides with the NSFD numerical method (2.1). In Chapter 2, Theorem 2.8 demonstrates that the limit of the numerical final size $S^\infty(h)$, as $h \to 0$, corresponds to the continuous-time final size, provided that this limit exists. The results of Section 6.2 and Theorem 6.8 then apply to ensure the existence of the aforementioned limit, under the smoothness assumption (2.4). As a results, we can assert that the numerical method (6.1) is asymptotically coherent with (1.1). We integrate problem (1.1) on $[0, 100]$ with $\beta = 10^{-4}$, $S^0 = 49950$, $N = 50000$ and select the infectivity function as follows

$$A(t) = \begin{cases} 0 & 0 \le t \le \tau_a, \\ \dfrac{(t-\tau_a)(\tau_h - t)}{(\tau_b - \tau_a)(\tau_h - \tau_e)} & \tau_a < t < \tau_b, \\ \dfrac{\tau_h - t}{\tau_h - \tau_e} & \tau_b \le t < \tau_h, \\ 0 & t \ge \tau_h, \end{cases} \tag{6.21}$$

with $\tau_e = 12$, $\tau_a = 14$, $\tau_b = 16$, $\tau_h = 19$ (we refer to [2] for further details on the low regularity kernel). The results of the simulation by (6.1) for $h = 0.1$, presented in Figure 16, comply with the theoretical findings. The dot at the left end point of the integration interval represents the value $S(\infty) = 148.83$ of the continuous final size, obtained by solving the non-linear equation (6.20) through the Matlab routine fzero. We compare this value with the discrete final size $S^\infty(h)$ obtained by running the method (6.1) in the interval $[0, 1000]$. More specifically, we have $S^\infty(10^{-3}) = 149.97$ and the accuracy in

the approximation improves linearly as the stepsize $h \to 0$. Furthermore, in compliance with (6.7), the endpoint approximation of φ is numerically zero. Other numerical tests are reported in Section (2.3).

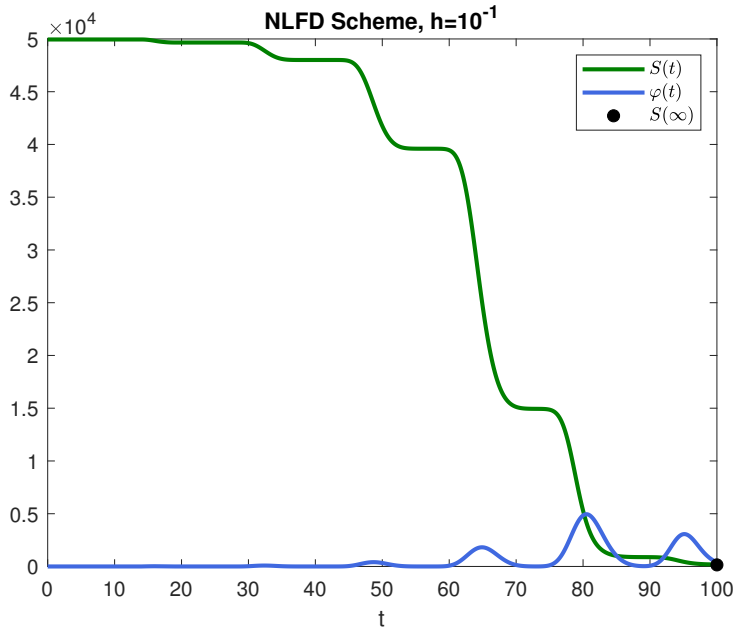

Figure 16: Long time behaviour of the non-local finite difference numerical solution to problem (1.1)-(6.21).

THE SYMPTOMATIC AND ASYMPTOMATIC AGE-OF-INFECTION MODEL

The comprehensive renewal system (1.20) incorporates the age-of-infection model which considers both symptomatic and asymptomatic infection pathways. In fact, (1.10) can be derived from (1.20) by configuring the parameters as described in II. In this case, the final size of the epidemic $S(\infty)$ is the root of the non-linear equation

$$\log \frac{S^0}{x} - \mathcal{F}\left(\frac{S_0 - x}{N}\right) - \frac{a}{N}\left(\int_0^{+\infty} \varphi_0^s(t)\, dt + \int_0^{+\infty} \varphi_0^a(t)\, dt\right) = 0, \quad (6.22)$$

where $\mathcal{F} = a\int_0^{+\infty} f(t)A^s(t)\, dt + a\int_0^{+\infty}(1-f(t))A^a(t)\, dt$, is considered to be finite. Thus, if $f(t)$ is constant with respect to t, $\mathcal{F} = R_0$ and the relation (1.13) is recovered. The theoretical results of Section 6.2 establish the uniqueness of $S(\infty)$ as a root of (6.22), within the interval $(0, S^0]$. Furthermore, the con-

vergence of the discrete final size provided by (6.19) validates the numerical method (6.1) as a dependable tool for predicting the epidemic's asymptotic behaviour and the total count of symptomatic and asymptomatic patients. These insights expand upon the research conducted in [7].

Our test concerns problem (1.10) with $0 \leq t \leq 30$ and

$$\begin{aligned} A^s(t) &= \pi^s(t)B^s(t), & B^s(t) &= \exp(-\sqrt{t}/2), & \pi^s(t) &= 5\gamma(t;1,2), \\ A^a(t) &= \pi^a(t)B^a(t), & B^a(t) &= (1+0.6t)^{-1}, & \pi^a(t) &= \gamma(t;3,2), \\ \varphi_0^s(t) &= (N-S^0)A^s(t), & \varphi_0^a(t) &= (N-S^0)A^a(t), & f(t) &= 0.783, \end{aligned} \tag{6.23}$$

where

$$\gamma(t;k,\theta) = \frac{t^{k-1}\theta^{-k}e^{-t/\theta}}{\int_0^{+\infty} x^{k-1}e^{-x}\,dx},$$

is the gamma probability density function. Here, we approximate the number of symptomatic and asymptomatic individuals at time t_n, $I^s(t_n)$ and $I^a(t_n)$ respectively, by employing for (1.11) the same non-local discretization technique of (6.1), as follows

$$\begin{aligned} I^{s,n} &= I_0^s(t_n) + h\frac{a}{N}f\sum_{j=0}^{n-1} B^s(t_{n-j})S^{j+1}(\varphi^{s,j}+\varphi^{a,j}), \\ I^{a,n} &= I_0^a(t_n) + h\frac{a}{N}(1-f)\sum_{j=0}^{n-1} B^a(t_{n-j})S^{j+1}(\varphi^{s,j}+\varphi^{a,j}). \end{aligned}$$

Here, we take $I_0^* = (N-S_0)B^*(t)$, for $* \in \{a,s\}$. Since no demographic turnover is accounted for in the model, the number of recovered people at time t is given by $R(t) = N - (S(t) + I^a(t) + I^s(t))$. Thus, we compute it by

$$R^n = N - (S^n + I^{s,n} + I^{a,n}), \qquad n \in \mathbb{N}_0.$$

Figure 17 shows the approximation of $S(t)$, $I^s(t)$, $I^a(t)$ and $R(t)$ by (1.20), as well as the continuous final size $S(\infty)$, root of (6.22).

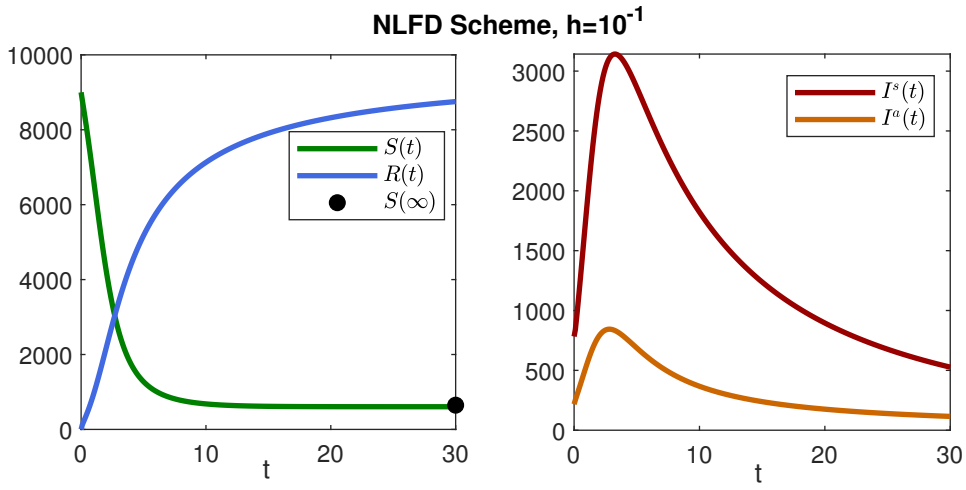

Figure 17: Long time behaviour of the non-local finite difference numerical solution to problem (1.10)-(6.23).

THE AGE-OF-INFECTION MODEL WITH HETEROGENEOUS MIXING

When the conditions in III are fulfilled, the integro-differential system (1.20) coincides with the age-of-infection model (1.16), involving static heterogeneity in the host population. From equation (1.18), the non-linear system governing the final size of the epidemic in group i, $S_i(\infty)$, for $i = 1, \dots, d$, can be expressed as

$$\log \frac{S_i^0}{x_i} - a_i \sum_{j=1}^{M} \frac{p_{ij}}{N_j} \left((S_j^0 - x_j) \int_0^{+\infty} A_j(t)\, dt + \int_0^{+\infty} \varphi_{j0}(t)\, dt \right) = 0. \quad (6.24)$$

Thus, (6.16) corresponds to (6.24) under the assumptions in III.

For our test, we consider a host population of $N = 1000$ individuals divided in 2 subgroups of sizes $N_1 = 0.1N$ and $N_2 = 0.9N$, respectively. Furthermore, we set

$$A_1(t) = A_2(t) = \frac{1}{\sigma\sqrt{2\pi}} e^{-\frac{(t-\mu)^2}{2\sigma^2}}, \qquad \mu = 0.2, \qquad \sigma = 3\mu, \quad (6.25)$$

we choose $S_1^0 = 99$, $S_2^0 = 899$, $a_1 = 5$, $a_2 = 10$, $p_{11} = 0.4$, $p_{12} = 0.6$, $p_{21} = 0.5$, $p_{22} = 0.5$ and

$$\varphi_{i0}(t) = (N_i - S_i^0)A_i(t), \qquad i = 1, 2.$$

The results of the numerical simulation by (6.1) are reported in Figure 17.

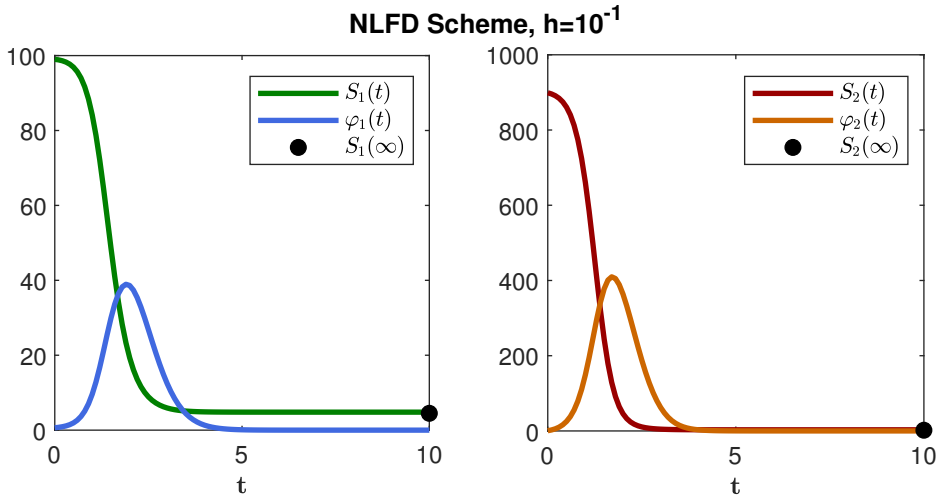

Figure 18: Long time behaviour of the non-local finite difference numerical solution to problem (1.16)-(6.25).

In order to check the asymptotic properties of the numerical solution, we have solved problem (1.16) by (6.1) on a $[0, 100]$ many times, each time halving the value of the stepsize h. Then we have used the numerical solution at the end point of the integration interval to evaluate the expression (6.24) and compute the final size residual

$$r^\infty(h) = \|\mathcal{R}(S_1^\infty(h), S_2^\infty(h))\|, \quad \text{with} \quad \mathcal{R} : \mathbb{R}^2 \to \mathbb{R}^2 \quad \text{such that for} \quad i = 1, 2,$$
$$\mathcal{R}_i(x_1, x_2) = \log \frac{S_i^0}{x_i} - a_i \sum_{j=1}^{2} p_{ij} \left(1 - \frac{x_j}{N_j}\right) \int_0^{+\infty} A_j(t)\, dt.$$

This procedure gives a measure for the errors in approximating $S(\infty) = (S_1(\infty), S_2(\infty))^T$ which are listed in Table 10, where it is clear that the numerical final size converges linearly to its continuous counterpart.

DISCRETE ASYMPTOTIC DYNAMICS						
h	$S_1^\infty(h)$	$S_2^\infty(h)$	$\|S(\infty)-S^\infty\|$	$r^\infty(h)$	EXP. ORDER	
2^{-1}	4.836	5.238	3.351	0.991	On $S(\infty)$	On r^∞
2^{-2}	4.953	4.257	2.397	0.787	0.48	0.33
2^{-3}	4.850	3.294	1.434	0.536	0.74	0.55
2^{-4}	4.716	2.652	0.780	0.325	0.88	0.72
2^{-5}	4.618	2.290	0.405	0.181	0.94	0.84
2^{-6}	4.560	2.100	0.206	0.096	0.97	0.92

Table 10: Long time behaviour of the numerical solution to (1.16)-(6.25) by the NLFD method: numerical final size convergence.

THE VIRUS SHEDDING MODEL The virus shedding epidemic model (1.23) is a particular instance of (1.20), obtained with the identifications in IV. Here we assume that

$$P_0(t) = \int_{-\infty}^{t} \Gamma(t-s)(r_1\varphi_1(s)+r_2\varphi_2(s))ds, \varphi_{i0} = \int_{-\infty}^{t} A_i(t-s)S(s)P(s)ds,$$

for $i = 1,2$, are known functions respectively of the form $\varphi_{i0}(t) = (N_i - S_i^0)A_i(t)$, and $P_0(t) = P_0\Gamma(t)$. In this case the final size relation (1.21) for $i = 1,2$, reads

$$\log\frac{S_i^0}{x_i} - \beta_i\left(R_{01}\left(1-\frac{x_1}{N_1}\right) + R_{02}\left(1-\frac{x_2}{N_2}\right) + P_0\int_0^{+\infty}\Gamma(t)dt\right) = 0, \quad (6.26)$$

where N_i is the size of the $i-$th group and

$$R_{0i} = r_i N_i \int_0^{+\infty} A_i(t)\,dt \int_0^{+\infty} \Gamma(t)\,dt, \qquad i = 1,2,$$

is the corresponding basic reproduction number. The uniqueness of $S(\infty) = (S_1(\infty), S_2(\infty))^T$ as a solution to the final size system (6.26) immediately comes from Theorem 6.6, since it corresponds to (6.16) under the conditions in IV.

For our experiment we consider

$$A_1(t) = A_2(t) = \frac{1}{\sigma\sqrt{2\pi}} e^{-\frac{(t-\mu)^2}{2\sigma^2}}, \qquad \mu = 0.2, \qquad \sigma = 3\mu, \qquad \Gamma(t) = \frac{1}{(1+t)^2},$$
$$N_1 = 200, \qquad N_2 = 300, \qquad S_1^0 = 199, \qquad S_2^0 = 298, \qquad P_0 = 2,$$
$$\beta_1 = 0.015, \qquad \beta_2 = 0.03, \qquad r_1 = 0.1, \qquad r_2 = 1. \tag{6.27}$$

The outcomes of the numerical simulation by the NLFD scheme (6.1) are reported in Figure 19. Again an at least linear convergence for the numerical final size $S_i^\infty(h)$, $i = 1, 2$, to the continuous one can be experimentally observed from Table 11. There, the values of the numerical final sizes and the residuals

$$r^\infty(h) = \|\mathcal{R}(S_1^\infty(h), S_2^\infty(h))\|, \quad \text{with} \quad \mathcal{R} : \mathbb{R}^2 \to \mathbb{R}^2 \quad \text{such that for} \quad i = 1, 2,$$
$$\mathcal{R}_i(x_2, x_2) = \log \frac{S_i^0}{x_i} - \beta_i \left(R_{01}\left(1 - \frac{x_1}{N_1}\right) + R_{02}\left(1 - \frac{x_2}{N_2}\right) + P_0 \int_0^{+\infty} \Gamma(t)dt \right),$$

on the relation (6.26) are shown, for different values of h.

DISCRETE ASYMPTOTIC DYNAMICS						
h	$S_1^\infty(h)$	$S_2^\infty(h)$	$\|S(\infty) - S^\infty\|$	$r^\infty(h)$	EXP. ORDER	
2^{-1}	2.891	0.140	6.639	1.954	On $S^\infty(h)$	On $r^\infty(h)$
2^{-2}	5.279	0.299	4.245	0.995	0.65	0.97
2^{-3}	7.194	0.458	2.324	0.475	0.87	1.06
2^{-4}	8.403	0.574	1.109	0.206	1.07	1.21
2^{-5}	9.082	0.644	0.427	0.070	1.38	1.56

Table 11: Long time behaviour of the numerical solution to (1.23)-(6.27) by the NLFD method: numerical final size convergence.

In conclusion, our study introduced a general framework for analyzing and comparing qualitative aspects of analytical solutions in epidemic models, along with their numerical approximations. The numerical method, characterized by a non-standard discretization approach, faithfully reproduces

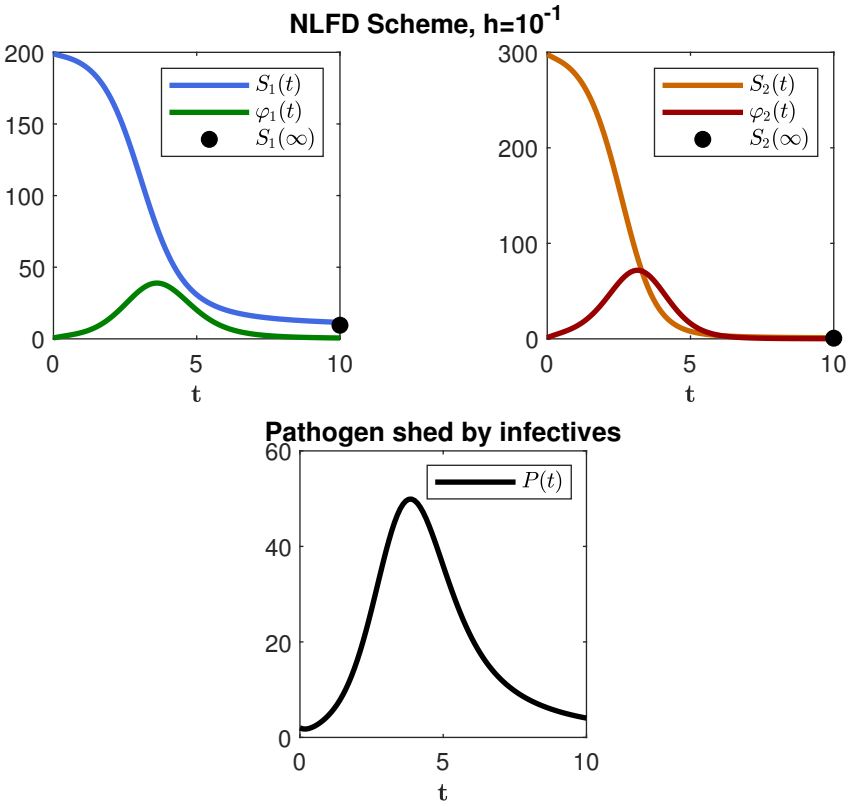

Figure 19: Long time behaviour of the non-local finite difference numerical solution to problem (1.23)-(6.27).

key qualitative features of the analytical solution, irrespective of the chosen step size. We demonstrated the uniqueness of the asymptotic numerical solution and its convergence to the analytical counterpart as step size tends to zero. The framework encompasses a range of epidemic models, making it a valuable tool for stability analysis and providing insights into epidemic dynamics. This method's reliability suggests its applicability to more complex scenarios, such as models with disease-related mortality or time-varying coefficients, which we intend to explore in future research within this general framework.

CONCLUSIONS AND FUTURE INSIGHTS

In this final section, we highlight the significant accomplishments and contributions of our research, which have unfolded across the chapters of this dissertation. Considering the advantages offered by integral and integro-differential equations in modeling the spread of infectious diseases, we systematically described age-of-infection models and the related well-established theoretical results, with a principal emphasis on the qualitative and asymptotic properties of the solutions. Notably, we have developed a rigorous integro-differential framework with the capacity to unify different age-of-infection models, providing a robust foundation for future investigations.

The necessity for numerical simulations to comprehend, predict and effectively address the spread of epidemics, coupled with the dearth of efficient integration methods for this class of models, motivated our interest in designing dynamically consistent numerical schemes. Our principal objective revolved around the formulation of discretization techniques that preserve both positivity and asymptotic behaviour of the continuous-time solution. To attain this goal, we adopted Non-Standard Finite Differences (NSFD) and Direct Quadrature (DQ) methods and investigated the properties of the corresponding numerical solutions within the theoretical framework of implicit Volterra discrete equations.

The origin of our research traces back to [71] and to Chapter 2, where an unconditionally positive and linearly implicit NSFD numerical method was presented. Despite its dynamical consistency and its capability to capture the asymptotic behaviour of the model, this method was constrained by a solely linear convergence rate. Therefore, seeking for higher precision we rewrote, employing an exponential operator, the original integro-differential model as an implicit Volterra integral equation and then discretized the integral terms via DQ approaches with Gregory weights. The resultant methodology, presented in [72] and Chapter 3, yielded positive, bounded and highly ac-

curate numerical solutions, which replicated the long-term behaviour of the epidemic.

The need to prove the existence of the discrete final size and its convergence to the continuous limit compelled our analysis towards the solutions of non-linear implicit Volterra discrete equations, with a particular focus on DQ methods as a specific instance. In [74] and Chapter 4, we provided insights into the existence, uniqueness and boundedness of the solution to general discrete VIEs under mild assumptions on the non-linearity. Additionally, we established theoretical results governing the existence of the asymptotic limit of the discrete solution and addressed the onset of oscillations. These outcomes resolved the question regarding the existence of the DQ numerical final size and confirmed its suitability as an approximation for the asymptotic behavior of the epidemic.

Recognizing the inherent benefits of the methodologies we developed, it was a natural progression to extend their application to multidimensional age-of-infection models. The paper [73] and the Chapter 5 introduced a DQ numerical method tailored to the integro-differential system involving static heterogeneity in the host population. The resulting scheme not only preserved positivity but also inherited high-order convergence. Of paramount significance, the discrete final size was unequivocally proved to converge to its continuous counterpart as the integration step size dwindled toward zero. Finally, following [75], Chapter 6 delved into non-local approximations for general renewal-type systems, expanding the purview of our methods to a wider range of scenarios.

Through our research, we have contributed to the field of mathematical epidemiology simulation, addressing the challenges posed by limited experimental validation and emphasizing the need for robust and efficient numerical tools. The properties of our approximated solutions, combined with the consideration of time-dependent infectivity in age-of-infection models, establish our methods as reliable instruments for understanding, predicting and mitigating infectious disease outbreaks. As we look ahead to future research, it is clear that there are opportunities to improve and extend these methodologies to more complex epidemic scenarios for which some simplifying modeling assumptions are relaxed.

One common characteristic among the models explored in this dissertation is the assumption of a closed population and constant sizes for its sub-

groups over time. While demographic turnover may be disregarded in cases of rapidly progressing epidemics, it holds considerable implications in other situations, as it could lead to the establishment of an endemic disease. Moreover, the inclusion of disease-related mortality is essential to yield accurate insights into the dynamics of an outbreak. For continuous-time models with extensions in this direction, we refer to [14, 16, 24, 36]. The numerical simulation of these models poses additional challenges. First of all, in these cases, the approximation of the time-varying non-negative population size $N(t)$ has to be addressed. Furthermore, the continuous final size relation turns to an inequality and offers limited insights into the long-term behaviour of the epidemic (see, for instance [5, 16]). In this perspective, it becomes crucial to provide numerical simulations that replicate the unknown asymptotic behaviour of the solution.

Generalizing the equation governing the incidence dynamics and the contact rate β is a viable option, as well. In fact, the widely employed mass action incidence and the standard incidence [18] are just two specific instances. Furthermore, it is often more realistic to assume that the contact rate is a non-increasing function of the total population size (see, for instance, [14, 18]). Thus numerical simulations, in conjunction with real-world data, may help to identify and characterize more complex contact patterns and modeling constitutive laws.

Our research has led to the development of efficient numerical methods for the age-of-infection model within a multi-group, heterogeneously mixed host population. Throughout the investigation, we maintained the assumption of a discrete trait space and static heterogeneity, with no interchanges among the multiple groups. However, we remark that, despite the generality of the model we considered, this assumption may not accurately represent scenarios in which group structures evolve over time, resulting in distinct dynamics. This becomes particularly relevant in the context of age-structured models, where the aging process introduces variations in individuals' group membership and corresponding infection characteristics. To address this modeling challenge, the work in [24] introduced a dependency on continuous-time age variables. Thus, the presence of partial derivatives and integral terms in the model complicates the extension of our numerical approaches, necessitating further in-depth investigation.

BIBLIOGRAPHY

[1] R. P. Agarwal. *Difference Equations and Inequalities*. CRC Press, 2000. DOI: 10.1201/9781420027020.

[2] G. K. Aldis and M. G. Roberts. "An integral equation model for the control of a smallpox outbreak". In: *Math Biosci.* 195.1 (2005), pp. 1–22. DOI: 10.1016/j.mbs.2005.01.006.

[3] R. M. Anderson. "Discussion: The Kermack-McKendrick epidemic threshold theorem". In: *Bulletin of Mathematical Biology* 53.1 (1991), pp. 3–32. ISSN: 0092-8240. DOI: 10.1016/S0092-8240(05)80039-4.

[4] J. A. D. Appleby and D. D. Patterson. "Large fluctuations and growth rates of linear Volterra summation equations". In: *Journal of Difference Equations and Applications* 23.6 (2017), pp. 1047–1080. DOI: 10.1080/10236198.2017.1315110.

[5] J. Arino, F. Brauer, P. van den Driessche, J. Watmough, and J. Wu. "A final size relation for epidemic models". In: *Mathematical Biosciences and Engineering* 4.2 (2007), pp. 159–175. ISSN: 1551-0018. DOI: 10.3934/mbe.2007.4.159.

[6] F. Ashraf, and M. O. Ahmad. "Nonstandard finite difference scheme for control of measles epidemiology". In: *International Journal of ADVANCED AND APPLIED SCIENCES* 6.3 (2019), pp. 79–85. DOI: 10.21833/ijaas.2019.03.012.

[7] F. Bai. "An age-of-infection model with both symptomatic and asymptomatic infections". In: *Journal of Mathematical Biology* 86.5 (2023). DOI: 10.1007/s00285-023-01920-w.

[8] A. D. Barbour. "Macdonald's model and the transmission of bilharzia". In: *Transactions of the Royal Society of Tropical Medicine and Hygiene* 72.1 (1978), pp. 6–15. ISSN: 0035-9203. DOI: 10.1016/0035-9203(78)90290-0.

[9] C. Barril, À. Calsina, and J. Ripoll. "A practical approach to Ro in continuous-time ecological models". In: *Mathematical Methods in the Applied Sciences* 41.18 (2018), pp. 8432–8445. DOI: 10.1002/mma.4673.

[10] D. Bernoulli. "Réflexions sur les avantages de l'inoculation". In: *Mercure de France* (1760), pp. 11656–11675.

[11] D. Bernoulli. "Essai d'une nouvelle analyse de la mortalite causee par la petite verole, et des avantages de l'inocula-tion pour la prevenir". In: *Histoire de l'Acad., Roy. Sci. (Paris) avec Mem* (1766), pp. 1–45.

[12] M. C. J. Bootsma, K. M. D. Chan, O. Diekmann, and H. Inaba. "Separable mixing: The general formulation and a particular example focusing on mask efficiency". In: *Mathematical Biosciences and Engineering* 20.10 (2023), pp. 17661–17671. ISSN: 1551-0018. DOI: 10.3934/mbe.2023785.

[13] M. C. J. Bootsma, K. M. D. Chan, O. Diekmann, and H. Inaba. *The effect of host population heterogeneity on epidemic outbreaks*. 2023. arXiv: 2308.06593.

[14] F. Brauer. "The Kermack–McKendrick epidemic model revisited". In: *Mathematical Biosciences* 198.2 (2005), pp. 119–131. ISSN: 0025-5564. DOI: 10.1016/j.mbs.2005.07.006.

[15] F. Brauer. "Some simple epidemic models". In: *Mathematical Biosciences and Engineering* 3.1 (2006), pp. 1–15. ISSN: 1551-0018. DOI: 10.3934/mbe.2006.3.1.

[16] F. Brauer. "Age-of-infection and the final size relation". In: *Mathematical Biosciences and Engineering* 5 (2008), p. 681. ISSN: 1551-0018. DOI: 10.3934/mbe.2008.5.681.

[17] F. Brauer. "Epidemic Models with Heterogeneous Mixing and Treatment". In: *Bulletin of Mathematical Biology* 70.7 (2008), p. 1869. ISSN: 1522-9602. DOI: 10.1007/s11538-008-9326-1.

[18] F. Brauer. "Age of Infection Epidemic Models". In: *Mathematical and Statistical Modeling for Emerging and Re-emerging Infectious Diseases*. Cham: Springer International Publishing, 2016, pp. 207–220. DOI: 10.1007/978-3-319-40413-4_13.

[19] F. Brauer. "A new epidemic model with indirect transmission". In: *Journal of Biological Dynamics* 11.sup2 (2017). PMID: 27430120, pp. 285–293. DOI: 10.1080/17513758.2016.1207813.

[20] F. Brauer, C. Castillo-Chavez, and Z. Feng. *Mathematical Models in Epidemiology*. Springer New York, 2019. DOI: 10.1007/978-1-4939-9828-9.

[21] F. Brauer, Z. Feng, and C. Castillo-Chávez. "Discrete epidemic models". In: *Mathematical Biosciences and Engineering* 7.1 (2010), pp. 1–15. DOI: 10.3934/mbe.2010.7.1.

[22] F. Brauer, Z. Shuai, and P. van den Driessche. "Dynamics of an age-of-infection cholera model". In: *Mathematical Biosciences and Engineering* 10.5&6 (2013), pp. 1335–1349. ISSN: 1551-0018. DOI: 10.3934/mbe.2013.10.1335.

[23] F. Brauer and J. Watmough. "Age of infection epidemic models with heterogeneous mixing". In: *Journal of Biological Dynamics* 3.2 (2009), pp. 324–330. DOI: 10.1080/17513750802415822.

[24] D. Breda, O. Diekmann, W. F. de Graaf, A. Pugliese, and R. Vermiglio. "On the formulation of epidemic models (an appraisal of Kermack and McKendrick)". In: *Journal of Biological Dynamics* 6.sup2 (2012), pp. 103–117. DOI: 10.1080/17513758.2012.716454.

[25] D. Breda, F. Florian, J. Ripoll, and R. Vermiglio. "Efficient numerical computation of the basic reproduction number for structured populations". In: *Journal of Computational and Applied Mathematics* 384 (2021), p. 113165. ISSN: 0377-0427.

[26] H. Brunner. *Collocation Methods for Volterra Integral and Related Functional Differential Equations*. Cambridge Monographs on Applied and Computational Mathematics. Cambridge University Press, 2004. DOI: 10.1017/CBO9780511543234.

[27] H. Brunner. *Volterra Integral Equations: An Introduction to Theory and Applications*. Cambridge Monographs on Applied and Computational Mathematics. Cambridge University Press, 2017. DOI: 10/kpm9.

[28] H. Brunner and P. J. van der Houwen. *The numerical solution of Volterra equations*. North-Holland Pub. Co., 1986. ISBN: 0-444-70073-0.

[29] T. A. Burton. *Volterra Integral and Differential Equations: SECOND EDITION (Mathematics in Science and Engineering)*. USA: Elsevier Science Inc., 2005. ISBN: 0444517863.

[30] A. Cardone, L. Gr. Ixaru, B. Paternoster, and G. Santomauro. "Ef–Gaussian direct quadrature methods for Volterra integral equations with periodic solution". In: *Mathematics and Computers in Simulation* 110 (2015). 7th edition of the workshop "Structural Dynamical Systems: computational aspects, pp. 125–143. ISSN: 0378-4754. DOI: 10.1016/j.matcom.2013.10.005.

[31] A. Cori, A. J. Valleron, F. Carrat, G. Scalia Tomba, G. Thomas, and P.Y. Boëlle. "Estimating influenza latency and infectious period durations using viral excretion data". In: *Epidemics* 4.3 (2012), pp. 132–138. DOI: 10.1016/j.epidem.2012.06.001.

[32] M. R. Crisci, V. B. Kolmanovskii, E. Russo, and A. Vecchio. "Stability of Continuous and Discrete Volterra Integro-Differential Equations by Liapunov Approach". In: *Journal of Integral Equations and Applications* 7.4 (1995), pp. 393 –411. DOI: 10.1216/jiea/1181075895.

[33] J. F. David. "Epidemic models with heterogeneous mixing and indirect transmission". In: *Journal of Biological Dynamics* 12.1 (2018), pp. 375–399. DOI: 10.1080/17513758.2018.1467506.

[34] P. J. Davis and P. Rabinowitz. *Methods of Numerical Integration*. Elsevier, 1984. DOI: 10.1016/c2013-0-10566-1.

[35] O. Diekmann, M. Gyllenberg, and J. A. J. Metz. "Finite Dimensional State Representation of Linear and Nonlinear Delay Systems". In: *Journal of Dynamics and Differential Equations* 30.4 (2018), pp. 1439–1467. ISSN: 1572-9222. DOI: 10.1007/s10884-017-9611-5.

[36] O. Diekmann and J. A. P. Heesterbeek. *Mathematical epidemiology of infectious diseases: model building, analysis and interpretation*. English. Wiley series in mathematical and computational biology. United States: John Wiley & Sons, 2000. ISBN: 9780471986829.

[37] O. Diekmann, J. A. P. Heesterbeek, and J. A. J. Metz. "On the definition and the computation of the basic reproduction ratio Ro in models for infectious diseases in heterogeneous populations". In: *Journal of Mathematical Biology* 28.4 (1990), pp. 365–382. ISSN: 1432-1416. DOI: 10.1007/BF00178324.

[38] O. Diekmann and H. Inaba. "A systematic procedure for incorporating separable static heterogeneity into compartmental epidemic models". In: *Journal of Mathematical Biology* 86.2 (2023), p. 29. ISSN: 1432-1416. DOI: 10.1007/s00285-023-01865-0.

[39] O. Diekmann, J. A. J. Metz, and J. A. P. Heesterbeek. "The legacy of Kermack and McKendrick". In: *Epidemic Models: Their Structure and Relation to Data*. Ed. by D. Mollison. Cambridge: Cambridge University Press, 1995.

[40] O. Diekmann, H. G. Othmer, R. Planqué, and M. C. J. Bootsma. "The discrete-time Kermack & McKendrick model: A versatile and computationally attractive framework for modeling epidemics". In: *Proceedings of the National Academy of Sciences* 118.39 (2021). DOI: 10.1073/pnas.2106332118.

[41] K. Dietz and J. A. P. Heesterbeek. "Daniel Bernoulli's epidemiological model revisited". In: *Mathematical Biosciences* 180.1 (2002), pp. 1–21. ISSN: 0025-5564. DOI: 10.1016/S0025-5564(02)00122-0.

[42] A. Domoshnitsky, A. Sitkin, and L. Zuckerman. "Mathematical Modeling of COVID-19 Transmission in the Form of System of Integro-Differential Equations". In: *Mathematics* 10.23 (2022). DOI: 10.3390/math10234500.

[43] S. Elaydi. "Periodicity and Stability of Linear Volterra Difference Systems". In: *Journal of Mathematical Analysis and Applications* 181.2 (1994), pp. 483–492. ISSN: 0022-247X. DOI: 10.1006/jmaa.1994.1037.

[44] S. Elaydi. *An Introduction to Difference Equations*. Undergraduate Texts in Mathematics. Springer-Verlag, 2005. DOI: 10.1007/0-387-27602-5.

[45] S. Elaydi, E. Messina, and A. Vecchio. "On the asymptotic stability of linear Volterra difference equations of convolution type". In: *Journal of Difference Equations and Applications* 13.12 (2007), pp. 1079–1084. DOI: 10.1080/10236190701264529.

[46] Z. Feng, D. Xu, and H. Zhao. "Epidemiological Models with Non-Exponentially Distributed Disease Stages and Applications to Disease Control". In: *Bulletin of Mathematical Biology* 69.5 (2007), pp. 1511–1536. DOI: 10.1007/s11538-006-9174-9.

[47] Z. Fodor, S. D. Katz, and T. G. Kovacs. "Why integral equations should be used instead of differential equations to describe the dynamics of epidemics". In: *arXiv* (2020). DOI: 10.48550/ARXIV.2004.07208.

[48] C. Fraser. "Estimating Individual and Household Reproduction Numbers in an Emerging Epidemic". In: *PLOS ONE* 2.8 (2007), pp. 1–12. DOI: 10.1371/journal.pone.0000758.

[49] L. Fumanelli, M. Ajelli, P. Manfredi, A. Vespignani, and S. Merler. "Inferring the Structure of Social Contacts from Demographic Data in the Analysis of Infectious Diseases Spread". In: *PLoS Computational Biology* 8.9 (2012). Ed. by Marcel Salathé, e1002673. DOI: 10.1371/journal.pcbi.1002673.

[50] J. Glasser, Z. Feng, A. Moylan, S. Del Valle, and C. Castillo-Chavez. "Mixing in age-structured population models of infectious diseases". In: *Mathematical Biosciences* 235.1 (2012), pp. 1–7. ISSN: 0025-5564. DOI: 10.1016/j.mbs.2011.10.001.

[51] I. Győri, F. Hartung, and N. A. Mohamady. "Existence and uniqueness of positive solutions of a system of nonlinear algebraic equations". In: *Periodica Mathematica Hungarica* 75 (2017), pp. 114–127. DOI: 10.1007/s10998-016-0179-3.

[52] I. Győri and D. W. Reynolds. "On admissibility of the resolvent of discrete Volterra equations". In: *Journal of Difference Equations and Applications* 16.12 (2010), pp. 1393–1412. DOI: 10.1080/10236190902824196.

[53] W. Hamer. "Epidemiology, Old and New". In: *Southern Medical Journal* 22.5 (1929), p. 516. DOI: 10.1097/00007611-192905000-00036.

[54] T. Harko, F. S. N. Lobo, and M. K. Mak. "Exact analytical solutions of the Susceptible-Infected-Recovered (SIR) epidemic model and of the SIR model with equal death and birth rates". In: *Applied Mathematics and Computation* 236 (2014), pp. 184–194. ISSN: 0096-3003. DOI: 10.1016/j.amc.2014.03.030.

[55] Italian National Institute of Statistics. *CENSUS OF POPULATION AND HOUSING, Age structure - municipalities. Demographic characteristics and citizenship*. http://dati-censimentipermanenti.istat.it. Accessed: 2022-06-09.

[56] A. Keimer and L. Pflug. "Modeling infectious diseases using integro-differential equations: Optimal control strategies for policy decisions and Applications in COVID-19". In: *ResearchGate* (2020). DOI: 10.13140/RG.2.2.10845.44000.

[57] A. Kergaßner, C. Burkhardt, D. Lippold, M. Kergaßner, L. Pflug, D. Budday, P. Steinmann, and S. Budday. "Memory-based meso-scale modeling of Covid-19". In: *Computational Mechanics* 66.5 (2020), pp. 1069–1079. ISSN: 1432-0924. DOI: 10.1007/s00466-020-01883-5.

[58] W. O. Kermack and A. G. McKendrick. "A contribution to the mathematical theory of epidemics". In: *Proceedings of the Royal Society of London. Series A, Containing Papers of a Mathematical and Physical Character* 115.772 (1927), pp. 700–721. DOI: 10.1098/rspa.1927.0118.

[59] Xiao-Lan L. and Cheng-Cheng Z. "A Non-Standard Finite Difference Scheme for a Diffusive HIV-1 Infection Model with Immune Response and Intracellular Delay". In: *Axioms* 11.3 (2022). ISSN: 2075-1680. DOI: 10.3390/axioms11030129.

[60] L. A. C. Ladeira. "Continuity of fixed-points". In: *J. Math. Anal. Appl.* 169.2 (1992), pp. 350–358. DOI: 10.1016/0022-247X(92)90083-P.

[61] J. D. Lambert. *Numerical Methods for Ordinary Differential Systems: The Initial Value Problem*. John Wiley and Sons, 1991.

[62] R. Laurio Dizon. "The heterogeneous age-mixing model of estimating the covid cases of different local government units in the National Capital Region, Philippines". In: *Clinical Epidemiology and Global Health* 9 (2021), pp. 12–16. ISSN: 2213-3984. DOI: 10.1016/j.cegh.2020.06.003.

[63] P. Linz. *Analytical and numerical methods for Volterra equations*. SIAM, 1985.

[64] J. M.-S. Lubuma and Y. A. Terefe. "A nonstandard Volterra difference equation for the SIS epidemiological model". In: *Revista de la Real Academia de Ciencias Exactas, Físicas y Naturales. Serie A. Matemáticas* 109.2 (2015), pp. 597–602. ISSN: 1579-1505. DOI: 10.1007/s13398-014-0203-5.

[65] Y. Ma, J. Deng, Q. Liu, M. Du, M. Liu, and J. Liu. "Long-Term Consequences of Asymptomatic SARS-CoV-2 Infection: A Systematic Review and Meta-Analysis". In: *International Journal of Environmental Research and Public Health* 20.2 (2023). ISSN: 1660-4601. DOI: 10.3390/ijerph20021613.

[66] R. K. Mallik and K. V. Rangarao. "On the impulse response of a discrete-time linear IIR system". In: *Digital Signal Processing* 13.1 (2003), pp. 128–143. ISSN: 1051-2004. DOI: 10.1016/S1051-2004(02)00010-6.

[67] M. Martcheva. *An Introduction to Mathematical Epidemiology*. Springer US, 2015. DOI: 10.1007/978-1-4899-7612-3.

[68] L. Mazzei, D. L. Marchisio, and P. Lettieri. "Direct Quadrature Method of Moments for the Mixing of Inert Polydisperse Fluidized Powders and the Role of Numerical Diffusion". In: *Industrial & Engineering Chemistry Research* 49.11 (2010), pp. 5141–5152. ISSN: 0888-5885. DOI: 10.1021/ie901116y.

[69] I. McCulloh, K. Kiernan, and T. Kent. "Inferring True COVID19 Infection Rates From Deaths". In: *Frontiers in Big Data* 3 (2020). ISSN: 2624-909X. DOI: 10.3389/fdata.2020.565589.

[70] S. Merler, M. Ajelli, B. Camilloni, S. Puzelli, A. Bella, M. C. Rota, A. E. Tozzi, M. Muraca, M. Meledandri, A. M. Iorio, et al. "Pandemic influenza A/H1N1pdm in Italy: age, risk and population susceptibility". In: *PLoS One* 8.10 (2013), e74785.

[71] E. Messina, M. Pezzella, and A. Vecchio. "A non-standard numerical scheme for an age-of-infection epidemic model". In: *Journal of Computational Dynamics* 9.2 (2022), pp. 239–252. ISSN: 2158-2491. DOI: 10.3934/jcd.2021029.

[72] E. Messina, M. Pezzella, and A. Vecchio. "Positive Numerical Approximation of Integro-Differential Epidemic Model". In: *Axioms* 11.2 (2022). ISSN: 2075-1680. DOI: 10.3390/axioms11020069.

[73] E. Messina, M. Pezzella, and A. Vecchio. "A long-time behavior preserving numerical scheme for age-of-infection epidemic models with heterogeneous mixing". In: *Applied Numerical Mathematics* (2023). ISSN: 0168-9274. DOI: 10.1016/j.apnum.2023.04.009.

[74] E. Messina, M. Pezzella, and A. Vecchio. "Asymptotic solutions of nonlinear implicit Volterra discrete equations". In: *Journal of Computational and Applied Mathematics* 425 (2023), p. 115068. ISSN: 0377-0427. DOI: 10.1016/j.cam.2023.115068.

[75] E. Messina, M. Pezzella, and A. Vecchio. "Nonlocal finite difference discretization of a class of renewal equation models for epidemics". In: *Mathematical Biosciences and Engineering* 20.7 (2023), pp. 11656–11675. ISSN: 1551-0018. DOI: 10.3934/mbe.2023518.

[76] E. Messina and A. Vecchio. "A sufficient condition for the stability of direct quadrature methods for Volterra integral equations". In: *Numerical Algorithms* 74.4 (2017), pp. 1223–1236. ISSN: 1572-9265. DOI: 10.1007/s11075-016-0193-9.

[77] E. Messina and A. Vecchio. "Stability and boundedness of numerical approximations to Volterra integral equations". In: *Applied Numerical Mathematics* 116 (2017). New Trends in Numerical Analysis: Theory, Methods, Algorithms and Applications (NETNA 2015), pp. 230–237. ISSN: 0168-9274. DOI: 10.1016/j.apnum.2017.01.011.

[78] R. E. Mickens. *Nonstandard Finite Difference Models of Differential Equations*. WORLD SCIENTIFIC, 1993. DOI: 10.1142/2081.

[79] R. E. Mickens. "Nonstandard Finite Difference Schemes for Differential Equations". In: *Journal of Difference Equations and Applications* 8.9 (2002), pp. 823–847. DOI: 10.1080/1023619021000000807.

[80] R. E. Mickens. "Numerical integration of population models satisfying conservation laws: NSFD methods". In: *Journal of Biological Dynamics* 1.4 (2007), pp. 427–436. DOI: 10.1080/17513750701605598.

[81] J. Migda, M. Nockowska-Rosiak, and M. Migda. "Asymptotic properties of solutions to discrete Volterra type equations". In: *Mathematical Methods in the Applied Sciences* 45.5 (2022), pp. 2674–2684. DOI: 10.1002/mma.7946.

[82] C. B. Moler. *Numerical Computing with Matlab*. Society for Industrial and Applied Mathematics, 2004. DOI: 10.1137/1.9780898717952.

[83] F. P. Pijpers. "A non-parametric method for determining epidemiological reproduction numbers". In: *Journal of Mathematical Biology* 82.5 (2021). DOI: 10.1007/s00285-021-01590-6.

[84] "Prevalence and incidence". In: *Bull World Health Organ* 35.5 (1966), pp. 783–784.

[85] Y. N. Raffoul. *Qualitative Theory of Volterra Difference Equations*. Springer International Publishing, 2018. DOI: 10.1007/978-3-319-97190-2.

[86] M. G. Roberts and J. A. P. Heesterbeek. "Model-consistent estimation of the basic reproduction number from the incidence of an emerging infection". In: *Journal of Mathematical Biology* 55.5 (2007), pp. 803–816. ISSN: 1432-1416. DOI: 10.1007/s00285-007-0112-8.

[87] R. Ross. *The Prevention of malaria*. J. Murray, 1910.

[88] P. Sah, M. C. Fitzpatrick, C. F. Zimmer, E. Abdollahi, L. Juden-Kelly, S. M. Moghadas, B. H. Singer, and A. P. Galvani. "Asymptomatic SARS-CoV-2 infection: A systematic review and meta-analysis". In: *Proceedings of the National Academy of Sciences* 118.34 (2021), e2109229118. DOI: 10.1073/pnas.2109229118.

[89] Y. Song and C. T. H. Baker. "Linearized stability analysis of discrete Volterra equations". In: *Journal of Mathematical Analysis and Applications* 294.1 (2004), pp. 310–333. DOI: 10.1016/j.jmaa.2004.02.019.

[90] L. Stella, A. P. Martínez, D. Bauso, and P. Colaneri. "The Role of Asymptomatic Infections in the COVID-19 Epidemic via Complex Networks and Stability Analysis". In: *SIAM Journal on Control and Optimization* 60.2 (2022), S119–S144. DOI: 10.1137/20M1373335.

[91] H. R. Thieme and C. Castillo-Chavez. "On the Role of Variable Infectivity in the Dynamics of the Human Immunodeficiency Virus Epidemic". In: *Lecture Notes in Biomathematics*. Springer Berlin Heidelberg, 1989, pp. 157–176. DOI: 10.1007/978-3-642-93454-4_7.

[92] H. R. Thieme and C. Castillo-Chavez. "How May Infection-Age Dependent Infectivity Affect the Dynamics of HIV /AIDS?" In: *SIAM Journal on Applied Mathematics* 53.5 (1993), pp. 1447–1479. DOI: 10.1137/0153068.

[93] S. Treibert, H. Brunner, and M. Ehrhardt. "A nonstandard finite difference scheme for the SVICDR model to predict COVID-19 dynamics". In: *Mathematical Biosciences and Engineering* 19.2 (2022), pp. 1213–1238. ISSN: 1551-0018. DOI: 10.3934/mbe.2022056.

[94] A. Vecchio. "Volterra discrete equations: summability of the fundamental matrix". In: *Numerische Mathematik* 89.4 (2001), pp. 783–794. DOI: 10.1007/s002110100270.

[95] M. A. Vink, M. C. J. Bootsma, and J. Wallinga. "Serial Intervals of Respiratory Infectious Diseases: A Systematic Review and Analysis". In: *American Journal of Epidemiology* 180.9 (Oct. 2014), pp. 865–875. ISSN: 0002-9262. DOI: 10.1093/aje/kwu209.

[96] B. Wacker and J. C. Schlüter. "A non-standard finite-difference-method for a non-autonomous epidemiological model: analysis, parameter identification and applications". In: *Mathematical Biosciences and Engineering* 20.7 (2023), pp. 12923–12954. ISSN: 1551-0018. DOI: 10.3934/mbe.2023577.

[97] P. H. M. Wolkenfelt. "The Construction of Reducible Quadrature Rules for Volterra Integral and Integro-differential Equations". In: *IMA Journal of Numerical Analysis* 2.2 (1982), pp. 131–152. ISSN: 0272-4979. DOI: 10.1093/imanum/2.2.131.

[98] P. H. M. Wolkenfelt. "On the Relation between the Repetition Factor and Numerical Stability of Direct Quadrature Methods for Second Kind Volterra Integral Equations". In: *SIAM Journal on Numerical Analysis* 20.5 (1983), pp. 1049–1061. DOI: 10.1137/0720074.